STRUCTURAL BASES OF PLEXIN SIGNAL TRANSDUCTION

APPROVED BY SUPERVISORY COMMITTEE

_____

Xuewu, Zhang, Associate Professor

_____

Zhe, Chen, Assistant Professor

_____

YuhMin, Chook, Professor

_____

Qiu-Xing, Jiang, Assistant Professor

Dedicated to my beautiful wife, family, friends, colleagues and mentor without whose help none of this would have been possible

STRUCTURAL BASES OF PLEXIN SIGNAL TRANSDUCTION

By

HEATH GARRICK PASCOE

DISSERTATION

Presented to the Faculty of the Graduate School of Biomedical Sciences

The University of Texas Southwestern Medical Center at Dallas

In Partial Fulfillment of the Requirements

For the Degree of

DOCTOR OF PHILOSOPHY

The University of Texas Southwestern Medical Center

Dallas, Texas

July, 2015

STRUCTURAL BASES OF PLEXIN SIGNAL TRANSDUCTION

HEATH GARRICK PASCOE, Ph.D.

The University of Texas Southwestern Medical Center at Dallas, 2015

Xuewu Zhang, Ph.D.

Plexins are a family of transmembrane receptors for the Semaphorin family of repulsive axon guidance molecules. Plexin mediated signal transduction is critical for a variety of cellular processes including regulation of adhesion and actin organization. Aberrant plexin signaling is associated with numerous pathologies. Despite plexin's essential cellular functions, a detailed understanding of the structural basis underlying plexin singling remains elusive. Here, the structural bases for two aspects of plexin signaling are revealed.

Plexins relay signals in part by accelerating the GTP hydrolysis reaction catalyzed by the small GTPase Rap. This discovery appears at odds with the known structural features of plexin GAP domains. Plexin GAPs are structurally related to RasGAPs and possess RasGAP catalytic machinery. Conversely, plexins are structurally unrelated to canonical RapGAPs and don't possess their associated catalytic machinery. Here, the structural basis underlying the non-canonical RapGAP activity of plexins is revealed. Plexins induce a unique configuration of Rap's Switch II loop to utilize a non-canonical catalytic residue.

Plexins also regulate RhoA activity. The B family plexins recruit two RhoGEFs (PDZ-RhoGEF and Leukemia Associated RhoGEF) by specifically binding to the PDZ domains of these GEFs. Conversely, these PDZ domains bind promiscuously to a variety of ligands. The structural basis by which plexins specifically recognize these two PDZ domains is revealed here. B family plexins interact with the PDZ domain of PDZ-

RhoGEF using a secondary interface outside the canonical PDZ binding site. This secondary interface contributes to tight binding and is important for RhoA activation following plexin activation. Secondary interfaces may be a general mechanism utilized by modular protein-protein interaction domains to achieve specificity.

Structural and biochemical characterization of plexins can be difficult. Here, two methods for studying plexins are described. These methods were critical to the success of the above studies. First, a method used to generate fusion proteins in-vitro for use in crystallography is described. This method allowed for the successful crystallization of a plexin/Rap complex. Second, a biochemical assay is described for easily measuring Plexin GAP activity in-vitro. This method circumvents the difficulties of many alternative approaches to measuring GAP activity.

Table of Contents

Prior Publications

Heath G. Pascoe*, Yuxiao Wang*, et al. "In vitro assay for the Rap GTPase Activating Protein activity of the purified cytoplasmic domain of plexin." Methods in Molecular Biology, Springer. In press.
* Co-first author

Heath G. Pascoe, et al. "Structural mechanisms of plexin signaling." Progress in Biophysics and Molecular Biology, Elsiver. In press.

Heath G. Pascoe, et al. "A secondary PDZ domain-binding site on class B plexins enhances the selectivity towards PDZ-RhoGEF." Under review.

Yuxiao Wang*, Heath G. Pascoe*, et al. "Structural basis for activation and non-canonical catalysis of the Rap GTPase activating protein domain of plexin." eLife 2, e01279.
* Co-first author

Figure and Table List

Chapter 1:

Chapter 2:

Chapter 3:

Chapter 4:

Chapter 5:

Chapter6:

CHAPTER ONE

An Introduction to Semaphorin/Plexin Signaling

Relevance

From the point of conception through development, the human body must orchestrate numerous miracles of organization; perhaps the most complex of which is the development of the nervous system. With hundreds of billions of individual neurons, hundreds of trillions of individual synaptic connections must be formed in a highly organized fashion to ensure proper signal transduction. The plexin family receptors and their associated ligands, the semaphorins, are critical regulators of nervous system morphogenesis. Signals through semaphorin/plexin play essential roles in many aspects of nervous system development including axon guidance, fasciculation, branching and synapse formation (Tran, Kolodkin et al. 2007). In addition to their roles in neuronal development, plexins/semaphorins are critical regulators of additional processes including: cardiovascular development, angiogenesis, immune responses, and wound healing (Yaron and Zheng 2007, Sakurai, Doci et al. 2012, Takamatsu and Kumanogoh 2012, Gu and Giraudo 2013, Worzfeld, Swiercz et al. 2014). Malfunction of the plexin signaling pathway has been implicated in human diseases, including neurological disorder and cancer (Sakurai, Doci et al. 2012, Tamagnone 2012, Gu and Giraudo 2013). There is then, an obvious and strong clinical motivation underlying the study of this ligand/receptor pair as well as an opportunity to discover the fundamental processes governing nervous system development.

Semaphorins

Overview

The semaphorins comprise a large family of secreted and membrane bound proteins that mediate signaling processes in a variety of tissues. Over 20 semaphorins have been identified to date and are divided, according to sequence conservation, into eight classes (Figure 1-1) (Kolodkin, Matthes et al. 1993, Semaphorin_Nomenclature_Committee 1999). The majority of semaphorins are cell surface attached through a transmembrane region or glycosylphosphatidylinositol(GPI)-linker (Semaphorin_Nomenclature_Committee 1999). Classes 2,3, and a viral semaphorin, however, are secreted.

While semaphorins are expressed largely throughout the nervous system, they are expressed in the majority of peripheral tissues as well. Genetic knockout of semaphorins or their plexin receptors are often embryonically lethal, causing severe defects in the development of the nervous and cardiovascular systems (Worzfeld, Swiercz et al. 2014).

Semaphorins regulate axon guidance

First characterized for their role in the developing nervous system, the semaphorins were shown to induce collapse of axon growth cones (Messersmith, Leonardo et al. 1995, Takahashi, Fournier et al. 1999). Growth cones are dynamic structures that lead migrating axons and ensure proper pathfinding by constantly sensing the extracellular environment for both attractive and repulsive axon guidance cues. Semaphorins regulate axon pathfinding by binding to and activating their primary receptors on the growth cone surface, the plexin family of transmembrane receptors.

Plexin activation following semaphorin binding induces loss of attachment to the extracellular matrix though integrin inactivation as well as reorganization of the cytoskeleton through a variety of small GTPase mediated pathways described below. Together these processes facilitate axon turning away from regions of high semaphorin concentration. In the context of the nervous system then, semaphorins function primarily as repulsive guidance cues. Semaphorins in conjunction with additional repulsive and attractive guidance molecules including: slit, netrin, and ephrin, direct axon pathfinding by defining pathways of permissive and restrictive growth by repelling and attracting migrating axons at the appropriate boundaries. While semaphorins are known to act primarily as repulsive guidance cues, Semaphroin3A has been reported to attract migrating axons in the context of elevated cellular cyclic Guanosine MonoPhosphate (cGMP) levels. The molecular details by which this repulsive/attractive switch is made, however, remain obscure (Song, Ming et al. 1998, Kruger, Aurandt et al. 2005, Tran, Kolodkin et al. 2007).

In addition to the plexins, semaphorins have been shown to interact with a small handful of additional proteins including: neuropilin 1 and 2 (Npn 1, 2), T-cell immunoglobulin and mucin domain (Tim2), CD72, syndecan-3 (Syn-3), heparin sulfate proteoglycan (HSPG), and chondroitin sulfate proteoglycan (CSPG) reviewed in (Kruger, Aurandt et al. 2005). Some plexins require neuropilin (neuropilin 1 or 2) to act as a co-receptor to form holo-receptors for secreted class 3 semaphorins (Figure 1-1) (Takahashi, Fournier et al. 1999).

Semaphorins regulate cardiovascular development

Apart from their role in regulating nervous system morphology, semaphorins have also been investigated for their ability to regulate cardiovascular development. In retrospect, it is perhaps unsurprising that semaphorins would regulate vascular patterning given the organizational similarities between the highly branched network of neuronal connections and that of the vascular network. As axon growth physically defines the neuronal network, endothelial cell growth defines the vascular network. Various semaphorins and plexins are expressed in endothelial cells including Semaphorin 3A and its receptor PlexinA1, which together regulate endothelial cell adhesion. This regulation appears crucial for proper vascular remodeling as dominant negative PlexinA1 disrupts vascular remodeling in developing chick brains (Takahashi, Fournier et al. 1999, Serini, Valdembri et al. 2003). Semaphorin3E is expressed in developing somites while its receptor PlexinD1 is also expressed in endothelial cells. Semaphorin/plexin signaling appears to be crucial for restricting excessive vascularization of developing somites as Semaphorin3E knockout mice exhibit highly vascularized somites, as do PlexinD1 knockouts (Gitler, Lu et al. 2004, Gu, Yoshida et al. 2005, Kruger, Aurandt et al. 2005). Additional roles have been described for semaphorin/plexin signaling in regulating heart morphogenesis as well as liver vascularization (Kruger, Aurandt et al. 2005, Worzfeld, Swiercz et al. 2014).

Semaphorins in the immune system

Many poxviruses express a secreted form of semaphorin, presumably to inhibit host immune responses. The viral semaphorin is most closely related by sequence

homology to Semapohrin7A, which is expressed on the surfaces of activated T-cells (Yamada, Kubo et al. 1999). The viral semaphorin, like Semaphorin7A, binds PlexinC1 (Figure 1-1). PlexinC1 is expressed in antigen presenting dendritic cells and binding of the viral semaphorin has been shown to affect migration of both monocytes and dendritic cells (Walzer, Galibert et al. 2005, Walzer, Galibert et al. 2005). The role of the viral semaphorin may then be to inhibit T-cell activation by interfering with plexin's ability to regulate migration processes.

Semaphorin organization

The eight classes of semaphorins display diverse topologies within their C-terminal regions (Figure 1-1). Domains found in the C-terminal portion of semaphorins include: Plexin-Semaphorin-Integrin (PSI), thrombospondin, Ig like-Plexin-Transcription-Factors (IPT), PSD95-Dlg1-Zo-1 (PDZ), and Ig-like (Kruger, Aurandt et al. 2005). While these C-terminal domains apparently do not mediate the plexin/semaphorin interaction, they are functionally important. The Ig-like domain of Semaphorin3A potentiates its ability to induce growth cone collapse and the thrombospondin domains of Semaphorin5A regulate its effect on axon guidance (Koppel, Feiner et al. 1997, Oster, Bodeker et al. 2003, Kantor, Chivatakarn et al. 2004, Yazdani and Terman 2006). All semaphorins, however, posses a conserved N-terminal "Sema" domain (~500 residues) which mediates the semaphorin/plexin interaction. The sema domains have been the focus of extensive crystallographic and biochemical investigations that have revealed both the structure and ligand binding modes of several sema domains. To date crystal structures of the sema domains from Semaphorins: 6A, 3A, 4D, and 7A have been

determined alone or in complex with plexin (Antipenko, Himanen et al. 2003, Janssen, Robinson et al. 2010, Liu, Juo et al. 2010, Nogi, Yasui et al. 2010). Despite variations in sequence between semaphorin classes, the sema domains adopt a conserved 7 bladed beta propeller fold and homodimerize along the face of the propeller via inter-molecular interactions with a second sema domain (Figure 1-2). In some cases the dimerization is enforced through inter-chain disulfide bonds mediated by the PSI domain immediately C-terminal to the sema domain (Klostermann, Lohrum et al. 1998, Koppel and Raper 1998, Antipenko, Himanen et al. 2003, Love, Harlos et al. 2003).

Plexins

Overview

Plexins are the major cell surface receptors for the semaphorin family of axon guidance proteins (Winberg, Noordermeer et al. 1998, Tamagnone, Artigiani et al. 1999). Invertebrates have two plexins (Plexins A and B), whereas the nine vertebrate plexins are organized into four classes (A, B, C and D) (Figure 1-1)(Tamagnone, Artigiani et al. 1999).

Plexins are large type I transmembrane receptors with their N-terminal regions mediating extracellular engagement of semaphorins and their C-terminal regions transducing the activating signal to the cell interior. Plexins, like the semaphorins, possess a conserved N-terminal sema domain that engages the semaphorin sema domain. Similar to semaphorins, the plexin sema domains have been reported to homodimerize. Unlike the semaphorins, however, plexin sema domains dimerize in a head to head

fashion as seen for PlexinA2 (Nogi, Yasui et al. 2010) rather than face to face (Figure 1-3).

Plexin Signal Transduction

The additional features of the plexin extracellular region are conserved across the plexin families (Figure 1-1 and 1-4A). C-terminal to the sema domain, every plexin possesses 3 PSI domains followed by 3 IPT domains, and a single pass transmembrane helix. The ~600-residue cytoplasmic regions of the plexin family members are highly conserved and share a common architecture. It was discovered over a decade ago that this region contains two segments (C1 and C2) that show sequence similarity to GTPase Activating Proteins (GAPs) for Ras (Figure 1-4B) (Rohm, Rahim et al. 2000, Hu, Marton et al. 2001). The two segments are interrupted by an insertion region. Despite this interruption, structural studies have shown that the two GAP-homology segments fold together into one intact GAP domain, which indeed structurally resembles RasGAPs such as p120GAP and neurofibromin (Figure 1-4B) (He, Yang et al. 2009, Tong, Hota et al. 2009). There are two conserved arginine residues in the plexin GAP domain, one in each of the two segments, corresponding to the two catalytically essential arginine residues in RasGAPs (Figure 1-4). Mutating these arginine residues abolishes plexin activity both in vitro and in vivo, demonstrating the essential role of the GAP domain in plexin function (Rohm, Rahim et al. 2000, Worzfeld, Swiercz et al. 2014).

Plexin GAP Specificity

The identification of the GAP domain in plexins was of particular significance for establishing the fundamental signaling mechanisms underlying plexin function. Small GTPases such as Ras and Rac1 are master regulators of many fundamental cellular processes such as proliferation and cytoskeletal dynamics. They act as molecular switches, cycling between the GDP-bound inactive and GTP-bound active states. GAPs turn off GTPases by accelerating hydrolysis of the bound GTP to GDP, whereas guanine nucleotide exchange factors (GEFs) activate them by promoting the exchange of GDP for GTP. The presence of the GAP domain makes it possible for plexins to directly control the activity of small GTPases, consistent with their roles in regulating cell morphology and migration. To date, plexins remain unique as the only group of cell surface receptors known to contain a GAP domain.

A recent biochemical study established the first in vitro reconstitution of plexin GAP activity (Wang, He et al. 2012). This study demonstrated the specificity of the plexin GAP domains for the Rap family of small GTPases, despite the structural similarity of plexin GAP domains to known RasGAPs (Figure 1-5). The discovery that plexin GAPs specifically catalyze Rap mediated GTP hydrolysis is consistent with the cell-matrix detachment and actin reorganization seen upon plexin activation (Wang, He et al. 2012), as Rap is a known activator of integrins and also plays a negative regulatory role in Rho activation. This discovery also raised the question of how plexins catalyze Rap mediated GTP hydrolysis given plexins' lack of canonical RapGAP catalytic machinery, this question will be discussed in greater detail below.

The Plexin RBD and Juxtamembrane Segment

The ~200-residue insertion segment between the two GAP homology regions forms an independent domain that packs against one side of the GAP domain (Figure 1-4B) (Tong, Chugha et al. 2007, He, Yang et al. 2009, Tong, Hota et al. 2009). This domain interacts with Rho family small GTPases such as Rac1, RND1 and RhoD, and is therefore referred to as the RhoGTPase Binding Domain (RBD) (Rohm, Rahim et al. 2000, Vikis, Li et al. 2000, Driessens, Hu et al. 2001, Hu, Marton et al. 2001, Vikis, Li et al. 2002, Zanata, Hovatta et al. 2002, Oinuma, Katoh et al. 2003, Turner, Nicholls et al. 2004, Tong, Chugha et al. 2007). The RBD/RhoGTPase interaction plays an important regulatory role in plexin signaling, acting as either an activator or inhibitor of plexin signaling depending upon the identity of the particular RhoGTPase bound. In addition to the GAP domain and the RBD, crystal structures also revealed a juxtamembrane segment at the N-terminus of the plexin cytoplasmic region (Figure 1-4B) (He, Yang et al. 2009, Wang, He et al. 2012)

The Semaphorin/Plexin Interaction

Overview

In the past few years, the understanding of the mechanisms governing the regulation and signaling of plexin/semaphorin has grown tremendously (Jones 2015). This progress is owned largely to insights from structural studies of both the extracellular and intracellular regions of several plexin family members in various states. The N-terminal sema domain in the plexin extracellular region binds semaphorin, on it's own or

together with the extracellular region of the neuropilin co-receptor (Janssen, Robinson et al. 2010, Liu, Juo et al. 2010, Nogi, Yasui et al. 2010, Gu and Giraudo 2013).

Multiple lines of biochemical evidence suggest that activation of plexin signaling following semaphorin binding involves plexin clustering of some form, likely dimerization. Mutation of the PSI domain cysteine residues that strengthen the semaphorin Sema dimer though disulfide linkages, for example, strongly attenuate semaphorin's ability to activate plexin (Klostermann, Lohrum et al. 1998, Koppel and Raper 1998). Treatment of a cluster-inducing antibody against the plexin extracellular region induces activation of plexin signaling similar to semaphorin treatment (Oinuma, Ishikawa et al. 2004, Oinuma, Katoh et al. 2004). Furthermore, chimeric receptors of the plexin intracellular region fused to the ectodomain of the TrkA receptor are effectively activated upon treatment of the TrkA ligand, NGF (nerve growth factor), which is known to induce dimerization of TrkA.

Plexin/semaphorin Binding Mode

Recent structural studies have elucidated the binding mode between semaphorin and plexin, mediated by the N-terminal sema domains from both molecules (Janssen, Robinson et al. 2010, Liu, Juo et al. 2010, Nogi, Yasui et al. 2010, Gu and Giraudo 2013). The crystals structures revealed that plexin and semaphorin indeed interact as dimers, binding in a 2:2 fashion where each plexin protomer engages 1 semaphorin protomer. The head-to-head sema dimer seen for apo plexin is lost upon semaphorin engagement, but a similar binding mode is recapitulated through interactions with semaphorin (Figure 1-3, 1-6). Each plexin sema domain binds a semaphorin sema domain in a head-to-head

fashion similar to the plexin sema domain dimer. The geometry of the semaphorin face-to-face homodimer is largely maintained before and after binding plexin (Figure 1-2, 1-6). Additional inter-molecular interactions involving the membrane proximal domains may also contribute to semaphorin/plexin clustering on the cell surface, offering another layer of regulation to plexin signaling (Janssen, Robinson et al. 2010, Janssen, Malinauskas et al. 2012, Gu and Giraudo 2013).

Plexins are Activated Following Dimerization

The cytoplasmic region of neuropilin is short (~30 residues) and appears non-essential for semaphorin signaling (Nakamura, Tanaka et al. 1998). For semaphorin/plexin pairs that require the neuropilin co-receptor, neuropilin serves to strengthen the interaction but does not alter the binding mode (Figure 1-7) (Janssen, Malinauskas et al. 2012, Gu and Giraudo 2013). All the sema domain structures were solved by using plexin ectodomain constructs with multiple membrane proximal domains truncated. The C-termini of the two plexin molecules in these structures are placed away from each other. In full-length plexin, this distance could in principle be bridged by the membrane proximal domains, allowing the two cytoplasmic regions to interact and form an activating dimer that triggers intracellular signaling. On the other hand, these structures are also consistent with a model in which the semaphorin/plexin complex activates the plexin cytoplasmic region by driving dissociation of a pre-formed inhibitory dimer of this region. A recent study provided the first biochemical demonstration that plexin dimerization regulates its signaling activity (Figure 1-5). Engineered dimers of the plexin cytoplasmic regions from several plexin family members displayed dramatically

higher RapGAP activity than the corresponding monomers, supporting the model that activation of the plexin cytoplasmic region is triggered by dimerization (Figure 1-5) (Wang, He et al. 2012).

The discovery that plexin cytoplasmic regions form active dimers does not preclude the existence of a preformed inhibitory dimer, which is disrupted upon semaphorin binding. Both the extracellular and intracellular regions of plexins have been implicated in mediating inhibitory dimerization (Takahashi and Strittmatter 2001, Tong, Chugha et al. 2007, Tong, Hota et al. 2009, Nogi, Yasui et al. 2010). Further studies are required to elucidate the nature of an inhibitory oligomeric form of plexin on the cell surface and its role in plexin regulation.

Plexin Cytoplasmic Signal Transduction

The activating signal initiated by semaphorin binding propagates through plexin's multiple membrane proximal domains and the transmembrane helix to the cytoplasmic region inducing formation of an active cytoplasmic plexin dimer. The cytoplasmic region is responsible for triggering intracellular signaling cascades, which ultimately lead to a variety of cellular responses that underlie the biological functions of plexin. Therefore, the cytoplasmic region of plexin and proteins associated with it have been subjected to extensive investigations to elucidate the signaling mechanisms of plexin. The major plexin interacting proteins that are known to transduce plexin signals are reviewed below. The structural basis for activation of the cytoplasmic region of plexin upon semaphorin binding, however, remains obscure.

Plexin Cytoplasmic Interacting Proteins

For comprehensive discussions on the interactions between plexins and their intracellular binding partners, please refer to recent review articles (Gay, Zygmunt et al. 2011, Hota and Buck 2012). The focus here will be upon the GAP domain and the RBD of plexins, because they constitute the core signaling and regulatory components, and their mechanisms of action are better understood in light of recent structural studies.

Guanine Nucleotide Exchange Factors (GEFs)

Over 20 proteins have been reported to interact with the cytoplasmic region of plexins and contribute to signaling. Some plexin family members contain unique protein-interaction sites that mediate member-specific signaling pathways. For example, Class B plexins (PlexinB1, B2 and B3) specifically interact with two related GEFs, PDZ-RhoGEF and LARG (leukemia-associated RhoGEF) (Figure 1-1, 1-4B). The interaction is mediated by a conserved C-terminal "VTDL" motif in class B plexins and the PDZ (PSD-95, Dlg-1 and ZO-1) domains in PDZ-RhoGEF and LARG (Aurandt, Vikis et al. 2002, Driessens, Olivo et al. 2002, Hirotani, Ohoka et al. 2002, Perrot, Vazquez-Prado et al. 2002, Swiercz, Kuner et al. 2002, Oinuma, Katoh et al. 2003). The "VTDL" conforms to the consensus sequence for Type I PDZ ligands, which consists of three C-terminal residues "S/T-X-ϕ" where X and ϕ are any residue and any hydrophobic residue respectively. PDZ-RhoGEF and LARG recruited by Class B plexins activate RhoA, mediating an important branch of the signaling pathway (Worzfeld, Swiercz et al. 2014).

The structural basis by which plexins and the PDZ domains from these two GEFs achieve specificity, however, remains a mystery. The PDZ domains from both LARG and PDZ-RhoGEF bind to peptidic ligands promiscuously with similar or tighter affinity

than they bind peptides derived from B plexins (Smietana, Kasztura et al. 2008). In contrast, plexins have been shown bind tightly and specifically to these two PDZ domains in the physiological context (Aurandt, Vikis et al. 2002, Hirotani, Ohoka et al. 2002, Perrot, Vazquez-Prado et al. 2002). Understanding the basis of this specificity may require studies of the interaction in the context full-length plexin cytoplasmic regions.

Class A plexins interact with two other highly related GEFs FARP1 (FERM, RhoGEF, and pleckstrin homology domain protein 1) and FARP2 (Figure 1-4B) (Toyofuku, Yoshida et al. 2005, Zhuang, Su et al. 2009). FARP1 and FARP2 contribute to plexin-mediated dendrite growth and axonal repulsion, respectively. FARP2 has also been implicated in osteoprotection by Semaphorin3A/PlexinA1 (Hayashi, Nakashima et al. 2012). FARPs are normally autoinhibited by adopting a closed conformation that blocks the GEF active site (He, Kuo et al. 2013). The mechanism by which plexin binds FARPs and regulates their activity is not clear at present.

RhoGTPases

Two early studies implicated a role for Rac1 in semaphorin signaling (Jin and Strittmatter 1997, Kuhn, Brown et al. 1999). A series of later studies, through genetic association, yeast two-hybrid and biochemical co-purification, found that the insertion region between the two GAP-homology segments binds directly to some Rho family GTPases in a GTP-dependent manner (Rohm, Rahim et al. 2000, Vikis, Li et al. 2000, Driessens, Hu et al. 2001, Hu, Marton et al. 2001, Zanata, Hovatta et al. 2002, Oinuma, Katoh et al. 2003, Turner, Nicholls et al. 2004). A systematic survey has shown that the

RBD of PlexinB1 binds Rac1, Rac2, Rac3, Rnd1, Rnd2, Rnd3 and RhoD, but not RhoA, Cdc42, RhoG or Rif (Fansa, Dvorsky et al. 2013).

Binding of the RhoGTPases by plexin may sequester them from their effectors such as the PAK kinase, indicating that the RhoGTPases are downstream of plexin in the signaling pathway (Hu, Marton et al. 2001, Vikis, Li et al. 2002). However, the plexin/RhoGTPase interactions are rather weak, with the dissociation constant in the 3-40 μM range (Tong, Chugha et al. 2007, Hota and Buck 2009, Tong, Hota et al. 2009, Wang, Hota et al. 2011, Fansa, Dvorsky et al. 2013). It seems unlikely such a weak interaction can effectively compete with the RhoGTPase/effector interactions, which are often tighter. Over-expression of Rac1 has been shown to increase cell surface expression of plexin and its interaction with semaphorin, suggesting an inside-out signaling mechanism in which Rac1 acts as an upstream activator of plexin (Vikis, Li et al. 2002). The upstream role of Rac1 is further supported by a study showing that a constitutively active mutant of plexin is able to induce cell collapse independent of Rac1 (Turner, Nicholls et al. 2004). Strikingly, binding of over-expressed RND1 to plexin has been shown to trigger cell collapse in the absence of semaphorin, suggesting that RND1 is a more potent activator than Rac1 for plexin (Zanata, Hovatta et al. 2002). RND1 has also been shown to promote the interaction between PlexinB1 and PDZ-RhoGEF or LARG (Oinuma, Katoh et al. 2003). Intriguingly, although RhoD binds plexin with similar affinity, and presumably in the same mode as Rac1 and RND1, it strongly inhibits, rather than activates, plexin signaling (Zanata, Hovatta et al. 2002).

Structural analyses have revealed that the middle portion of the insertion region forms the RBD with an ubiquitin-like fold (Tong, Chugha et al. 2007, He, Yang et al.

2009, Tong, Hota et al. 2009). One side of the RBD is packed against the GAP domain, whereas the other side mediates the interactions with RhoGTPases (Figure 1-8). The RBD/RhoGTPase interface is dominated by interactions between a hydrophobic patch on the RBD and the switch II helix of the Rho GTPases in the GTP-bound active conformation (Bell, Aricescu et al. 2011, Wang, Hota et al. 2011, Wang, He et al. 2012). Binding of the RhoGTPases does not induce any significant conformational change to plexin (Bell, Aricescu et al. 2011, Wang, He et al. 2012). The bound RhoGTPase is located far away from the active site of the GAP domain, and is therefore unlikely to affect the GAP/Rap interaction directly (Figure 1-8). Consistently, activity assays in solution showed that the RhoGTPases do not alter the RapGAP activity of plexin either in the monomeric or the active dimer state (Wang, He et al. 2012). A model of plexin activation involving RhoGTPase-mediated oligomerization has been proposed (Bell, Aricescu et al. 2011), but existence of this oligomeric structure in solution or on the cell surface has not been established (Paduch, Biernat et al. 2007, Siebold and Jones 2013). These observations together suggest that the RhoGTPases may only regulate full-length plexin in the context of the cell membrane. Regulation of phospholipase C-beta by several elements has been proposed to rely on the membrane as the "conduit" of allostery (Charpentier, Waldo et al. 2014). The membrane may play a similar role in plexin regulation by the RhoGTPases.

RasGTPases

Since the discovery of the GAP domain in plexin over a decade ago, many studies have been devoted to identifying its small GTPase substrate and experimentally

demonstrating its catalytic activity (Kruger, Aurandt et al. 2005). The two studies that originally identified the GAP domain did not report GAP activity to any small GTPase (Rohm, Rahim et al. 2000, Hu, Marton et al. 2001). Later, a study showed that PlexinB1 is active specifically to the Ras homolog R-Ras but not Ras (Oinuma, Ishikawa et al. 2004). This study further showed that plexin signaling is critically dependent on inactivation of R-Ras. The GAP activity, assessed by the levels of GTP-bound R-Ras in cells expressing PlexinB1, appeared to rely on concomitant binding of plexin by both semaphorin and the RhoGTPase RND1. By using the crude membrane fraction of cells over-expressing PlexinB1, GAP activity towards R-Ras was also observed in vitro. The same group later found that the PlexinB1 GAP was also active to another Ras homolog, M-Ras (Saito, Oinuma et al. 2009). In contrast, Sakurai et al, using similar assays, failed to detect GAP activity of PlexinD1 to R-Ras, although binding between PlexinD1 and R-Ras was observed through co-immunoprecipitation (Sakurai, Gavard et al. 2010). Similarly, another study showed that the purified cytoplasmic region of PlexinB1 had no GAP activity towards R-Ras, while it displayed weak binding to R-Ras in a manner independent of the form of the bound nucleotide (Tong, Hota et al. 2009). More recently, Worzfeld et al provided strong in vivo genetic evidence that the developmental functions of PlexinB2 and PlexinD1 are not mediated by inactivation of R-Ras or M-Ras (Worzfeld, Swiercz et al. 2014).

A systematic analysis of most plexin family members from mouse demonstrated that the purified plexin cytoplasmic region displayed no GAP activity to either R-Ras or M-Ras (Figure 1-5) (Wang, He et al. 2012). Rather, these plexins displayed robust GAP activity to the Rap proteins, a distinct sub-family of Ras homologs (Figure 1-5B). There

are five members in the Rap sub-family: Rap1A, 1B, 2A, 2B and 2C. Rap1B and Rap2A were examined, and both responded to the plexin GAP. The RapGAP activity varies among different plexin family members, but in general is quite low when compared with the RasGAP activity of p120GAP. The low basal activity and its activation by dimerization are consistent with the role of plexin as an off/on signaling switch under the control of its semaphorin ligand. In addition, the low activity may be required for plexin to induce localized inhibition of Rap without perturbing the overall pool of active Rap in the cell, which is involved in many other signaling processes independent of the plexin pathway (Wang, He et al. 2012).

Importantly, the RapGAP activity of plexins can be stimulated by semaphorin in cells, and is required for plexin-induced neuronal growth cone collapse (Wang, He et al. 2012). GTP-bound Rap is an activator of integrin for promoting cell-matrix adhesion (Gloerich and Bos 2011). Taken together, these analyses establish that Rap is a bona fide substrate of the plexin GAP domain, and plexin-mediated Rap inactivation constitutes the core plexin signaling pathway. Inactivation of Rap by the plexin GAP would weaken integrin-mediated cell-matrix adhesion, contributing to repulsive axon guidance and other cell morphological changes. Moreover, Rap is known to inhibit RhoA activity through activating RhoGAPs (Yamada, Sakisaka et al. 2005, Jeon, Kim et al. 2010). Inactivation of Rap by plexin may relieve the inhibition on RhoA, leading to stress fiber formation and growth cone collapse.

A Non-Canonical RapGAP Catalytic Mechanism

The RapGAP activity of plexin was unexpected because the plexin GAP domain structurally belongs to the RasGAP family (Figure 1-4), and is unrelated to canonical RapGAPs. RasGAPs such as p120GAP all adopt the same structure fold and contain two conserved arginine residues critically required for facilitating GTP hydrolysis for Ras (Scheffzek, Ahmadian et al. 1997). One of the two arginine residues is termed the "arginine finger", which plays an essential role in catalysis by neutralizing the negative charge on the leaving γ-phosphate group. The second arginine residue stabilizes the conformation of the loop in which the arginine finger resides. Concomitantly, Ras provides in cis an essential catalytic residue, Gln61, which coordinates the nucleophilic water (Figure 1-9). All known RasGAPs also act on R-Ras and M-Ras using the same catalytic mechanism (Li, Nakamura et al. 1997, Scheffzek, Ahmadian et al. 1997, Scheffzek, Ahmadian et al. 1998, Quilliam, Castro et al. 1999, Ohba, Mochizuki et al. 2000, Padilla and Yeates 2003, Bos, Rehmann et al. 2007, Tong, Hota et al. 2009, Winn, Ballard et al. 2011). This is not surprising, as Ras, R-Ras and M-Ras are virtually identical in the regions that interact with the GAPs. Rap is a unique member in the Ras family, containing a threonine at position 61 that lacks the ability to coordinate a nucleophilic water (Figure 1-9). Canonical RapGAPs are structurally unrelated to RasGAPs and do not use an arginine finger for catalysis. Instead, they contain a conserved asparagine residue, referred to as the "asparagine thumb", which fulfills the water coordination role of Gln61 in Ras (Scrima, Thomas et al. 2008).

The plexin GAP domain structurally resembles RasGAPs and contains two conserved arginine residues but not an asparagine thumb, appearing unsuited for

facilitating GTP hydrolysis for Rap. The first clue to the catalytic mechanism of the plexin GAP came from a comparison of plexin with several GAPs that show dual GAP activity towards both Ras and Rap. These include SynGAP (Synaptic GAP), and three GAP1 family members RASAL (Ras-GTPase-activating-like protein), CAPRI (Ca^{2+}-promoted Ras inactivator) and $GAP1^{IP4BP}$ (tetrakisphosphate binding protein) (Krapivinsky, Medina et al. 2004, Kupzig, Deaconescu et al. 2006, Pena, Hothorn et al. 2008). The dual-specificity GAPs share the same domain fold and catalytic residues with the plexin GAP domain. They facilitate GTP hydrolysis for Ras using the same mechanism as p120GAP, but it was less clear how they act on Rap. Kinetic analyses of various structure-guided mutants of Ras, Rap, RASAL and $GAP1^{IP4BP}$ showed that Gln63 in Rap is critical for GTP hydrolysis catalyzed by the dual-specificity GAPs (Sot, Kotting et al. 2010). These analyses suggested that the dual-specificity GAPs induce a specific conformation of Rap, allowing Gln63 to adopt the catalytic role that is normally performed by Gln61 in Ras (Sot, Kotting et al. 2010). Mutating Gln63 in Rap abolishes GTP hydrolysis catalyzed by plexins, suggesting that they use the same Gln63-dependent catalytic mechanism(Wang, He et al. 2012).

Summary and Questions of Interest

The intracellular signaling events triggered following semaphorin/plexin engagement underlie a variety of essential processes. A mechanistic understanding of how plexins initiate many of these signaling events however, remains obscure. Most notably, (1) how plexin GAP domains catalyze the non-canonical GTP hydrolysis reaction for the Rap family of small GTPases, (2) how plexins are activated upon

dimerization, and (3) how plexins specifically recognize Rap remain mysteries. Additionally, it is unclear how the B family plexins are able to derive binding specificity for the PDZ domains of the two RhoGEFs known to bind B family plexins, Leukemia Associated RhoGEF and PDZ RhoGEF. These PDZ domains bind promiscuously to peptidic ligands, how plexin is able to specifically recruit these two PDZ domains in particular remains unclear. My thesis work answers these key questions. The development of the experimental tools required to complete these studies is also discussed.

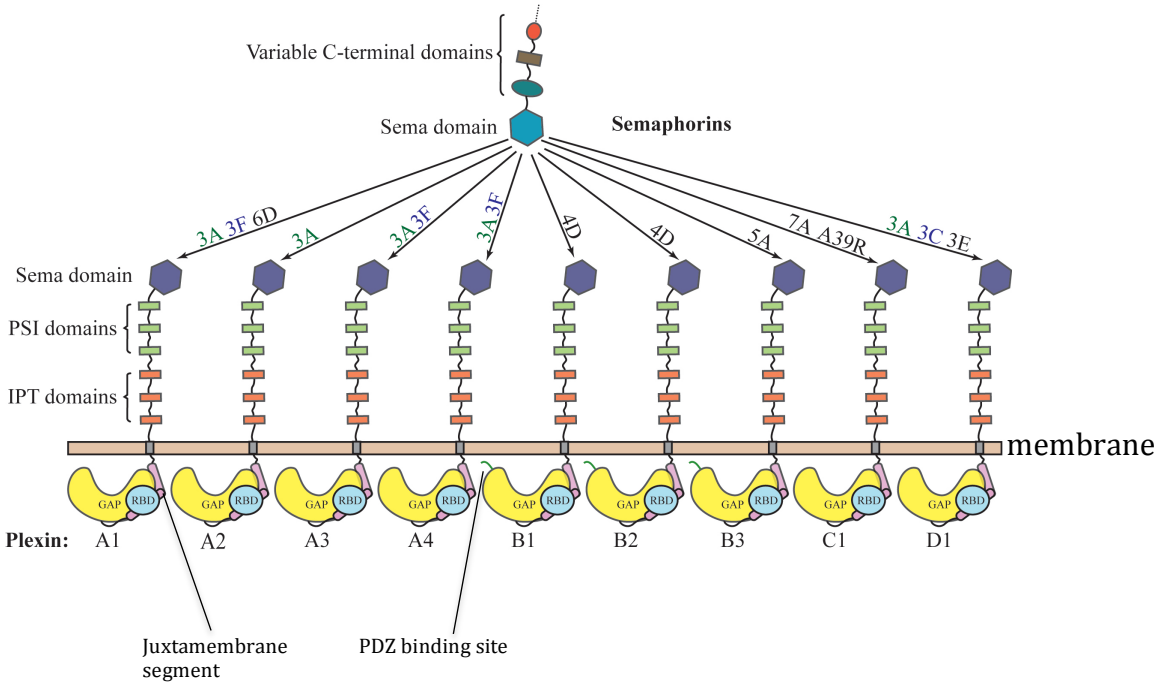

Figure 1-1. Semaphorin/plexin interactions and domain organization
Arrows and labels represent the semaphorin family members that interact with each plexin respectively. Green and blue semaphorin labels indicate the requirement for concomitant binding of neuropilin 1 or 2 respectively. The plexin intracellular juxtamembrane segment is colored in pink, the B family plexin PDZ domain binding site is colored green.

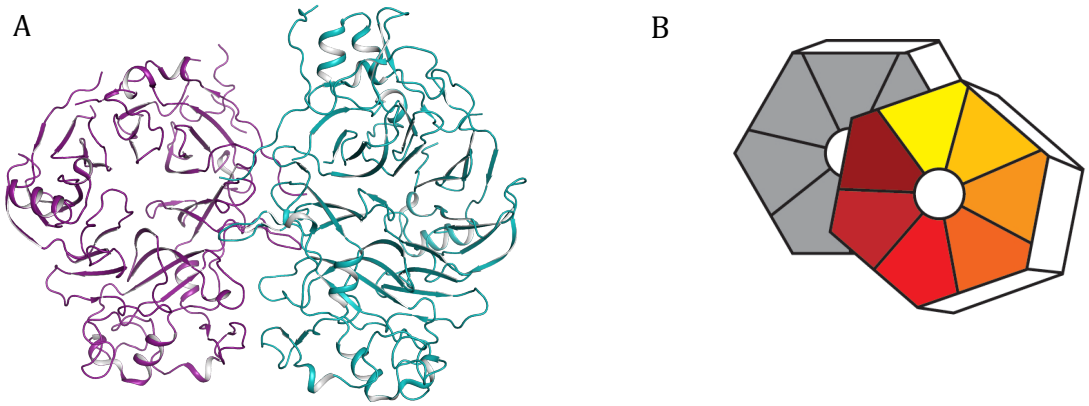

Figure 1-2. Crystal structure of the apo Semaphorin6A sema domain dimer
(A) The structure reveals the semaphorin sema domains adopt a staggered face-to-face dimer. The two sema domains are colored dark purple and teal respectively. PDB ID: 3AFC.

(B) The cartoon representation delineates each of the 7 beta strands in the sema domain as a different color and emphasizes their face-to-face interaction mode.

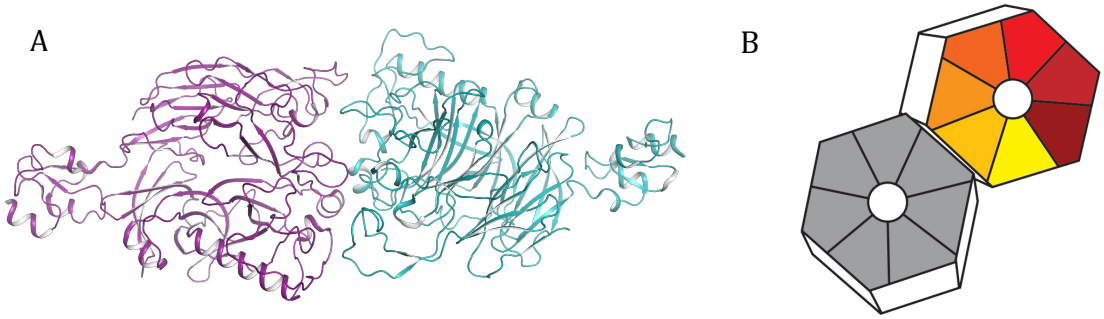

Figure 1-3. Crystal structure of the apo PlexinA2 sema domain dimer
(A) The structure reveals the PlexinA2 sema domains adopt a head-to-head dimer. The two sema domains are colored dark purple and teal respectively. PDB ID: 3AL9.

(B) The cartoon representation delineates each of the 7 beta strands as a different color and emphasizes the distinct head-to-head dimerization mode seen for plexin sema domains.

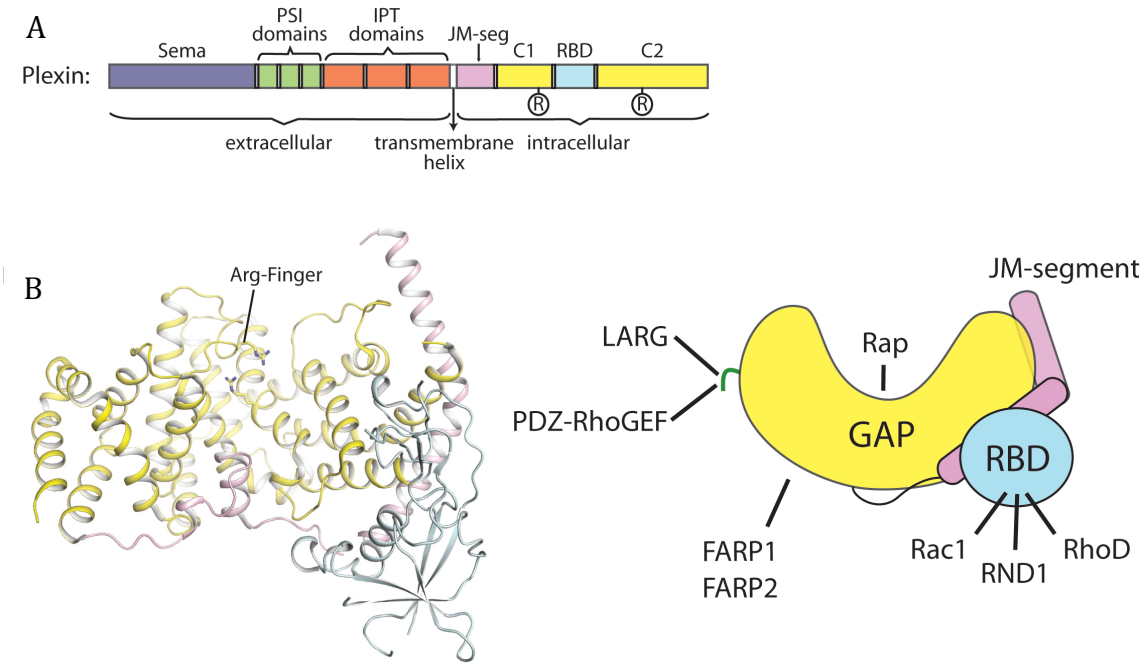

Figure 1-4. Overall structure of the plexin cytoplasmic region
(A) Domain organization of plexin. The cartoon describes the general architectures of plexin, with variations among different family members omitted.

(B) Structure of the cytoplasmic region of plexin. The structure of mouse PlexinA3 (PDB ID: 3IG3) is shown as a representative. The right panel shows a schematic of the structure. The color scheme is the same as in (A). The green line represents the C-terminal tail in class B plexins that interacts with LARG and PDZ-RhoGEF. The two GAP homology regions, C1 and C2 in (A), fold together to form one GAP domain. The two conserved arginine residues in the GAP domain are highlighted. The catalytic arginine finger residue is labeled “Arg-Finger”. JM-segment: juxtamembrane segment.

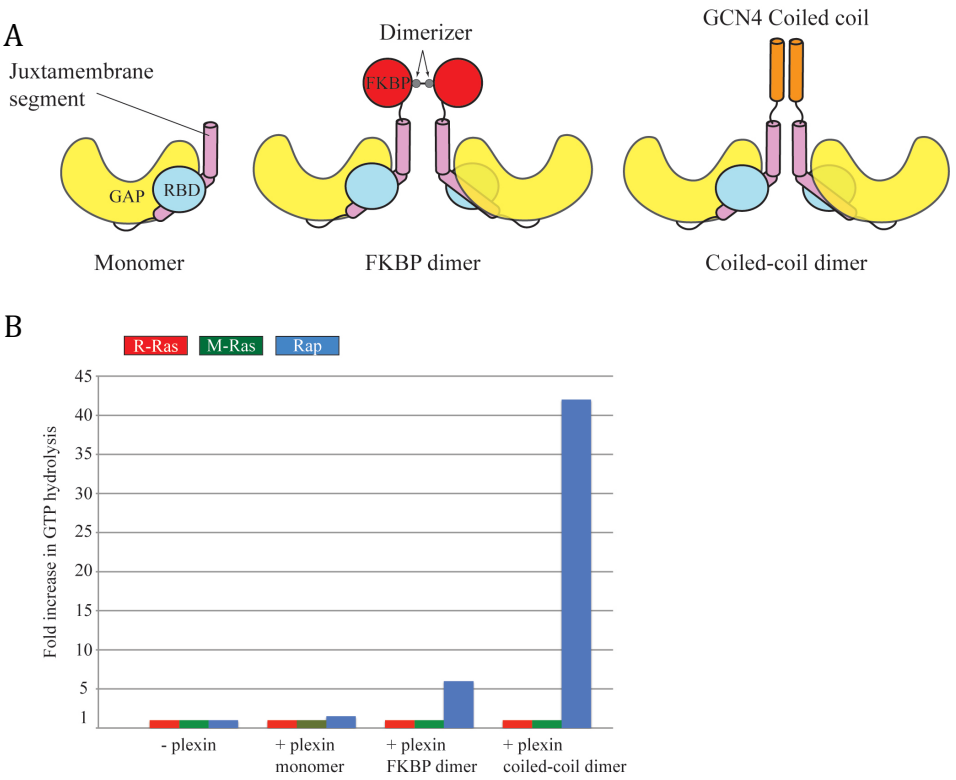

Figure 1-5. Plexin GAP activity towards Rap and Ras small GTPases
(A) Constructs of the plexin cytoplasmic regions used in GAP activity assays. Dimer constructs were generated by fusing the N-terminal Juxtamembrane segment of plexins to a constitutive (GCN4 coiled coil) or inducible (FKBP) dimerization motif through a flexible linker.

(B) PlexinA1 cytoplasmic regions display GAP activity only towards the Rap small GTPase. Activity is increased upon dimerization of the plexin cytoplasmic regions.

Note: The data used to generate the figures and plot above is found in Wang et al., 2012.

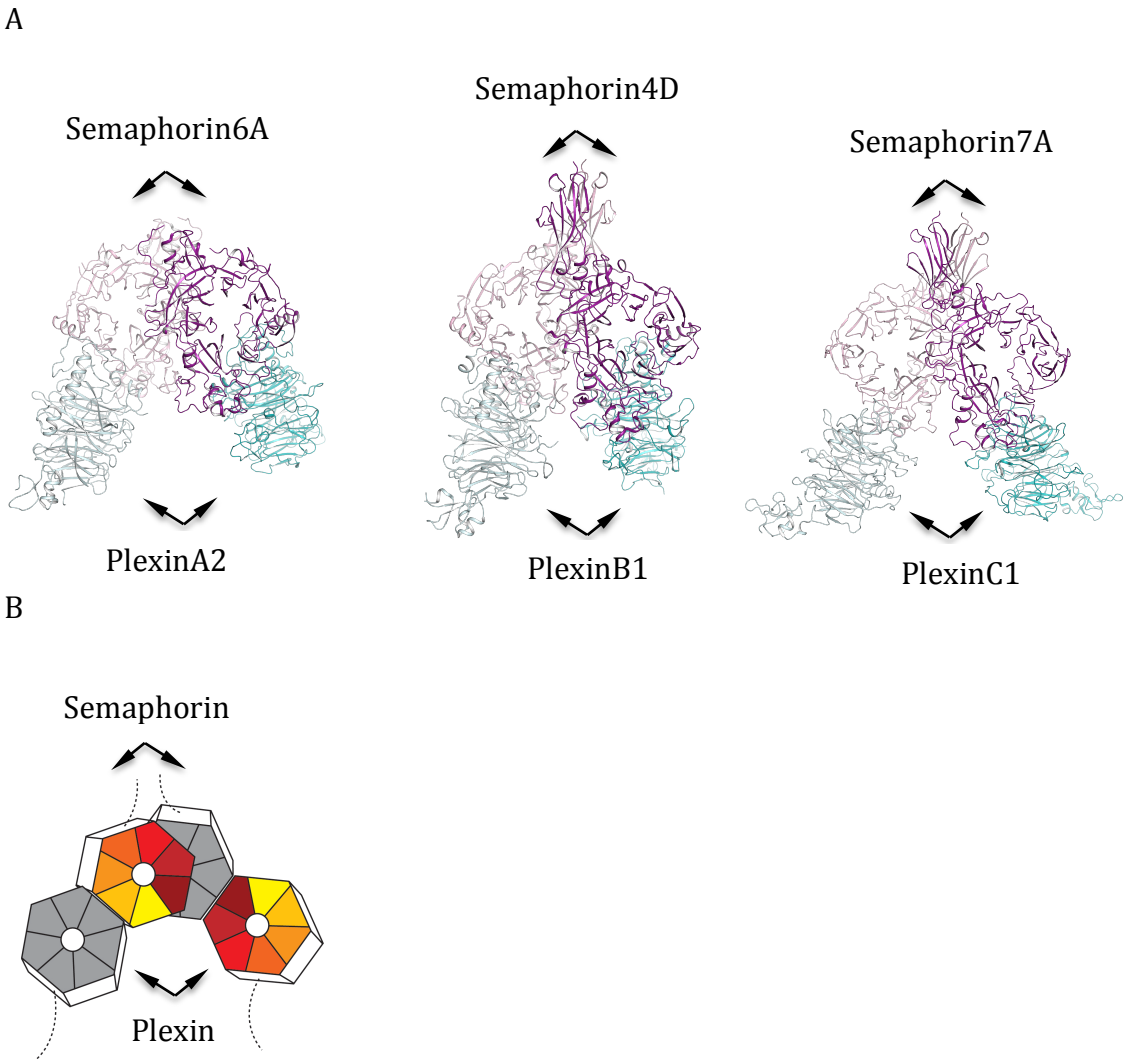

Figure 1-6. Crystal structures of the plexin/semaphorin sema domain complexes

(A) The structures reveal the semaphorin/plexin interaction mode is conserved. Additionally, the semaphorin sema domain dimer geometry is largely maintained before and after plexin binding. The head to head apo plexin dimer is lost upon semaphorin engagement. The head to head style interaction, however, is recapitulated with sema domains from semaphorin. Semaphorin sema domains are colored light pink and dark purple, plexin sema domains are colored light cyan and teal. PDB ID: 3AL8, 3OL2, 3NVQ

(B) The cartoon representation of the interaction delineates each of the 7 beta strands in plexin and semaphorin as a different color.

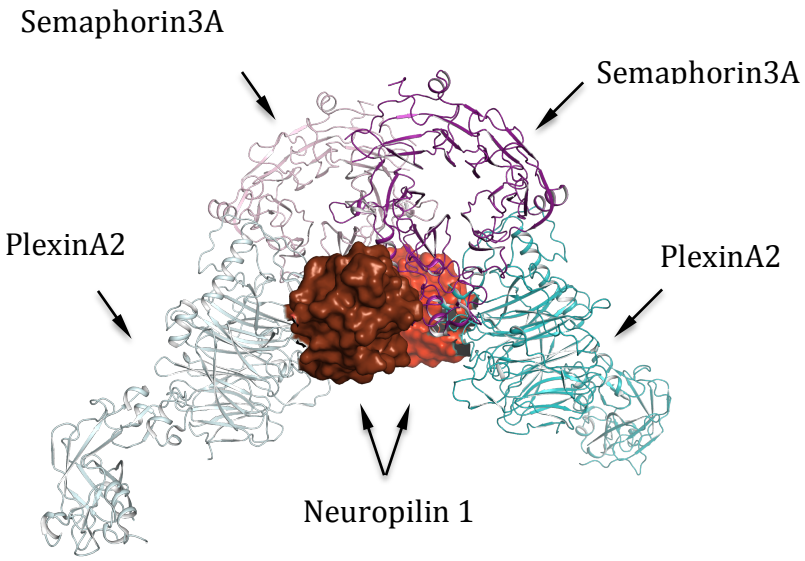

Figure 1-7. Crystal structure of the PlexinA2/Semaphorin3A/Neuropillin1 complex
The structure reveals that binding of Neuropilin does not alter the nature of the plexin/semaphorin interaction seen in Figure 1-6. Plexins and semaphorins are colored as in Figure 1-6, Neuropilin is colored brown or red and shown in surface. PDB ID: 4GZA.

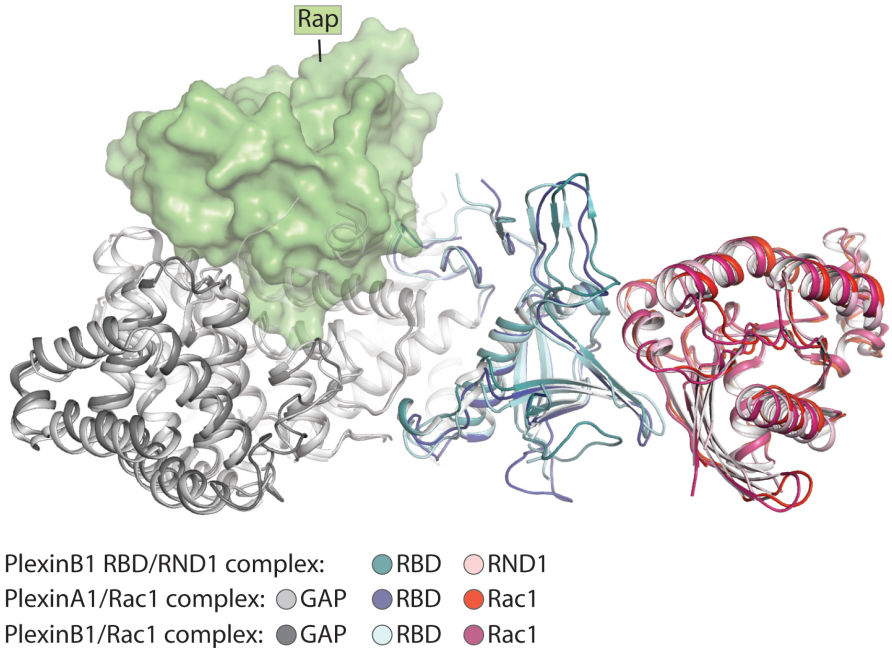

Figure 1-8. Interaction between the RhoGTPases and the plexin RBD
The structures of the PlexinA1/Rac1 complex (PDB ID: 3RYT), the PlexinB1/Rac1 complex (PDB ID: 3SUA) and the PlexinB1 RBD/RND1 complex (PDB ID: 2REX) are superimposed. Rap is modeled to indicate the location of the active site in the plexin GAP domain. It is clear that the RhoGTPases bound to the RBD are placed far away from the GAP active site.

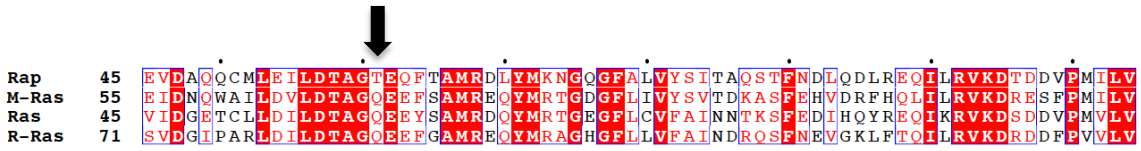

Figure 1-9. Sequence alignment of Rap and Ras small GTPases
Rap does not posses a catalytic glutamine residue at the 61 position. Instead it possesses a threonine, which is not competent to coordinate a nucleophilic water molecule. The black arrow indicates residue 61.

CHAPTER TWO

Sortase Mediated Ligation For Fusion Protein Production

Summary

Generating bioconjugates of proteins coupled to a variety of targets including: small molecules, affinity or solubility tags, matrices, cell surfaces, and other proteins has garnered a lot of attention in recent years. Several methods have been developed for this purpose, each with its own benefits and limitations. Structural biology is a field of research that continues to benefit greatly from these tools, as generating stable bioconjugates can be experimentally valuable. Fusion proteins for example, have been used in X-ray crystallography to produce critical lattice contacts that promote crystal formation. Fusion proteins have also been used in crystallography to promote the interaction of weakly associating proteins. NMR studies make frequent use of fusion proteins to attach solubility-enhancing tags to proteins of interest. Many fusion proteins, however, express poorly or are improperly folded, limiting their application. Here we describe the use of a bacterial transpeptidase, sortase, for the in-vitro generation of fusion proteins for use in X-ray crystallography and biochemical studies. Importantly, this method avoids the challenges of expressing fusion proteins from single gene constructs. We used this approach to covalently link the cytoplasmic regions of plexin to its substrate Rap for crystallization. This strategy was key to solving a crystal structure of a plexin/Rap complex, described in Chapter Four. Biochemical analysis of these fusion proteins demonstrates their interaction is promoted following fusion, which provides obvious advantageous for crystallography studies in general.

Introduction

Plexins (reviewed in Chapter One) are a large family of type I transmembrane receptors that serve as the primary receptors for the semaphorin family of repulsive axon guidance cues (Yazdani and Terman 2006, Tran, Kolodkin et al. 2007). The cytoplasmic regions of all plexins contain a GTPase Activating Protein (GAP) domain that is critical for plexin signal transduction as mutation of functionally important residues in the GAP domain abolish plexin mediated signaling (He, Yang et al. 2009, Wang, He et al. 2012). It was recently discovered that the GAP domains of plexins, despite being structurally and catalytically related to Ras GAPs such as p120, specifically catalyze the GTP hydrolysis reaction for the Rap family of small GTPases (Wang, He et al. 2012). This was an interesting discovery because plexin GAP domains do not posses the typical RapGAP fold or associated catalytic machinery, meaning they work on Rap through a non-canonical mechanism that remains poorly understood.

Plexin and Rap Interact Weakly in Solution

Motivated by the recent discovery of plexin's non-canonical GAP activity toward Rap, we sought to generate a crystal structure of the plexin cytoplasmic region in complex with Rap. Plexin GAP domains, however, interact weakly with Rap in solution and generating complexes stable enough to facilitate crystal formation appeared unlikely (Figure 2-1A). Indeed, extensive crystal screening efforts were undertaken using the cytoplasmic regions of various plexins ($plexin_{cyto}$) mixed with Rap family members without success. In an attempt to promote the interaction of $plexin_{cyto}$ and Rap in solution and hopefully facilitate crystal formation, single gene fusion constructs of

$plexin_{cyto}$ and Rap1B were generated with a 21 residue flexible linker connecting the proteins (Figure 2-1B). When covalently attached by a flexible linker, these proteins are effectively at saturating concentrations with respect to one another. In so far as the linker does not impose hindering restrictions on the geometry of the interaction, this approach should be an effective method for promoting interaction of plexin and Rap (Figure 2-1B). These proteins, however, were not well expressed and generating the amounts of protein necessary for structural studies was unfeasible.

Sortase Mediated Fusion of Plexin and Rap

In order to take advantage of the benefits plexin/Rap fusion proteins would have for crystallographic studies while avoiding the difficulties in expressing them as single gene fusion constructs, the bacterial transpeptidase sortase A was used. Sortases are found in many Gram-positive bacteria where they anchor proteins to the bacterial cell wall and are critical for pilin assembly. The *Staphylococcus aureus* sortase A (SrtA) recognizes the C-terminal amino acid motif "LPXTG" on one protein and an N-terminal "GG" motif on another protein where "X" is any amino acid, although natural substrates tend to posses a glutamic acid at this position. SrtA ligates these motifs together through a native peptide bond by first binding the C-terminal "LPXTG" motif (Figure 2-2A) (Popp, Antos et al. 2009). Binding positions the motif in proximity to a catalytic cysteine residue in the SrtA active site, which attacks the carbonyl group of the motif's threonine residue (Figure 2-3). This results in a SrtA/target-protein acyl intermediate product which further reacts with the nucleophilic N-terminal "GG" motif. Nucleophilic attack by the "GG" motif regenerates SrtA and results in the formation of a native amide bond

between the threonine of the C-terminal motif and the first glycine residue in the N-terminal motif (Figure 2-3) (Tian and Eriksson 2011). The mechanism is similar to that used by cysteine proteases except that water acts as the nucleophile in protease reactions. SrtA can also recognize the "LPXTG" motif within flexible loops provided steric restraints don't prevent binding to the active site (Popp, Antos et al. 2009, Proft 2010). It has also been observed that an additional C-termianl glycine residue improves ligation efficiency(Popp, Antos et al. 2009, Proft 2010). Consequently, "LPXTGG" motifs are frequently used.

Sortase Substrates and Constructs

Different bacteria possess sortase enzymes with differing substrate specificity. While SrtA from *Staphylococcus aureus* recognizes the "LPXTG" motif, the sortase from *S. pyogenes* (Sp-SrtA) can recognize both "LPXTG" as well as "LPXTA". Sp-SrtA can also utilize poly alanine N-terminal motifs in addition to poly glycine. While N-terminal poly alanine or glycine motifs are the native sortase substrates, various alkylamines have been reported to function as nucleophilic substrates as well. The efficiency of alkylamines as substrates, however, is diminished compared to the natural substrates (Kim, Siu et al. 2015).

Two soluble SrtA constructs are frequently described in the literature for use in ligations (Ton-That, Liu et al. 1999, Ilangovan, Ton-That et al. 2001). Both constructs possess N-terminal truncations of the signal peptide of 25 and 59 residues (SrtAΔ25 and SrtAΔ59) and replacement with a His_6 tag for ease of purification. SrtAΔ59 was used here.

Methods

Protein construct design and expression

To make use of the sortase system for generating $plexin_{cyto}$/Rap fusions, Rap1B constructs were generated with C-terminal Gly-Ser linkers of various lengths ranging from 0-26 residues and terminating in the "LPETGG" motif. Seven linkers in total were generated and used for ligation reactions: 0-residue ("LPETGG"), 11-residue (GGSGGSGSGSS-LPETGG), 14-residue (SGGSGSGSSGGSGS-LPETGG), 16-residue (GGSGGSGSGSSGGSGS-LPETGG), 21-resdiue (GGSGGSGSGSSGGSGSGGGSG-LPETGG), 24-residue (SGGSGSGSSGGSGSGGGSGSGSSG-LPETGG), and 26-residue (GGSGGSGSGSSGGSGSGGGSGSGSSG-LPETGG).

It is critical that SrtA be able to access the recognition motifs in order to catalyze the ligation reaction. The use of a linker may therefore be required in order to achieve ligation if the C-terminus of the target protein is tightly bound or otherwise sterically inaccessible. The necessity for a linker and its length, however, must be determined empirically on a case-by-case basis (Figure 2-2B). For use in crystallography experiments it is likely advantages to use the shortest linker possible, as flexible regions can be problematic for crystal formation.

The Rap constructs were generated using standard molecular cloning techniques and subcloned into a modified pET-28 vector (Novagen), which encodes an N-terminal His_6 tag with a cleavage site for the human rhinovirus C3 protease. The modified pET-28 vector originally encoded a glycine residue at the second amino acid position and a methionine in the first position. This results in exposure of an N-terminal glycine residue upon loss of the N-terminal methionine via naturally expressed methionine

aminopeptidases. This generates a Rap construct that would self ligate into polymers and severely hinder ligation efficiency of the desired reaction. The glycine residue within the vector was mutated to an aspartate using site directed mutagenesis. This example highlights the careful consideration that must be given to not only the protein but also the vector when designing constructs for the sortase reaction.

Pelxin$_{cyto}$ constructs with an N-terminal "GG" motif were generated using standard molecular cloning techniques and subcloned into a different modified pET-28 vector that encodes an N-terminal SUMO tag with a cleavage site for the Ulp1 protease. Upon treatment with the Ulp1 protease the N-terminal "GG" tag is exposed.

The incorporation of the C-terminal motif into the Rap constructs and the N-terminal motif into the plexin constructs was motivated by examination of the Ras/p120 complex crystal structure (Figure 2-4 and 2-5A). The structure reveals that the closest N-C terminus distance between Ras and p120 is located between the N-terminus of the GAP and C-terminus of Ras (Figure 2-4). This was expected to hold true for the Rap/plexin interaction as well given the structural similarities of the two GAPs and small GTPases. The choice of which protein will harbor the N and C-terminal motifs respectively should also be carefully considered using any structural information available.

In contrast to the difficulty of expressing plexin$_{cyto}$-Rap1B fusion constructs, plexin$_{cyto}$ and Rap1B individually express efficiently. The addition of the sortase motifs did not appear to impact expression efficiency. Please see Chapter Three for a detailed description of plexin$_{cyto}$ and Rap1B expression and purification procedures.

Ligation reaction

The ligation of GG-plexin$_{cyto}$ to His$_6$-Rap1B-LPETGG was accomplished by combining the two proteins at 69 and 450 μM respectively in the presence of SrtA at 25μM. The reaction was carried out in a reaction buffer containing 20 mM Tris pH 8, 150 mM NaCl, 10% glycerol, 2 mM $MgCl_2$, 2 mM DTT, and 10 mM $CaCl_2$. Note that calcium is a sortase cofactor and should be present in the reaction buffer to promote efficient ligation. This highlights another consideration for sortase-mediated ligations, buffer selection. While Tris was used here other common buffers are compatible with the reaction. Phosphate buffers however, should be avoided as calcium phosphate will precipitate out of solution and consequently deplete the calcium pool.

Reactions were dialyzed with stirring against 1 liter of reaction buffer for 3 hours at room temperature. At the end of the reaction, the extent of ligation can be assessed by SDS-PAGE electrophoresis with coomassie blue staining or immunoblotting. While 3 hours at room temperature was sufficient to complete the reaction for this protein pair, longer or shorter reaction times may be required to achieve complete ligation for other systems. Appropriate reaction times and temperatures should be determined empirically on a case-by-case basis. Also of note is that the poly glycine peptide byproduct of the ligation reaction is itself a nucleophilic competitor of subsequent reactions. Dialysis is performed to help remove the poly glycine byproduct and limit competition with subsequent reactions.

Using a molar excess of one of the proteins to be ligated provides a thermodynamic impetus to drive the reaction to completion with respect to the limiting reagent. Here the “LPETGG” tagged protein (Rap) was mixed at several fold molar

excess relative to the "GG" tagged protein (plexin). Rap was used in excess due to its relative ease of production. In general however, including an excess of the nucleophilic "GG" tagged protein is recommended in the literature (Kim, Siu et al. 2015).

Fusion protein purification

At the end of the reaction the unligated $plexin_{cyto}$ is removed from the sample by passing the reaction over a Ni-NTA column. The N-terminal His_6 tag on Rap1B allows for only unreacted Rap, and plexin that has been fused to Rap to be retained. To remove uncreated Rap a size exclusion column (GE Healthcare, Hi Load 160/600 Superdex200) was subsequently used. SDS-PAGE electrophoresis and Commassie blue staining was performed on the collected product, and the reaction was seen to have been successful (Figure 2-5B).

Fusions promote Rap/plexin interaction

To ensure the ligation process did not disrupt the ability of $plein_{cyto}$ and Rap1B to interact productively, the GAP activity of the $plexin_{cyto}$/Rap1B fusions was assessed and compared to that of unligated $plexin_{cyto}$ and Rap1B. If the fusion was successful, the GAP activity is expected to be higher for the fusion proteins as their covalent attachment should promote their association. Indeed a clear increase in the GAP activity of the fusion proteins relative to the unligated proteins at equimolar concentrations is seen (Figure 2-5C). The rate of phosphate release into solution was measured using a photometric assay. Please see Chapter Three for a detailed explanation of the GAP activity assay protocol.

Crystal screenings

The observation that the GAP activity of the fusion proteins was increased over that of the unligated proteins indicated that the fusions indeed promoted the interaction of plexin and Rap. Various $plexin_{cyto}$ family members were subsequently ligated to the Rap1B constructs of varying linker lengths. These constructs were subjected to crystallization screenings until a suitable construct was identified. Please see Chapter Four for a detailed description of the crystallization process and subsequent findings.

Troubleshooting

Inefficient ligation can be the result of numerous issues. The efficiency can however, usually be improved by making simple changes to the reaction protocol. The most serious problems will involve issues with construct design as discussed above. Varying the reaction time and temperature, however, are the two easiest parameters to adjust and can greatly effect the overall efficiency.

Additional sortase note

Although SrtA catalyzes only N-to-C ligation in the physiological context, recent work has demonstrated N-to-N and C-to-C ligations can also be accomplished. By incorporating an "LPXTG" motif conjugated to an azidohexanoic acid or an azadibenzocyclooctyne functional group, N-to-N or C-to-C ligations can be achieved through a cycloaddition reaction (Figure 2-6). This method makes any combination of ligations possible using the sortase system.

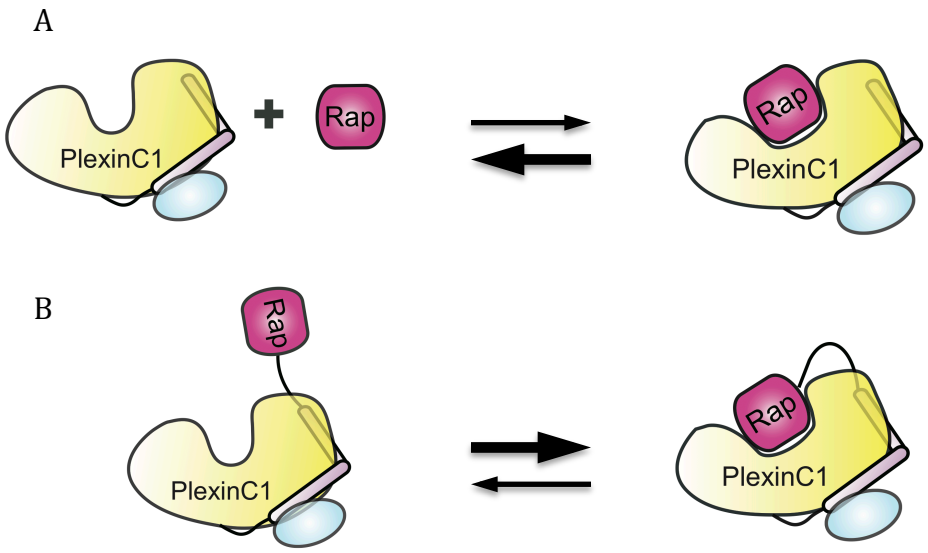

Figure 2-1. Fusion proteins promote interactions of fused proteins
(A) Plexin$_{cyto}$ and Rap interact weakly in solution. Consequently forming a stable plexin$_{cyto}$/Rap complex was a major challenge for early crystallization efforts. The GAP domain is colored in yellow, the juxtamembrane segment is colored in light pink, the Rho GTPase Binding Domain (RBD) is colored in cyan, an Rap is colored in dark pink.

(B) Fusion constructs of plexin$_{cyto}$ and Rap connected through a flexible linker keeps the two proteins in close proximity consequently promoting their interaction.

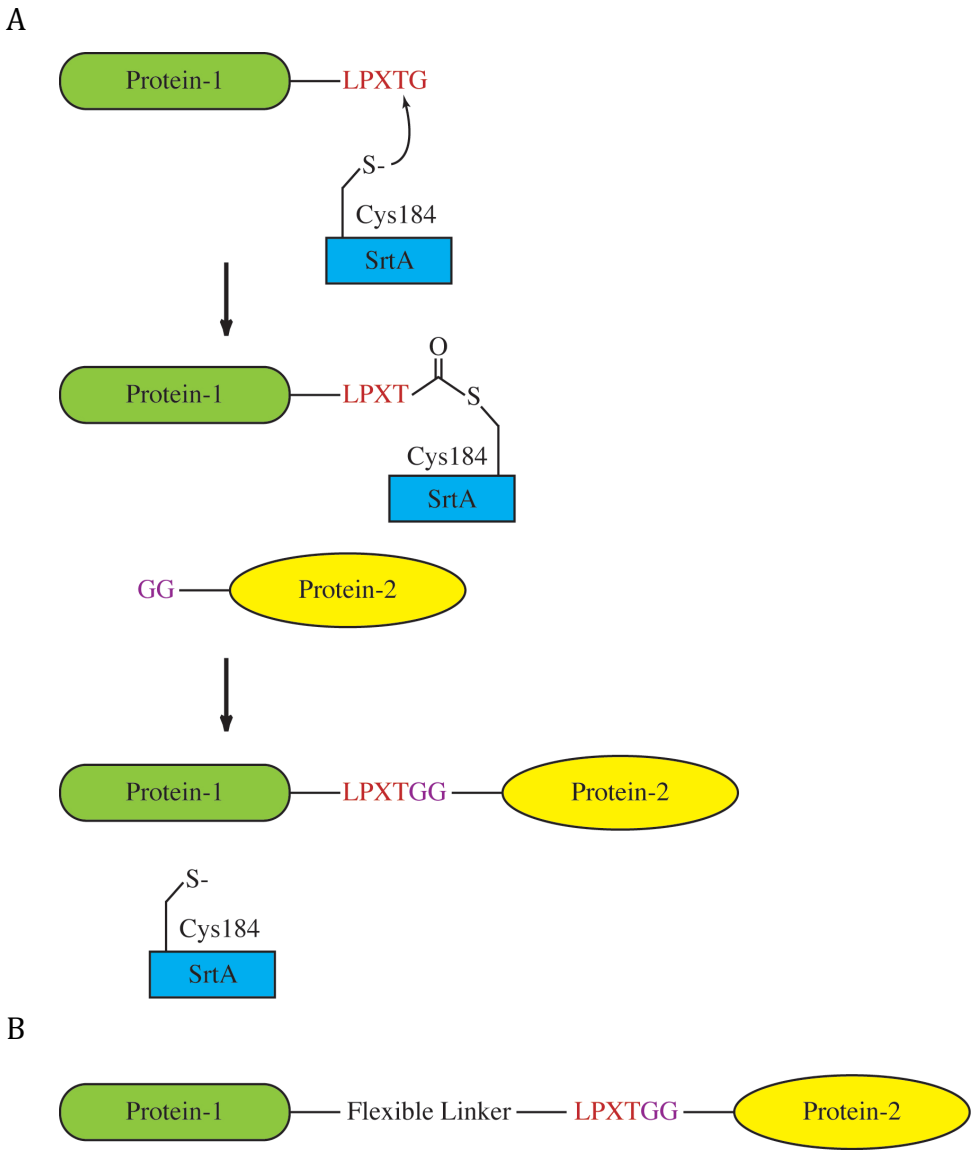

Figure 2-2. Sortase-mediated ligation reaction scheme
(A) The general reaction scheme for a sortase-mediated ligation is shown. Sortase is incubated with a target protein containing the C-terminal "LPXTG" motif and a probe protein containing the N-terminal "GG" motif. The reaction generates a native amide bond between the target and probe protein.

(B) It may be necessary to include a flexible linker between the target protein and the C-terminal motif to ensure accessibility of the motif.

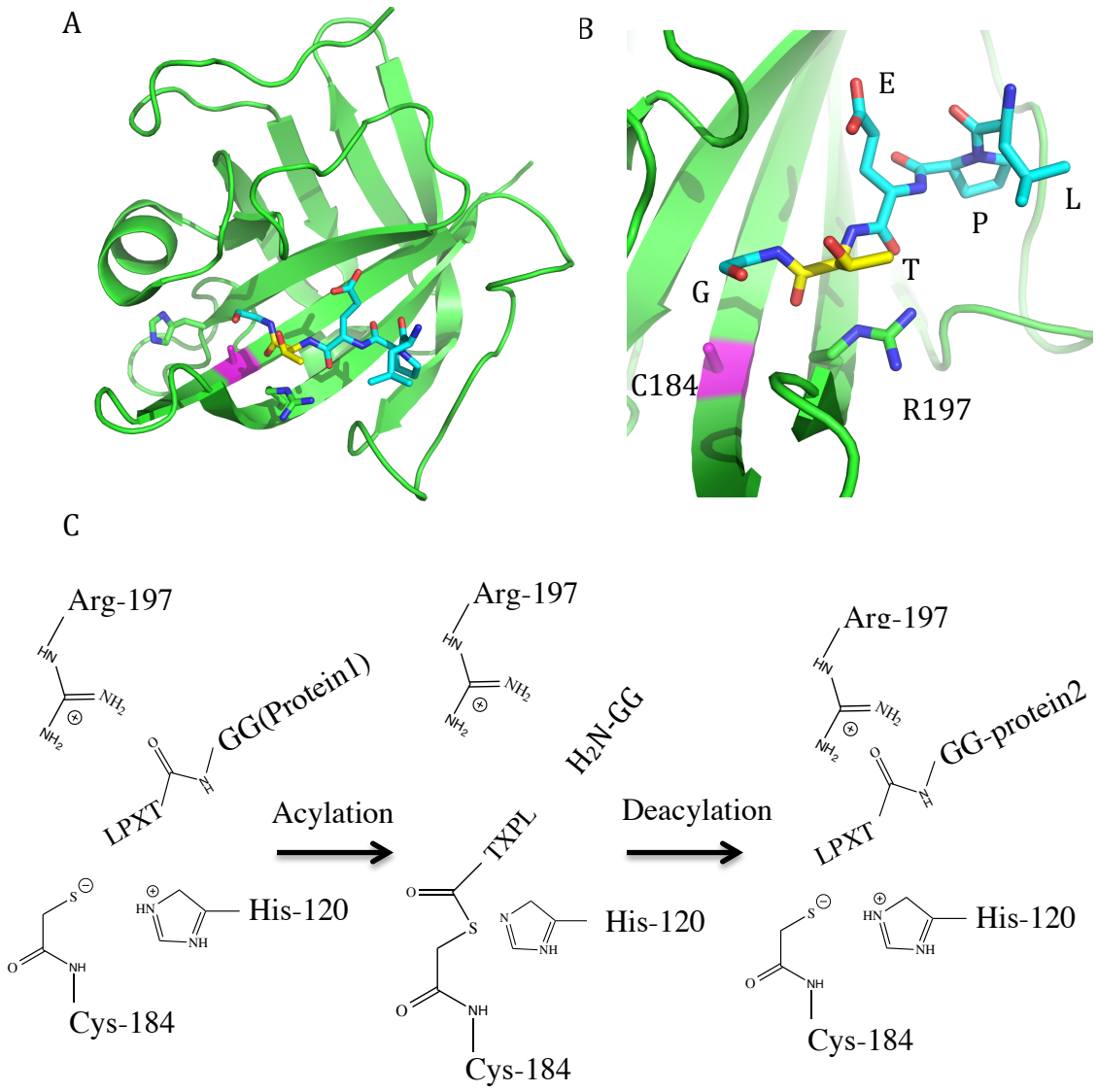

Figure 2-3. Sortase catalytic mechanism
(A) The crystal structure of SrtA from *Staphylococcus aureus* in complex with an "LPETG" peptide highlights the peptide binding mode and the location of the sortase catalytic triad (Cys184, Arg197, His120). The sortase enzyme is colored green and the catalytic triad residues are shown in stick representation. The catalytic Cys184 is mutated to alanine and is colored purple. The peptide is colored cyan and shown in stick representation. The threonine residue of the peptide, which is attacked during the reaction, is colored yellow. PDB ID: 1T2W

(B) A closer view of the SrtA active site shows that Cys184 is positioned appropriately to attack the carbonyl group of the peptide threonine residue.

(C) The mechanism utilized by sortase to achieve fusion is shown.

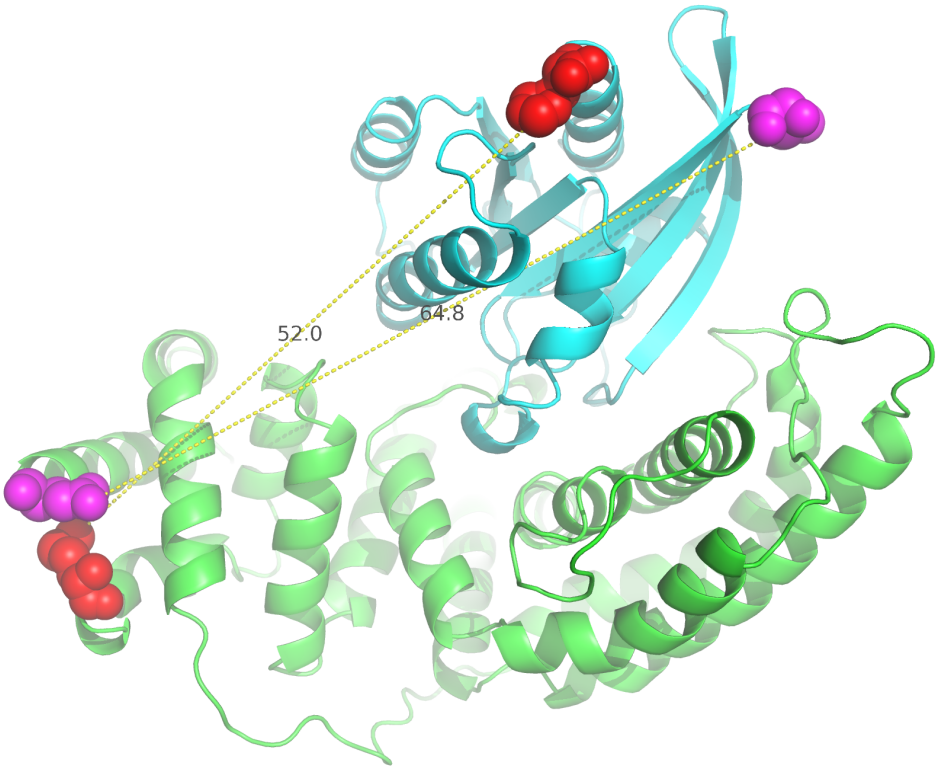

Figure 2-4. Structure of Ras/p120GAP complex
The crystal structure of p120GAP in complex with Ras is shown. The GAP is colored green and Ras is colored cyan. The yellow dashed lines indicate the two possible sortase-mediated N-C ligations. The residues involved are shown as spheres and colored red or purple. The minimum distances that a flexible linker would need to stretch to maintain the binding mode seen here are shown. Of the two possible ligations, the N-terminal residue of p120GAP and the C-terminal residue of Ras are closest at 52 Å. PDB ID: 1WQ1.

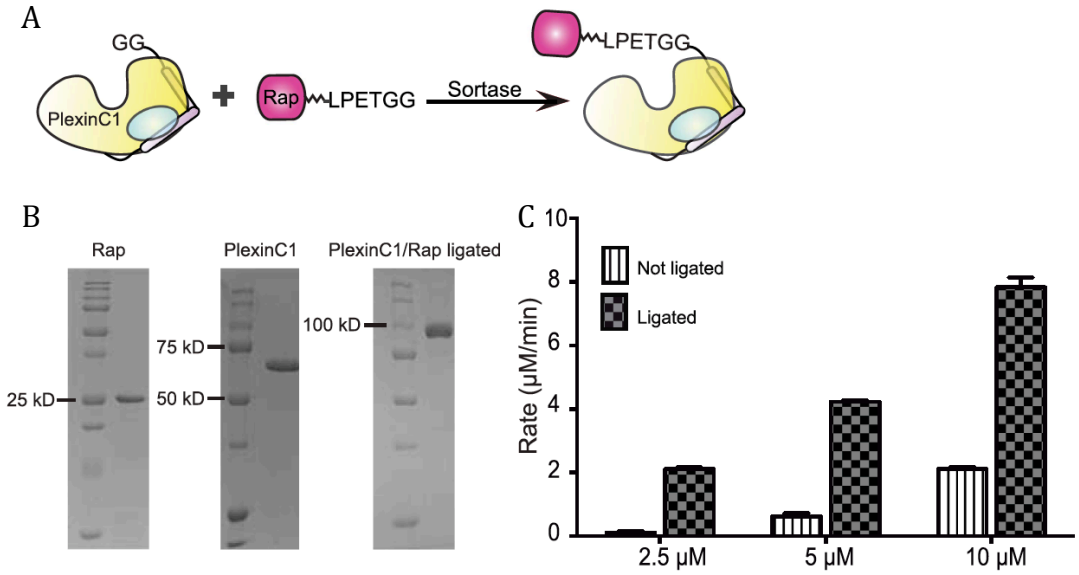

Figure 2-5. Plexin$_{cyto}$/Rap1B example ligation
(A) Scheme of the sortase-mediated ligation of PlexinC1$_{cyto}$ and Rap1B.

(B) Representative gel analyses of purified PlexinC1$_{cyto}$, Rap1B and the ligated PlexinC1$_{cyto}$/Rap1B complex.

(C) Comparison of the GTP hydrolysis activity between the ligated complex and the individual PlexinC1$_{cyto}$ and Rap1B proteins mixed at the same concentrations (2.5, 5 and 10 mM). The GTP hydrolysis rates are averages of three independent experiments. Error bars represent standard deviation of the mean.

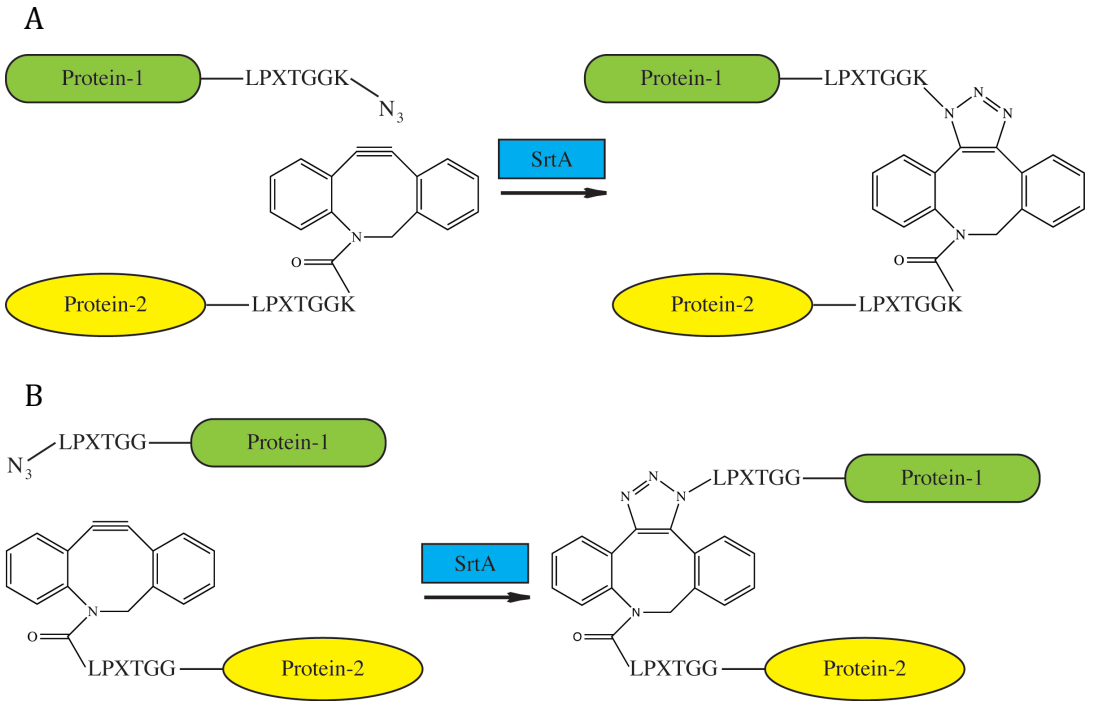

Figure 2-6. N-N and C-C sortase ligation strategies
(A) Schematic for generating C-C ligation products using cycloaddition.

(B) Schematic for generating N-N ligataion products using cycloaddition.

CHAPTER THREE

In Vitro Assay for the Rap GTPase Activating Protein Activity of the Purified Cytoplasmic Domain of Plexin

Summary

The ability to measure the GAP activity of the plexin intracellular region is a critical tool for studying plexin function. Many GAP activity measurements, however, can be difficult or time consuming and a convenient method for measuring plexin GAP activity has been lacking in the field. Here we describe the methods for expression and purification of the plexin cytoplasmic region in *E. coli*, and characterization of its GAP activity using a photometric assay. We also provide a protocol for measuring GAP activity of single-chain constructs with Rap covalently linked to the plexin cytoplasmic region. This method provides an easy and fast measurement of GAP activity for any plexin in-vitro. We employed this method frequently to investigate the structural basis for plexin GAP activity and substrate selectivity, described in Chapter Four.

Introduction

Plexins comprise a family of large cell surface receptors that bind the axon guidance molecules semaphorins and transduce their signal across the membrane (Yazdani and Terman 2006, Tran, Kolodkin et al. 2007, Sakurai, Doci et al. 2012). The plexin intracellular region contains a conserved GAP domain that is essential for function (Rohm, Rahim et al. 2000, He, Yang et al. 2009, Tong, Hota et al. 2009). Plexins relay the semaphorin signal, in part, by regulating the activity of the small GTPase Rap through the GTPase Activating Protein (GAP) domain (Wang, He et al. 2012).

Small GTPases such as Rap cycle between the GTP-bound active state and the GDP-bound inactive state. Two classes of proteins govern this cycle; GAPs accelerate the rate of GTP hydrolysis, while Guanine Nucleotide Exchange Factors (GEFs) promote exchange of nucleotide to allow GTP loading. The GAP domains of plexins are structurally related to RasGAP, but specifically catalyze GTP hydrolysis for Rap through a non-canonical mechanism (He, Yang et al. 2009, Sot, Kotting et al. 2010, Wang, He et al. 2012).

A quantitative in vitro RapGAP assay is important for rigorous characterization of the activity and regulation of plexin and will be utilized thoroughly in the studies related in subsequent chapters. The effects of dimerization or site-specific mutations on GAP activity, for example, can be directly assessed (Wang, He et al. 2012) The GTP hydrolysis reaction can be followed in vitro using radiolabeled nucleotide or fluorescent GTP analogs. These experiments, however, are often cumbersome or require the use of hazardous reagents. To characterize the GAP activity of plexins in vitro in a more convenient manner, we adopted the method described by Webb et al (Figure 3-1) (Webb 1992, Webb and Hunter 1992), which allows continuous monitoring of the GAP reaction photometrically. As the hydrolysis reaction proceeds, inorganic phosphate (P_i) is released as a byproduct. In the presence of free P_i, purine nucleoside phosphorylase (PNP) converts the guanosine analogue 2-amino-6-mercapto-7-methylpurine ribonucleoside (MESG) to its guanine base form (2-amino-6-mercapto-7-methylpurine) and ribose-1-phosphate. This reaction can be monitored photometrically by following the decay of absorbance at 320 nm (peak absorbing λ of MESG) and the increase in absorbance at 360 nm (peak absorbing λ of 2-amino-6-mercapto-7-methylpurine). With

only a handful of reagents and a desktop UV-Vis spectrophotometer, plexin catalyzed GTP hydrolysis by Rap can be easily monitored in real time.

This assay can be employed to monitor GTP hydrolysis for either single or multiple-turnover reactions (Webb 1992, Webb and Hunter 1992). For single-turnover reactions, GTP bound Rap is mixed with the plexin cytoplasmic region. Each Rap molecule carries out one hydrolysis reaction upon GAP binding. In the absence of a Rap GEF, the GDP bound Rap cannot exchange nucleotide for additional hydrolysis reactions. Multiple-turnover reactions can be achieved by addition of excess GTP and a small amount of ammonium sulfate and EDTA to the assay buffer. Ammonium sulfate and EDTA together mimic the activity of a Rap GEF by slightly destabilizing Rap and chelating its magnesium cofactor. Nucleotide is continuously exchanged until Rap has consumed all the excess GTP in solution.

Materials

All solutions are prepared with ultrapure water and analytical grade reagents. All pH adjustments are performed at room temperature unless otherwise stated. Store solutions at room temperature unless otherwise stated.

1.1. Reagents for protein expression

1. cDNA for plexins and Rap1B: cDNA could be obtained from OpenBiosystems (Part of ThermoFisher).
2. Expression vector: we used a modified pET-28 vector (Novagen), in which the original thrombin protease recognition site and T7 tag are replaced by a recognition

site for the human rhinovirus C3 protease (PreScission Protease from GE Healthcare) (Wang, He et al. 2012). The original pET-28 vector or similar expression vectors with an N-terminal His_6-tag could also be used.

3. *E. coli* cells for protein expression: ArcticExpress (Stratagene), BL21 (DE3).
4. LB plate: dissolve 10 g tryptone, 5 g yeast extract, 10 g NaCl, and 15 g agar in 900 mL water. Adjust pH to 7.0. Bring the pH-adjusted solution to 1 L with water and autoclave. Cool to approximately 55 °C. Add kanamycin to 50 μg/mL. Pour media into 10 cm plates. Store at 4 °C.
5. LB medium: dissolve 10 g tryptone, 5 g yeast extract, and 10 g NaCl in 900 mL water. Adjust pH to 7.0. Bring the pH-adjusted solution to 1 L with water and autoclave. Cool to room temperature prior to use. Supplement with 50 μg/mL kanamycin and 20 μg/mL gentamycin when instructed.
6. Basic TB (Terrific Broth) medium: dissolve 12 g tryptone, 24 g yeast extract and 4 mL glycerol in 900 mL water and autoclave.
7. 10x TB salt: dissolve 23.1 g KH_2PO_4 and 121.54 g K_2HPO_4 in 1 L water and autoclave.
8. Complete TB medium: combine 900 mL basic TB medium, 100 mL 10x TB salt, 2 mL 2 M $MgSO_4$, 50 mg kanamycin powder.
9. 2 M $MgSO_4$: dissolve 24.07 g $MgSO_4$ in 100 mL water and autoclave.
10. 1 M IPTG (isopropylthio-β-D-galactoside): dissolve 2.38 g IPTG powder in 10 mL water. Aliquot and store in -20ºC.

1.2. Reagents for protein purification

1. Lysis buffer: 50 mM Tris-HCl, pH 8.0, 500 mM NaCl, 20 mM Imidazole. Add β-mercaptoethanol to 3 mM final concentration immediately before use.
2. Ni-A buffer: 10 mM Tris-HCl, pH 8.0, 500 mM NaCl, 20 mM Imidazole, 5% Glycerol. Add β-mercaptoethanol to 3 mM final concentration immediately before use.
3. Ni-B buffer: 10 mM Tris-HCl, pH 8.0, 500 mM NaCl, 250 mM Imidazole, 5% Glycerol. Add β-mercaptoethanol to 3 mM final concentration immediately before use.
4. Q-dilution buffer: 10 mM Tris-HCl, pH 8.0, 10% Glycerol. Add dithiothreitol (DTT) to 2 mM final concentration immediately before use.
5. Q-A buffer: 10 mM Tris-HCl, pH 8.0, 10 mM NaCl, 5% Glycerol. Add DTT to 2 mM final concentration immediately before use.
6. Q-B buffer: 10 mM Tris-HCl, pH 8.0, 1 M NaCl, 5% Glycerol. Add DTT to 2 mM final concentration immediately before use.
7. A peristaltic pump is used to load bacteria lysate to a nickel column for affinity purification.
8. AKTA FPLC (GE Healthcare). (*see* **Note 1)**
9. 1 mL Histrap FF nickel column (GE healthcare)
10. UNO Q1 anion exchange column (Bio-Rad).
11. High-pressure cell disruptor (Avestin)
12. 0.45 μm nylon filter
13. PreScission Protease (GE Heathcare)
14. 10 kD molecular weight cut-off concentrators (Amicon)

15. 50 kD molecular weight cut-off concentrators (Amicon)

1.3. Reagents for GAP activity assay

1. 2x assay buffer: 100 mM Tris-HCl, pH 7.6, 100 mM NaCl, 2 mM $MgCl_2$, 20% Glycerol. Add 2 mM DTT immediately before use. (*see* **Note 2**)
2. 4 mM MESG stock solution: dissolve 25 mg MESG powder (Berry & Associates) into 20 mL water. Aliquot ~500 µL per tube and freeze in -80 ºC. (*see* **Note 3**)
3. 200 unit/mL PNP stock solution: Dissolve PNP (lyophilized powder, Sigma) in 1x assay buffer to 200 unit/mL. Centrifuge the solution at 14,000 g in 4 ºC for 10 min to remove insoluble materials, aliquot and store the stock solution in -80 ºC.
4. 25 mM GTP pH 7.0: dissolve GTP powder (Sigma) into water and slowly adjust the pH of the solution by adding small amount of 1 M NaOH. (*see* **Note 4**)
5. 100 mM ammonium sulfate: dissolve 1.32 g ammonium sulfate in water to a total volume of 100 mL.
6. 50 mM EDTA pH 8.0: dissolve EDTA in water by slowly adding 1M NaOH to adjust the pH of the solution. The solubility of EDTA increases as the pH increases.
7. SpectraMax Plus^{384} UV-Vis spectrophotometer (Molecular Devices). Any UV-Vis spectrophotometer capable of performing time course measurement of absorbance at 360/320 nm could be used.
8. 100 µL quartz crystal cuvette with 1 cm path length (Precision Cells Inc.).

Methods

2.1. Cloning and expression of plexin cytoplasmic region (plexin$_{cyto}$)

1. Amplify via polymerase chain reaction (PCR) the coding sequence for plexin$_{cyto}$ (*see* **Note 5)**.
2. Clone the amplified fragment into the modified pET28 vector using standard molecular biology techniques (Lorenz 2012). A STOP codon is included in the C-terminus of the plexin$_{cyto}$ coding sequence. The resulting recombinant protein is plexin$_{cyto}$ with an N-terminal His$_6$-tag and a PreScission protease recognition site, allowing removal of the His$_6$-tag after affinity purification (Wang, He et al. 2012).
3. Transform the plasmid into ArcticExpress cells. Use one vial of the competent cells and follow the instructions provided by the manufacturer. (*see* **Note 6**)
4. Spread the transformed bacteria onto one LB plate containing 50 µg/mL kanamycin and incubate at 37 ºC overnight.
5. The next day, pick multiple colonies and start an overnight culture in 100 mL LB medium supplemented with 50 µg/mL kanamycin and 20 µg/mL gentamycin in a 37 ºC shaker, 220 rpm.
6. Aliquot 1 L of the complete TB medium into each of three 1 L flasks. Inoculate each flask with 30 mL overnight culture from Step 5. (*see* **Note 7**)
7. Incubate culture in a shaker at 30 ºC, 220 rpm. Take $OD_{600\ nm}$ measurements of the culture until it reaches the range of 2.0-2.5. Pre-cool another shaker to 10 ºC for induction. Usually it takes 5-8 hr for the culture to reach the desired OD. (*see* **Note 8**)
8. Cool down the flasks containing the culture from Step 7 in an ice bath for 30-60 min.
9. Add 100-500 µL 1M IPTG solution to each flask for a final concentration of 100-500 µM. (*see* **Note 8**)
10. Incubate the flasks in the 10 ºC shaker, 220 rpm for 24 hr.

11. Transfer culture into a centrifuge bottle. Pellet cells by spinning at 5000 g for 15 min at 4 ºC.

2.2. Cloning and expression of Rap1B GTPase.

1. Amplify via polymerase chain reaction (PCR) the coding sequence for the G domain of human Rap1B (residues 2-167), without the C-terminal tail that is unstructured and likely affects protein expression level.
2. Clone the amplified fragment into the modified pET-28 vector as described above. A STOP codon is included in the C-terminus of Rap1B. The recombinant protein is Rap1B with an N-terminal His_6-tag and a PreScission protease recognition site, allowing removal of the His_6-tag after affinity purification (Wang, He et al. 2012).
3. Transform the pET-28 Rap1B vector into BL21(DE3) cells. Use one vial of the competent cells and follow the instructions provided by the manufacturer. (*see* **Note 6**)
4. Spread the transformed bacteria onto one LB plate containing 50 µg/mL kanamycin and incubate at 37 ºC overnight.
5. The next day, pick multiple colonies and start an overnight culture in 100 mL LB medium supplemented with 50 µg/mL kanamycin in a 37 ºC shaker, 220 rpm.
6. Aliquot 1 L of the complete TB medium into each of three 1 L flasks. Inoculate each flask with 30 mL overnight culture from Step 5. (*see* **Note 7**)
7. Incubate culture in a shaker at 37 ºC, 220 rpm. Take $OD_{600\ nm}$ measurement of the culture until it reaches the range of 2.0-2.5. Pre-cool another shaker to 16 ºC for induction. Usually it takes 3-5 hr for the culture to reach the desired OD.
8. Cool down the flasks from Step 7 in an ice bath for 30-60 min.

9. Add 500 μL 1 M IPTG solution to each flask for a final concentration of 500 μM.
10. Incubate the flasks in the 16 ºC shaker, 220 rpm for 16-18 hr.
11. Transfer culture into a centrifuge bottle. Pellet cells by spinning at 5000 g for 15 min in 4 ºC.

2.3. Purification of plexin$_{cyto}$ and Rap1B

All purification steps are conducted at 4 °C. Plexin$_{cyto}$ and Rap1B are purified using the same protocol unless specified otherwise. For all the purification steps of Rap1B, 2 mM $MgCl_2$ is added to the buffers to stabilize the nucleotide bound state of the protein.

1. Resuspend the cell pellet in Lysis buffer by vigorous vortexing. Use 50 mL Lysis buffer per 1 L of expression culture. Resuspended cells can be stored in -80 ºC for later purification if desired.
2. Lyse resuspended cells using a high-pressure cell disruptor with a peak cycling pressure of ~ 50,000 kPa. Pass the lysate through the cell disruptor 3-5 times to ensure complete lysis.
3. Clear cell debris by centrifuging the lysate at 17,000 *g* for 1 hour at 4 °C.
4. Decant the supernatant and discard the pellet.
5. Vacuum filter the supernatant through a 0.45 μm nylon filter.
6. Equilibrate a Histrap FF nickel column with at least 5 column volumes of Ni-A buffer. For 3 L of bacteria culture, a 1 mL Histrap FF column should be used as a starting point. Using a larger volume column may result in a significant increase in non-specific binding of impurities.

7. Use a peristaltic pump to load the filtered supernatant to the nickel affinity column. Set the flow rate though the column according to the recommendation from the manufacturer. Collect the flow through as the column is loaded. (*see* **Note 9**)
8. Wash the loaded nickel column with ~50 column volumes of Ni-A. Collect this wash.
9. Elute the bound plexin with ~ 20 column volumes of Ni-B buffer. Collect the eluted protein.
10. To ensure the proteins are expressed and purified, run an SDS-PAGE gel (12-15% acrylamide) with samples from the loading flow through, the Ni-A wash, and the Ni-B eluent. $Plexin_{cyto}$ and Rap1B will be a dominant band in the eluents at about 70 kD and 20 kD, respectively.
11. (Optional) The N-terminal histidine tag does not affect the GAP activity assay but may be removed at this point by addition of PreScission to the Ni-B eluent. Incubate overnight at 4 °C and then proceed to Step 12.
12. Concentrate the Ni-B eluent to 500 μL using Amicon 50 kD and 10 kD molecular weight cut-off concentrators for $plexin_{cyto}$ and Rap1B, respectively. Centrifuge the concentrated eluent for 10 min at 20,000 g in 4 ºC. Collect the supernatant and dilute into 10 mL Q-loading buffer.
13. Equilibrate a 1 mL anion exchange column with Q-A buffer.
14. Load the 10 mL protein sample from Step 12 to the anion column.
15. Program the FPLC to run a 20-column volume NaCl gradient (10-1000 mM) using buffers Q-A and Q-B. Collect 1 mL fractions throughout the elution.

16. Run an SDS-PAGE gel to identify the protein containing fractions. Combine those fractions.
17. Concentrate the protein solution to 100-500 μL using Amicon concentrators.
18. Determine the protein concentration by measuring the absorbance at 280 nm. The extinction coefficients of the proteins can be calculated from the sequences. For measuring Rap1B concentration, the extinction coefficient of the bound guanine nucleotide at 280 nm (7765 cm^{-1} M^{-1}) should also be taken into account.
19. Flash freeze any protein to be saved for an extended period in liquid nitrogen and store at -80 °C.

2.4. GAP activity assay of plexin$_{cyto}$: Single-turnover GAP activity assay

Reactions are carried out at room temperature in a 100 μL quartz crystal cuvette with 1 cm path length. Reagent volumes listed below assume 100 μL total reaction volume.

1. If plexin$_{cyto}$, Rap1B and PNP are stored frozen, thaw them quickly at room temperature and then spin at 20,000 g for 10 min at 4 ºC. Transfer the supernatant to a new centrifuge tube. This is to remove any protein aggregation/precipitation formed during freezing/thawing, which will interfere with the absorbance measurement. After this step, keep stock protein solutions on ice. MESG stock solution should also be thawed quickly and kept on ice.
2. Calculate the amounts of stock protein solutions to be used. We recommend the following final concentrations as a starting point: plexin$_{cyto}$ (1-10 μM), Rap1B (100 μM), MESG (300 μM), PNP (8 unit/mL). 50 μL 2x assay buffer is used for each

reaction. Calculate the volume of H_2O to be added to bring the total volume to 100 µL. (*see* **Note 10**)

3. Setup the spectrophotometer to record absorbance at 360 nm and 320 nm every 5 seconds. If the spectrophotometer cannot measure two wavelengths simultaneously, set the wavelength to 360 nm. (*see* **Note 11**)
4. Mix all the components except $plexin_{cyto}$ in the cuvette. Start measurement of the baseline for about 1 min. The baseline of $OD_{360\ nm}$ should be slightly increasing at about 2-5 mOD/min, due to slow intrinsic hydrolysis of GTP bound to Rap.
5. Add $plexin_{cyto}$ or the buffer as the control and mix quickly but thoroughly. Continue measurement of the reaction for 5-10 min (Figure 3-2A). (*see* **Note 12**)

2.5. GAP activity assay of $plexin_{cyto}$: Multiple-turnover GAP activity assay of $plexin_{cyto}$

$Plexin_{cyto}$ and Rap1B interact with low affinity in vitro, making some biochemical and biophysical experiments difficult. In order to promote the association of proteins that interact with low affinity, fusion proteins are frequently used as described in Chapter Two. Fusing $Plexin_{cyto}$ and Rap1B helps promote their association. When generating $Plexin_{cyto}$ / Rap1B fusions, characterizing the GAP activity of the protein is useful both in terms of analyzing whether the fusion protein retains function and if so how the catalytic rate compares to the non-fused proteins as well as other fusion constructs. Assaying the GAP activity of fusion proteins in vitro requires an altered protocol to that used for single-turnover reactions (Method 3.4). When $Plexin_{cyto}$ and Rap1B are fused, Rap1B is always in the vicinity of its GAP and cannot remain in the GTP-bound state, preventing

activity measurement using the single-turnover assay. This problem is addressed by measuring the GAP activity with a multiple-turnover assay where the fused Rap1B can exchange nucleotide and undergo multiple hydrolysis reactions. This is accomplished by the addition of ammonium sulfate, EDTA, and excess GTP to the reaction buffer. The presence of ammonium sulfate and EDTA help destabilize the interaction between Rap and the nucleotide, allowing release of the bound nucleotide and re-binding of the excess GTP. As listed for Method 3.4, reactions are carried out at room temperature in a 100 μL quartz crystal cuvette with 1 cm path length. Reagent volumes listed below assume 100 μL total reaction volume.

1. Perform steps 1-3 as described in Method 3.4. (*see* **Note 13**)
2. Combine the assay reagents as described in Method 3.4, Step 4, with the exception that no free Rap should be added. To this mixture add GTP, ammonium sulfate, and EDTA to final concentrations of 0.5 mM, 10 mM, and 1 mM, respectively. Measure the baseline as described in step 4 (Method 3.4). (*see* **Note 14,15**)
3. Add fusion protein or buffer control and mix quickly but thoroughly. Continue measurement of the reaction for 5-10 min (Figure 3-2B). (*see* **Note 16)**
4. Repeat the experiment using free Rap1B without any plexin to determine basal level Rap1B GTP hydrolysis.

4. Notes

1. Performing protein purification without the use of an FPLC (Materials 2.2) is not advisable. Ion exchange columns like the UNO Q1 (Materials 2.2) require higher pressure to pump fluid through the column than what peristaltic pumps could

typically provide. Additionally, an FPLC makes it easy to generate accurate and reproducible conductivity gradients for protein elution during ion exchange chromatography (Materials 2.2, Methods 3.3, Step 15).

2. The absorbance spectrum of MESG is pH dependent. The assay is most sensitive at pH 7.6 (Webb 1992). 20% Glycerol is added (the final concentration in the assay is 10%) to help stabilize $plexins_{cyto}$.
3. MESG solutions degrade over time, especially after several cycles of freezing/thawing. This can result in lower MESG concentrations than were intended. If too much MESG has degraded, it may become limiting during the course of the experiment. Once all the MESG is consumed, the 360/320 nm absorbance values will plateau, which may be mistakenly interpreted as the GTP hydrolysis reaction going to completion. To ensure that MESG is not limiting during the reaction, it is best to determine the maximal measurable change in absorbance before conducting the experiments. This is determined by mixing all the assay reagents except the proteins (plexin and Rap). Measure the 320/360 nm absorbance signals and incrementally add a known quantity of phosphate. Continue adding phosphate and measuring the absorbance values until absorbance no longer changes. The total change in absorbance defines the detection limit. The upper limit of detection can be extended by using higher concentrations of MESG, so far as the range of linearity of the UV-Vis spectrophotometer is not exceeded.
4. Stored GTP solutions will hydrolyze to GDP and P_i over time, even when frozen. This can be problematic for the continuous turnover reaction because adding free P_i to the solution will result in an absorbance change that can be mistaken for Rap

mediated GTP hydrolysis. It is best to make fresh GTP stocks regularly to minimize this free P_i contamination.

5. The plexins are a large family and choosing which plexin(s) to work with may be difficult. In our experience, mouse PlexinB2 and zebrafish PlexinC1 are the easiest plexins to express and are relatively stable. The specific questions being asked, however, should dictate which plexins are used.
6. Using the ArcticExpress cells, which co-express the cold-adapted chaperonins Cpn10 and Cpn60, significantly improves the expression level of $plexins_{cyto}$ compared to using BL21 cells. The yield of Rap1B is acceptable using BL21 cells.
7. It is optional to add 2 mL of antifoam B emulsion (Sigma) to each flask. Suppression of foaming improves gas exchange so that the bacteria culture grows faster.
8. If the expression level of $plexin_{cyto}$ is low, it may be helpful to keep $OD_{600\ nm}$ at about 1.6-2.0 before induction. Lowering the IPTG concentration to about 100 μM could also help.
9. Bacterial cell lysate contains not only the protein being expressed but also a mixture of cell debris, unlysed bacteria, bacterial proteases and other contaminant proteins. Using a peristaltic pump to load this mixture to the Histrap FF nickel column (Methods 3.3, Step 7) allows you to avoid introducing all these contaminants to the FPLC system which is much more difficult to clean.
10. Ideally Rap1B pre-loaded with GTP should be used as the substrate. Rap binds to nucleotide tightly, however, making it difficult to perform GTP loading. Rap1B purified from *E. coli*, remains ~70% GTP bound as determined by HPLC (unpublished result). GTP is incorporated into Rap during protein expression in *E.*

coli, and remains mostly unhydrolyzed due to the extremely low intrinsic hydrolysis activity of Rap.

11. 320 nm absorbance of MESG at this concentration is usually above the linear range of the spectrophotometer and is therefore unsuitable for quantitative analysis. However it is a useful indication of precipitation, as the $OD_{320\ nm}$ should decrease when phosphate is being generated from Rap GTP hydrolysis. If the absorbance of both 360 nm and 320 nm are increasing, the apparent "activity" is due to the increase of scattering from unstable proteins that are continuously precipitating out of solution. If the UV-Vis spectrophotometer cannot perform dual wavelength reads, measure the $OD_{320\ nm}$ once before addition of plexin. Move to 360 nm for data collection. Upon completion of the reaction, measure the $OD_{320\ nm}$ again to ensure the value hasn't increased.
12. Salt concentrations strongly affect the plexin GAP activity and should be consistent between any experiments that will be directly compared (Wiesmuller and Wittinghofer 1992, Wang, He et al. 2012). For example, when comparing the GAP activity of different plexin family members, the purified $plexin_{cyto}$ proteins should be diluted to the same final concentration using the same buffer.
13. Since using different ratios of Rap1B and $plexin_{cyto}$ is not possible when they are fused, we recommend using 5-20 μM of the fusion protein for the assay.
14. Even fresh GTP solutions contain some free P_i contaminant, which causes an initial spike in $OD_{360\ nm}$. Incubating the reagent mixture for 1-2 min before starting the baseline measurement will remove this spike from early readings.

15. Because Rap1B and PlexinC1$_{cyto}$ are fused in the multiple-turnover assay, Rap1B cannot be added to the cuvette for baseline measurement prior to addition of the fusion protein as in step 4 of the single-turnover assay (Method 3.4). Measurement of the baseline should be conducted only with the reagent components and no protein. Measure the basal Rap1B GTP hydrolysis rate separately (Method 3.5, Step 4).
16. For generating the fusion protein, we used human Rap1B (residues 2-167) with a C-terminal 24-residue linker that is followed by a "LPETGG" motif, and PlexinC1$_{cyto}$ from zebrafish (residues 552-1153, gene bank entry XM_6856674) with a N-terminal di-glycine motif. The bacterial transpeptidase Sortase recognizes these motifs and fuses Rap1B and plexin into one polypeptide chain, which is described in detail in Chapter Two.

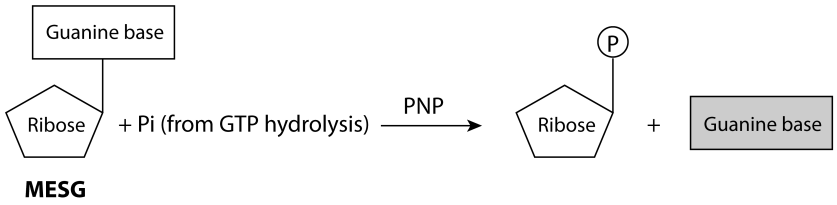

Figure 3-1. Coupling phosphate release to a photometric readout
GTP hydrolysis reactions release free P_i as a byproduct. P_i and MESG are converted to ribose-1-phosphate and a guanine base (2-amino-6-mercapto-7-methylpurine) by PNP. This conversion is accompanied by an increase in absorbance of the guanine base (λ_{Max}, 360 nm) and a decrease of MESG absorbance (λ_{Max}, 320 nm).

Note: Figure above was generated in collaboration with Yuxiao Wang

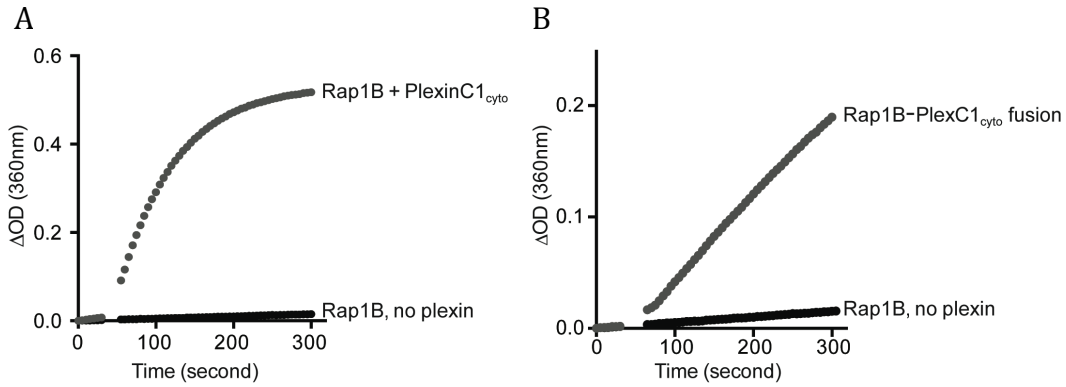

Figure 3-2. Single and multiple-turnover plexin GAP activity reactions
(A) Example data set from a single-turnover GAP activity measurement using 10 μM mouse PlexinC1$_{cyto}$ and 70 μM human Rap1B. Measurement of Rap1B with no plexin is used to establish the basal GTP hydrolysis rate. The GAP reaction proceeds as a single exponential and reaches completion at around 200 s.

(B) Data from a multiple-turnover GAP activity assay using 15 μM of a human Rap1B/zebrafish PlexinC1$_{cyto}$ fusion protein. Rap1B basal hydrolysis is measured as in

Note: Figure above was generated in collaboration with Yuxiao Wang

CHAPTER FOUR

Crystal Structure of a Plexin/Rap Complex Reveals the Non-Canonical Catalytic Mechanism for Rap Inactivation

Summary

Plexin function is critically dependent on its cytoplasmic GTPase activating protein (GAP) domain, which specifically inactivates the Ras homolog Rap for signaling. The plexin GAP is unrelated to canonical RapGAPs and facilitates Rap GTP hydrolysis through a poorly understood non-canonical mechanism. We determined the crystal structure of a PlexinC1/Rap complex, which shows that PlexinC1 induces an unprecedented conformation of Switch II in Rap. This conformation brings Gln63 in Rap into the active site to act as a key residue for catalyzing GTP hydrolysis. Several conserved residues in plexin make specific interactions to stabilize this "Gln63-in" conformation. Our mutational analyses validate this catalytic mechanism and its essential role in plexin signaling in the cell. Comparisons of plexins with RasGAPs suggest the basis for their different substrate preferences and catalytic mechanisms.

Introduction

The C-terminal cytoplasmic regions of plexins contain a RasGAP domain, a juxtamembrane segment and a RhoGTPase-binding domain (RBD) (Rohm, Rahim et al. 2000, Hu, Marton et al. 2001, He, Yang et al. 2009, Tong, Hota et al. 2009, Bell, Aricescu et al. 2011). It relays the signal from the semaphorin-bound extracellular region of plexins to downstream pathways. The essential role of the GAP domain in plexin signaling has been demonstrated by the loss of function upon mutating the conserved

arginine residue in this domain corresponding to the catalytic "arginine finger" in RasGAPs (Rohm, Rahim et al. 2000, He, Yang et al. 2009). While plexins have been previously reported to be GAPs for R-Ras and M-Ras (Oinuma, Ishikawa et al. 2004, Saito, Oinuma et al. 2009), a recent study has demonstrated that plexin GAPs act specifically on Rap (reviewed in Chapter One)(Wang, He et al. 2012).

RasGAPs such as p120GAP and neurofibromin facilitate GTP hydrolysis of Ras, R-Ras and M-Ras by providing the arginine finger to stabilize the leaving γ-phosphate group (Li, Nakamura et al. 1997, Scheffzek, Ahmadian et al. 1997, Scheffzek, Ahmadian et al. 1998, Quilliam, Castro et al. 1999, Ohba, Mochizuki et al. 2000, Bos, Rehmann et al. 2007). Concomitantly, a conserved glutamine in the GTPases (Gln61 in Ras) coordinates the nucleophilic water for hydrolysis (Figure 4-1). Rap is distinct from Ras/R-Ras/M-Ras in that it has a threonine at position 61, which lacks the ability to coordinate the catalytic water (Figure 4-1C).

Canonical RapGAPs are unrelated to RasGAPs and catalyze Rap GTP hydrolysis by providing an asparagine residue (the "Asn thumb") to fulfill the role of Gln61 in Ras (Scrima, Thomas et al. 2008). Plexins and a group of dual-specificity GAPs such as SynGAP (Synaptic GAP), and three GAP1 family members Rasal (Ras-GTPase-activating-like protein), CAPRI (Ca^{2+}-promoted Ras inactivator) and $GAP1^{IP4BP}$ (tetrakisphosphate binding protein) share the RasGAP fold that contains the arginine finger but lack a conserved Asn thumb (Kupzig, Deaconescu et al. 2006, Pena, Hothorn et al. 2008). They act on Rap through a distinct, poorly understood mechanism. An insightful mutational study has suggested that Gln63 in Rap plays a role analogous to Gln61 in Ras in the non-canonical catalysis of the dual-specificity GAPs (Figure 4-1B

and 1C) (Sot, Kotting et al. 2010). Mutating Gln63 in Rap abolishes GTP hydrolysis catalyzed by both the dual-specificity GAPs and plexins (Sot, Kotting et al. 2010, Wang, He et al. 2012).

Results

Sortase Mediated Plexin/Rap Ligation

To better understand plexin signaling and this non-canonical catalytic mechanism, we sought to crystallize the plexin cytoplasmic region ($plexin_{cyto}$) in complex with Rap. Our attempts to co-crystallize $plexins_{cyto}$ and Rap failed. To stabilize the plexin/Rap complex, we covalently linked $plexins_{cyto}$ and Rap1B by using a recently developed protein ligation system described in Chapter Two (Figure 4-2A and B) (Popp, Antos et al. 2009). The ligated complex of zebrafish $PlexinC1_{cyto}$ and human Rap1B catalyzes GTP hydrolysis at much higher rates than the two individual proteins mixed at the same concentrations (Figure 4-2C), indicating increased formation of the catalytically competent PlexinC1/Rap complex when the two proteins are tethered. It was shown concurrently in this study that induced dimerization promotes the active conformation of $plexins_{cyto}$ (work done by Yuxiao Wang). Conversely, stabilization of the active conformation by Rap binding is expected to facilitate formation of the plexin active dimer. Analytical ultracentrifugation experiments showed that while the ligated PlexinC1/Rap itself did not dimerize, it was induced to dimerize robustly by the transition-state analog aluminum tri-fluoride (AlF_3) (Figure 4-2D). These results support that binding of AlF_3 to GDP-bound Rap induces the transition-state complex between ligated PlexinC1 and Rap1B, which promotes plexin dimerization.

PlexinC1$_{Cyto}$/Rap1B Crystal Structure

We crystallized and determined the structure of the ligated complex of zebrafish PlexinC1$_{cyto}$ and human Rap1B in the presence of AlF_3 (Table 4-1). Our analyses show that the species mismatch does not affect the plexin/Rap interaction (Figure 4-3A). The asymmetric unit contains four protomers of the PlexinC1/Rap1B complex, which are virtually identical to one another. The four PlexinC1 molecules form two pairs of dimers (Figure 4-1A), consistent with the dimerization observed in solution. The conformation of PlexinC1 and its mode of dimerization are similar to those seen in the structure of a coiled-coil induced dimer of PlexinC1$_{cyto}$ (work done by Yuxiao Wang) (Figure 4-4). This chapter focuses on the specific interaction between plexin and Rap and the catalytic mechanism, but the dimerization-induced activation of plexin will be discussed briefly.

A structural superimposition of the PlexinC1/Rap and p120GAP/Ras complexes based on Rap and Ras shows that the overall binding modes of the two are similar (Figure 4-1B) (Scheffzek, Ahmadian et al. 1997). The GAP domain in PlexinC1 and Switches I (residues 30-38) and II (residues 59-67) in Rap constitute the majority of the binding interface, whereas the RBD in plexin is not involved (Figure 4-1B and Figure 4-5). The core of the interface is composed of several hydrophobic residues, which are surrounded by numerous charge-charge interactions at the periphery. Most of the Rap-binding residues are conserved among the plexin family members, suggesting that they all interact with Rap in the same mode (Figure 4-5). The presumed arginine finger (Arg711) in PlexinC1 superimposes well with the arginine finger (Arg789) in p120GAP, playing the same role in catalysis by interacting with the AlF_3 and GDP in the active site (Figure

4-1B). Likewise, the second conserved arginine (Arg1001) in PlexinC1 is equivalent to Arg903 in p120GAP in stabilizing the position of the arginine finger (Figure 4-1B). The functional importance of these two arginine residues in plexins has been demonstrated by previous mutational studies (Rohm, Rahim et al. 2000, Oinuma, Ishikawa et al. 2004, He, Yang et al. 2009).

Switch I Interactions with the Activation Segment

Switch I of Rap makes numerous interactions with the loop-helix segment (residues 1038-1058) between helices 15 and 17 in PlexinC1 (Figure 4-6A). We refer to this segment as the "activation segment" because it regulates the GAP activity by switching from the closed to the open conformation when plexin forms the active dimer. The activation segment "open" conformation seen here is very similar to that in the coiled-coil induced PlexinC1 dimer structure (work doe by Yuxiao Wang) (Figure 4-7C). In contrast, all the previously reported monomeric structures of plexins display the "closed" conformation, which is incompatible with Rap binding (Figure 4-7A,B) (He, Yang et al. 2009, Tong, Hota et al. 2009, Bell, Aricescu et al. 2011, Wang, He et al. 2012).

Pro1050 at the N-terminus of the helical portion of the activation segment packs against Tyr40 in Rap. Asn1052 forms two hydrogen bonds with the carboxyl group of Asp38 and the backbone amide of Ser39 in Rap. Lys1053 apparently makes electrostatic interactions with Asp38 in Rap and Asp1036 in plexin. Gln1032 in helix 15 also contributes to Switch I binding through forming three hydrogen bonds. GAP activity assays showed that while the P1050A mutation caused a modest activity decrease, the Q1032E, N1052E and K1053A mutations largely abolished the activity (Figure 4-6). We

further examined(Wang, Pascoe et al. 2013) some of these mutations using the COS7 cell collapse assay, which assesses plexin function based on its ability to induce cell collapse when activated by semaphorin (Takahashi, Fournier et al. 1999). Because the ligand of zebrafish PlexinC1 is not available, mouse PlexinA3 and its ligand Sema3F were used in these assays (He, Yang et al. 2009). The results showed that both the Q1754E and K1775A mutations of mouse PlexinA3, equivalent to zebrafish PlexinC1 Q1032E and K1053A respectively, greatly impaired the cell collapse activity (Figure 4-6C). Interestingly, Pro2032 in PlexinB1 and Lys1809 in PlexinB3, equivalent to Pro1050 and Lys1053 in zebrafish PlexinC1 respectively, have been found mutated in cancer patients (Cancer Genome Atlas Research 2012, Seshagiri, Stawiski et al. 2012).

Switch II Interactions and Gln63

Switch II of Rap in the PlexinC1/Rap complex adopts an unprecedented conformation that is markedly different from both the p120GAP/Ras and the RapGAP/Rap complexes (Figure 4-8B,C and Figure 4-3B) (Scheffzek, Ahmadian et al. 1997, Scrima, Thomas et al. 2008). Residues 60-63 in Switch II form a tight hairpin-like turn, which brings Gln63 close to AlF_3 (therefore named the Gln63-in conformation). The Gln63 sidechain is placed in a nearly identical position in the active site as Gln61 in the p120GAP/Ras complex (Figure 4-8B). This comparison strongly supports that Rap Gln63 indeed fulfills the catalytic role of Gln61 in Ras, i.e. stabilizing the nucleophilic water (Sot, Kotting et al. 2010, Wang, He et al. 2012). The segment following Gln63 (residues 64-67) adopts an extended conformation, allowing it to span the distance between Gln63 in the active site and the helix following Switch II. In contrast, the corresponding

segments in the p120GAP/Ras and the Rap/RapGAP complexes adopt helical structures, holding residue 63 away from the active site.

Gln63 Orientation

The Gln63-in conformation of Switch II is stabilized by numerous specific interactions between PlexinC1 and Rap (Figure 4-8D). The side chains of Arg1001, Asn1005 and Asn1009 in helices 13 and 14 of PlexinC1 form a network of hydrogen bonds with the backbone of Switch II. Pro611 in the second helix of the juxtamembrane segment makes van der Waals interactions with Thr65 in Switch II (Figure 4-9A). Mutation of either Asn1005 or Asn1009 dramatically decreases the GAP activity (Figure 4-8E). The N1728E mutation in mouse PlexinA3 (equivalent to N1005E of zebrafish PlexinC1) also abolishes the cell collapse activity (Figure 4-8F). Mutating Pro611 to glycine, which eliminates its interaction with Thr65 in Switch II, decreases the GAP activity (Figure 4-8E). Conversely, the wild type PlexinC1 shows decreased activity towards the Rap T65A mutant (Figure 4-8E). The Switch II-interacting residues are highly conserved among the plexin family members (Figure 4-5 and 4-9C), suggesting they all use the same mechanism to stabilize the Gln63-in conformation.

The dual-specificity GAPs do not share some of the Switch II-interacting residues with plexins (Figure 4-8C and 4-9C). For example, Asn1005 in PlexinC1 is replaced by a proline in the dual-specificity GAPs (Pro585 in SynGAP) (Pena, Hothorn et al. 2008), lacking the ability to stabilize the Gln63-in conformation of Rap through hydrogen bonds. This loss may be compensated by the extra domains outside of the GAP domain in the dual-specificity GAPs, which have been shown to be required for their RapGAP

activity but not for the RasGAP activity (Kupzig, Deaconescu et al. 2006, Pena, Hothorn et al. 2008, Kupzig, Bouyoucef-Cherchalli et al. 2009, Sot, Kotting et al. 2010). RasGAPs such as p120GAP and neurofibromin also contain a proline at the position of Asn1005 in PlexinC1. GAP1m, the only GAP1 family member that is active toward Ras but not Rap, has a valine at this position (Figure 4-9C). Proline-to-valine mutants of the dual-specificity GAP1 family members remain active toward Ras, but lose activity toward Rap (Kupzig, Bouyoucef-Cherchalli et al. 2009). The superimposition of the p120GAP/Ras and PlexinC1/Rap structures suggests an explanation for this selectivity (Figure 4-9B). While both Ras and Rap can accommodate a proline residue at this position, Switch II of Rap in the Gln63-in conformation likely clashes with the bulkier valine sidechain if present (Figure 4-9B).

Plexin/Rap Specificity Determinants

In addition to Switch II, the PlexinC1/Rap interface involves several other residues in Rap that diverge from Ras/R-Ras/M-Ras. Residue 31 in Rap and Ras is a known determinant for their effector specificity (Nassar, Horn et al. 1996). Rap possesses a lysine at this position, which is replaced by a negatively charged residue (aspartate or glutamate) in Ras/R-Ras/M-Ras (Figure 4-1C). Lys31 and Asp33 in Rap form a charge-charge pair and are buried by the activation segment in PlexinC1 (Figure 4-10B). We made a Rap(K31E) mutant to render it more similar to Ras/R-Ras/M-Ras. This mutation is predicted to destabilize the PlexinC1/Rap interaction, since it closely places two buried negative charges. The GAP assay indeed showed that PlexinC1 failed to catalyze GTP hydrolysis for the K31E mutant (Figure 4-10C). Asp95 in Rap and Lys666 in PlexinC1

are close to each other and potentially form a salt-bridge (Figure 4-10A). The corresponding residues of Asp95 in Ras, R-Ras and M-Ras are glutamine, lysine and arginine respectively (Figure 4-1C). Mutating Rap Asp95 to lysine, as in R-Ras, substantially decreases the rate of PlexinC1-catalyzed GTP hydrolysis (Figure 4-10C). Likewise, PlexinC1(K666D) displays lower GAP activity than the wild-type PlexinC1 (Figure 4-10C). Arg1384 in PlexinA1 (equivalent to Lys666 in zebrafish PlexinC1) has also been found mutated in cancer patients (Brautigam 2015, in press). These analyses together with the unique plexin/Switch II interface support the notion that plexins have evolved to recognize residues in Rap that have diverged from other Ras family members, leading to loss of activity toward Ras/R-Ras/M-Ras.

Plexin Active Dimer Formation

Formation of the active dimer induces a striking conformational change in the juxtamembrane segment (Figure 4-11A and B). The N-terminal helix portion of the juxtamembrane segment in several structures of plexins in the inactive state adopts a well-defined kinked conformation and wraps around the GAP domain (He, Yang et al. 2009, Tong, Hota et al. 2009, Wang, He et al. 2012). In one of the PlexinB1 structures the juxtamembrane segment is disordered (Bell, Aricescu et al. 2011). In the active dimer, the C-terminal part of the juxtamembrane helix unwinds, which allows the N-terminal portion to straighten and pull up in relation to the GAP domain (Figure 4-11B). It also undergoes a 90° pivotal rotation compared to the inactive conformation. The dimer interface is formed mostly by the juxtamembrane helix in this new conformation and one helix from the GAP domain. The two

juxtamembrane helices from the two subunits run in parallel, poised to connect to the transmembrane helices on the cell surface (Figure 4-11A).

The new conformation of the juxtamembrane helix in the active dimer is coupled to a conformational change in the activation segment (Figure 4-11C). The coupling is mediated by interactions between the juxtamembrane segment from one subunit and the activation segment from the other subunit. Through these interactions, the juxtamembrane segment pulls the activation segment away from the GAP active site, leading to the open conformation that is able to accommodate Rap as seen in the PlexinC1/Rap1B complex structure. Residues involved in these interactions as well as other parts of the dimer interface are highly conserved in the plexin family, and are critical for the dimerization-driven activation of the plexin GAP activity and induction of cell collapse.

Discussion

While sharing the same domain fold with RasGAPs and dual-specificity GAPs, plexins appear to be a unique group that are active to Rap, but not to Ras/R-Ras/M-Ras. Our analysis of the plexin/Rap complex reveals residues in both plexin and Rap that contribute to this specificity. The apparent GAP activity of plexins towards R-Ras and M-Ras reported previously may be caused indirectly by inactivation of Rap and alleviation of its inhibition on p120GAP. P120GAP has been shown to bind tightly to GTP-bound Rap, but fail to promote GTP hydrolysis. Rap therefore can act as an effective inhibitor of p120GAP (Frech, John et al. 1990). (Frech, John et al. 1990, Hata, Kikuchi et al. 1990, Yatani, Quilliam et al. 1991). Conversion of Rap to the GDP-bound form by plexin

relieves this inhibition on p120GAP, which can then decrease levels of GTP-bound Ras/R-Ras/M-Ras. This indirect effect may underlie the reported GAP activity of plexin towards R-Ras and M-Ras in the cell. Indeed, a recent study has shown that PlexinB1 uses this indirect mechanism to inhibit Ras and act as a tumor suppressor (Okada, Sinha et al. 2015). The induced Gln63-in conformation of Rap seen in our structure likely represents the general mechanism by which plexins and the dual-specificity GAPs facilitate GTP hydrolysis for Rap. This conformation is stabilized by specific interactions made by several conserved residues in plexins. The dual-specificity GAPs achieve this through different mechanisms that likely involve the extra domains, the precise basis for which awaits structural studies of these GAPs in complex with Rap.

Plexin must be autoinhibited to prevent spontaneous signaling in the absence of the semaphorin ligand. A structural comparison with the p120GAP/Ras complex has suggested that the GAP domain of the monomeric cytoplasmic region of PlexinA3 adopts a closed conformation that cannot accommodate its small GTPase substrate (He, Yang et al. 2009). The structure of the PlexinC1/Rap1B complex revealed that the major inhibitory element in monomeric plexin is a helix-loop segment in the GAP domain (Figure 4-7). This segment is referred to as the "activation segment", drawing analogy from protein kinases in which the activation segment controls the activity by switching between the inactive and active conformations. The activation segment in the PlexinA3 structure adopts a more "closed" conformation compared to that in active PlexinC1 in complex with Rap (Figure 4-7). This closed conformation is stabilized by a hydrogen bond between a pair of conserved residues in the activation segment and the following helix. Consistently, this conformation is

present in all the monomeric structures of several plexin family members, suggesting that it represents a free energy minimum (Tong, Hota et al. 2009, Bell, Aricescu et al. 2011, Wang, He et al. 2012).

Docking Rap based on the PlexinC1/Rap complex structure to the inactive plexin structures showed that several residues sterically clash with Rap (Figure 4-7A). In addition, the flexible loop region in the activation segment may sample conformations that conflict with Rap binding. In contrast, the activation segment in the PlexinC1/Rap complex structure adopts an open conformation and makes intimate interactions with the switch I region of Rap. Therefore, residues in the activation segment play dual roles. They stabilize the autoinhibited conformation to suppress the basal activity of the plexin GAP. When converted to the open conformation, these residues make numerous contacts with Rap and support the catalysis of GTP hydrolysis.

Materials and Methods

Protein Expression.

The human Rap1B construct (residues 2-167) in a modified pET28 vector (Novagen) that encodes a N-terminal His_6-tag and a recognition site for the human rhinovirus C3 protease has been described previously (Wang, He et al. 2012). The Rap1B constructs containing a C-terminal flexible linker followed by a sortase recognition motif (one letter-code sequence: LPETGG) were generated by PCR and subcloned into the same vector. Seven versions of the linker were generated: 0-residue (containing the LPETGG motif only), 11-residue (sequence: GGSGGSGSGSS), 14-residue (sequence:

SGGSGSGSSGGSGS), 16-residue (sequence: GGSGGSGSGSSGGSGS), 21-residue (sequence: GGSGGSGSGSSGGSGSGGGSG), 24-residue (sequence: SGGSGSGSSGGSGSGGGSGSGSSG) and 26-residue (sequence: GGSGGSGSGSSGGSGSGGGSGSGSSG). The vector encodes a glycine residue at the second position from the N-terminus, which becomes the N-terminal residue after removal of the methionine residue encoded by the start codon during protein expression. An N-terminal glycine on the Rap1B protein would hinder the sortase-mediated ligation with Plexin (see below) (Popp, Antos et al. 2009). To avoid this problem, the vector was mutated to replace the glycine residue with an aspartate using a Quikchange reaction (Stratagene). The Rap1B proteins were expressed in the bacteria strain BL21 (DE3) and purified as described previously (Wang, He et al. 2012). The coding region for the zebrafish PlexinC1$_{cyto}$ (residues 552-1147) with a N-terminal di-glycine tag was synthesized (GenScript) based on the gene bank entry XM685667. The gene was subcloned into another modified pET28 vector containing a N-terminal tandem His$_6$–SUMO tag (Wang, He et al. 2012). The protein was expressed in the bacteria strain ArcticExpress (Stratagene) and purified as described previously (He, Yang et al. 2009, Wang, He et al. 2012). Removal of the His$_6$-SUMO-tag by treatment with the SUMO-specific protease Ulp1 yielded the PlexinC1 protein with a N-terminal GG-tag. Mutants of Rap1B and PlexinC1 were generated by Quikchange reactions (Stratagene), and expressed and purified as the wild-type proteins.

Sortase-mediated ligation.

Ligation of the N-terminal His_6/C-terminal LPETGG-tagged Rap1B and the N-terminal GG-tagged PlexinC1 was catalyzed by the transpeptidase activity of sortase from *Staphylococcus aureus* (plasmid provide by Dr. Hidde Ploegh) *(Popp, Antos et al. 2009)* using the method described in Chapter Two. Briefly, sortase with a N-terminal His_6-tag was expressed and purified by using Ni-NTA chromatography. Sortase first cleaves the peptide bond between the threonine and first glycine within the LPETGG motif in Rap1B. In the second step, the GG-tagged PlexinC1 is added to the threonine to regenerate a native peptide bond between the two proteins. The reaction mix contained Rap1B, PlexinC1 and sortase at 450, 69 and 25 μM respectively. Reactions were performed at room temperature for 3 hours with simultaneous dialysis to remove the di-glycine byproduct. The dialysis buffer contained 20 mM Tris pH 8, 150 mM NaCl, 10% glycerol, 2 mM $MgCl_2$, 2 mM DTT, 10 mM $CaCl_2$. The ligated PlexinC1/Rap1B complex was purified by Ni-NTA, ion exchange and gel filtration chromatographic steps. The N-terminal His_6-tag was removed by treatment with the human rhinovirus C3 protease.

In vitro GAP assays.

Due to the high intrinsic GAP activity of the ligated PlexinC1/Rap1B complex, all the bound GTP molecules were hydrolyzed to GDP during the purification process. To measure the activity of the complex, we used the multiple-turnover assay as described in Chapter Three. Briefly, $(NH_4)_2SO_4$ at 10 mM and EDTA at 1 mM are used to promote constant exchange of GTP/GDP for Rap in the complex, allowing continuous GTP

hydrolysis provided sufficient GTP is present in the assay solution (Webb and Hunter 1992). Unligated PlexinC1 and Rap1B mixed at the same concentrations were subjected to the same assay for comparison. For analyzing various structure-based mutants of PlexinC1 and Rap1B, the single-turnover GAP assay described in Chapter Three was used with Rap1B pre-loaded with GTP (Webb and Hunter 1992, Wang, He et al. 2012). The concentrations of PlexinC1 and Rap1B in these assays were 5 mM and 60 mM respectively.

Analytical Ultracentrifugation.

Sedimentation velocity analytical ultracentrifugation experiments were carried out using the ligated $PlexinC1_{cyto}$/Rap1B complex samples that were prepared in Centrifugation Buffer (10 mM Tris pH 8, 50 mM NaCl, 2 mM TCEP, and 2 mM $MgCl_2$). Protein samples at 0.5, 4, and 20 μM were used for the experiments without AlF_3. Protein samples at 0.5, 4, 8 and 20 μM were used for the experiments in the presence of 2 mM AlF_3. Samples were equilibrated ~14 hours at 4 °C, then approximately 400 μL of the samples were loaded into the "sample" sides of dual-sectored charcoal-filled Epon centerpieces that were sandwiched between sapphire windows in a cell housing; the "reference" sectors were filled with the same volume of Centrifugation Buffer. Filled cells were placed in an An50Ti rotor and equilibrated for 2.5 hours under vacuum in the centrifuge at 20 °C prior to centrifugation. Experiments were conducted using a Beckman Optima XL-I analytical ultracentrifuge at 42,000 RPM at 20 °C. Absorbance data at 280 nm were collected using the Beckman control software until all components had fully sedimented. Protein partial-specific volume, solvent viscosity, and density

values were calculated using the program Sednterp (Laue, Shah et al. 1992). The data were analyzed using the *c*(*s*) distribution in the program SEDFIT (Schuck 2000). A regularization level of 0.68 was routinely employed. Time-invariant noise elements were removed from the data (Schuck and Demeler 1999). Data-acquisition timestamp errors (Zhao, Ghirlando et al. 2013) were examined with SEDFIT and were found to be approximately 0.1%,; we deemed this small error acceptable and did not correct the timestamps. Plots were generated with the program GUSSI (Brautigam 2015, in press).

Crystallization and Structure Determination.

Ligated complexes of human Rap1B and several plexins$_{cyto}$ from mouse and zebrafish each with one of the 7 versions of the linker mentioned above were purified. They were characterized by the multiple-turnover GAP assay and subjected to crystallization trails. The ligated complex of zebrafish PlexinC1$_{cyto}$ and human Rap1B with the 24-residue linker and the LPETGG-tag at 4 mg/ml crystallized initially at 20 °C in 0.1 M HEPES pH 7.5, 10% 2-propanol, 20% PEG 4K in sitting-drop 96-well plates. Larger crystals were grown by hanging-drop vapor diffusion at 20 °C in 0.1 M HEPES pH 7.3, 5% 2-propanol, 25% PEG 3350, 3.6% polypropylene glycol P400. Cryo-protection of the crystals was achieved using with the crystallization solution supplemented with 25% glycerol. Cryo-protected crystals were snap cooled in liquid nitrogen. Diffraction data were collected at the Advanced Photon Source (Argonne National Laboratory) on beamline 19ID at 100 K. Data were indexed, integrated and scaled using HKL2000 (Otwinowski and Minor 1997). The diffract pattern extended to 3.3 Å and was consistent with the symmetry of the P1 space group. One protomer from

the active plexin dimer structure solved by Yuxiao Wang (PDB ID: 4M8M) was used as the molecular replacement search model for plexin using the Phaser module in the Phenix package (Adams, Grosse-Kunstleve et al. 2002, Mccoy, Grosse-Kunstleve et al. 2007). The structure of Rap1B from the Rap1B/RapGAP complex (PDB ID: 3BRW) was used as the search model for Rap1B. Model building and iterative refinement were performed using the Phenix and Coot programs respectively (Adams, Grosse-Kunstleve et al. 2002, Emsley and Cowtan 2004). The linker between the C-terminus of Rap1B and the N-terminus of PlexinC1$_{cyto}$ is not included in the model due to lack of discernable electron density (Figure 4-3A). Assuming the complexes in the crystal are formed by the covalently linked pairs of Rap1B and PlexinC1$_{cyto}$, the linker and the disordered flanking residues from the two proteins (a total of ~32 residues) are sufficient for spanning the distance (~45 Å) between the two ends without imposing restraints on the plexin/Rap binding mode. Comprehensive model validation was performed by using MolProbity (Chen, Arendall et al. 2010). Detailed statistics of data collection and refinement are listed in Table 4-1. Structure figures were prepared in PyMOL (the PyMOL Molecular Graphics System, Schrodinger). Sequence alignments were generated with ESPript (Gouet, Courcelle et al. 1999).

COS7 Cell assay.

Zebrafish PlxC1$_{cyto}$ equivalent mutants in mouse PlexinA3 were generated based on a sequence alignment of all mouse plexins with zebrafish PlexinC1. Full-length mouse PlexinA3 was used for the COS7 cell collapse assays, and performed as previously described (He, Yang et al. 2009). Briefly, 1x10^5 COS7 cells were plated in each well of a 6-well plate one day prior to transfection. FuGENE 6 (Promega) was used

to transfect each well with PlexinA3 (1 μg plasmid) and Neuropilin2 (0.5 μg plasmid) following the manufacturers instructions. Two days post transfection, 5 nM alkaline phosphatase-tagged Sema3F was added to each well and incubated for 25 minutes at 37ºC. The cells were washed, fixed and heat-treated to inactivate endogenous phosphatases (65ºC for 1 hour). Cells were stained with BCIP/NBT alkaline phosphatase substrate (Sigma). Cells were prepared and counted using a randomized and blind method. Representative cell images are shown in Figure 4-12.

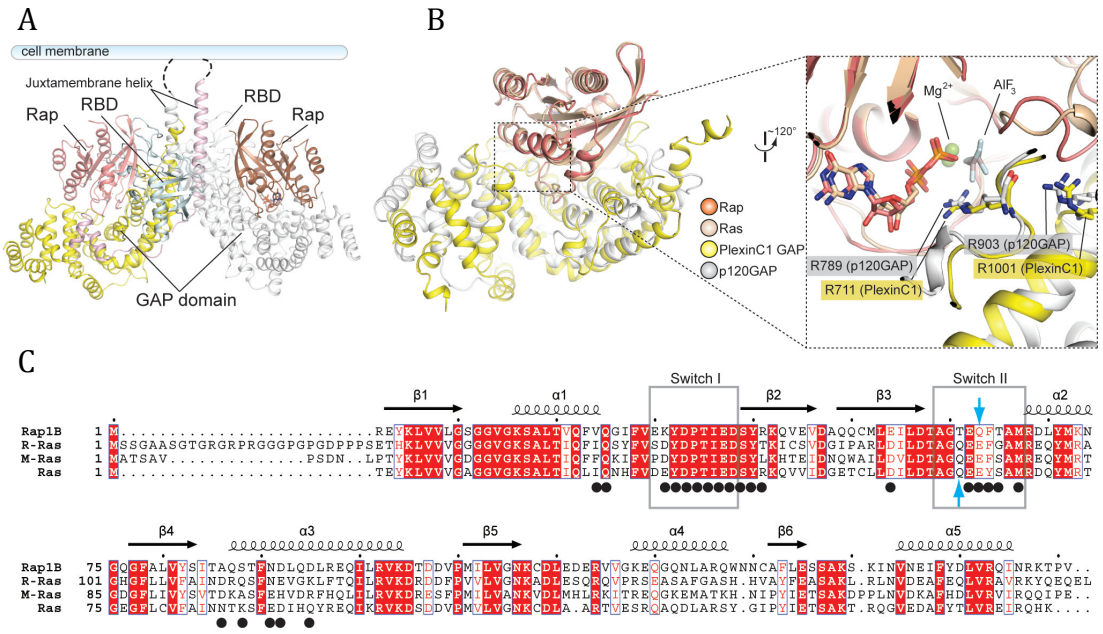

Figure 4-1. Crystal structure of the complex between zebrafish PlexinC1$_{cyto}$ and human Rap1B.

(A) The overall structure of the PlexinC1$_{cyto}$ dimer bound to two Rap1B molecules. For one plexin molecule, the juxtamembrane segment, the GAP domain and the RBD are colored pink, yellow and cyan respectively. The bound Rap1B is colored salmon. The other plexin molecule and the bound Rap1B are colored gray and brown, respectively.

(B) Structural comparison of the PlexinC1$_{cyto}$/Rap1B and the p120GAP/Ras complexes (PDB ID: 1WQ1). The left panel shows the overall view of a superimposition of the two structures based on Rap1B and Ras. The juxtamembrane segment and the RBD in PlexinC1 are omitted for clarity. The right panel shows a detailed view of the active site around the arginine finger. **(C)** Sequence alignment of human Rap1B, R-Ras, M-Ras and Ras. Black circles denote residues in Rap1B that are involved in interactions with PlexinC1$_{cyto}$. Gln63 in Rap1B and Gln61 in Ras are highlighted by blue arrows.

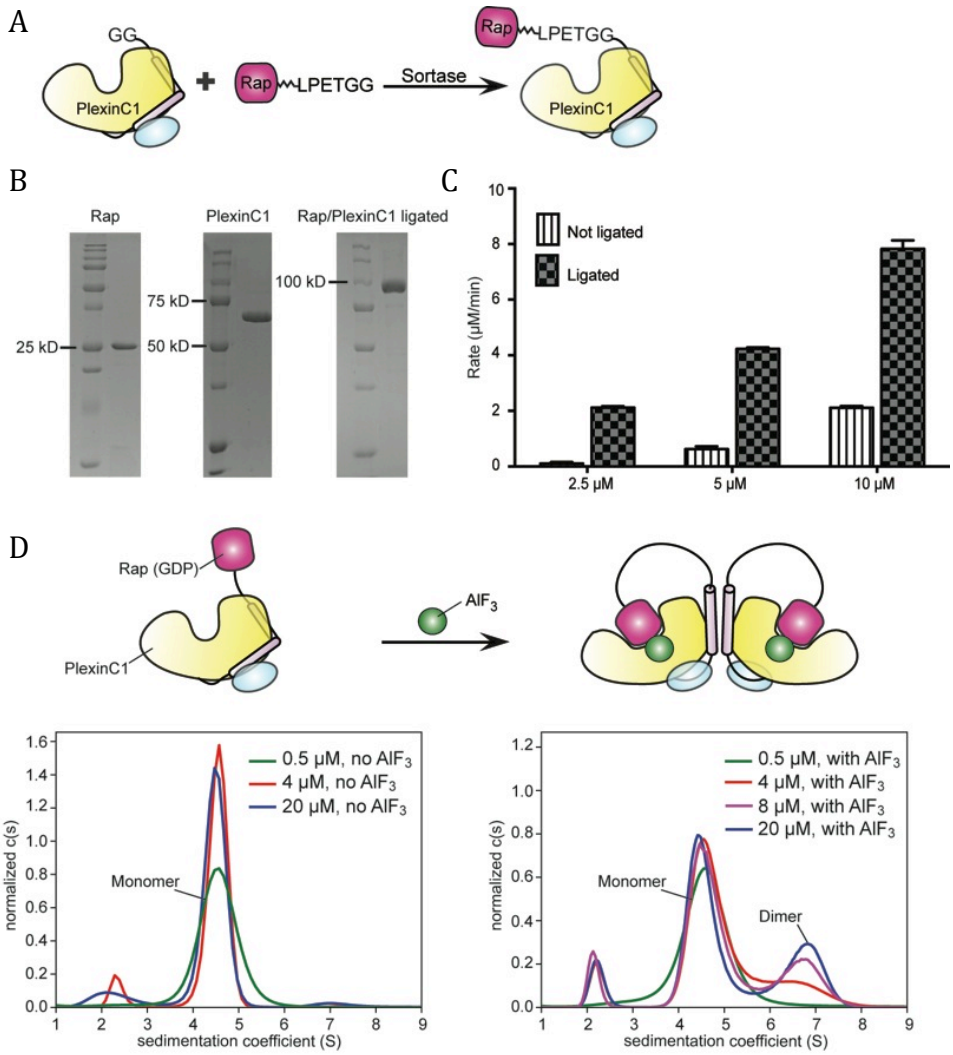

Figure 4-2. Sortase-$_{me6\ diated}$ ligation and characterization of the ligated PlexinC1$_{cyto}$/Rap1B complex.

(A) Scheme for the sortase mediated production of plexin$_{cyto}$ Rap1B fusion proteins.

(B) Representative gel analyses of purified PlexinC1$_{cyto}$, Rap1B and the ligated PlexinC1$_{cyto}$/Rap1B complex.

(C) Comparison of the GTP hydrolysis activity between the ligated complex and the individual PlexinC1$_{cyto}$ and Rap1B proteins mixed at the same concentrations (2.5, 5 and 10 mM). The GTP hydrolysis rates are averages of three independent experiments. Error bars represent standard deviation of the mean.

(D) Analytical ultracentrifugation showing AlF_3-induced dimerization of the ligated PlexinC1$_{cyto}$/Rap1B complex. In the absence of AlF_3 (the left panel), the majority of the complex behaves as a monomer with a sedimentation coefficient of 4.5 S. In the presence of AlF_3 (the right panel), a dimeric species (sedimentation coefficient of 6.7 S) appears and becomes more abundant at higher protein concentrations.

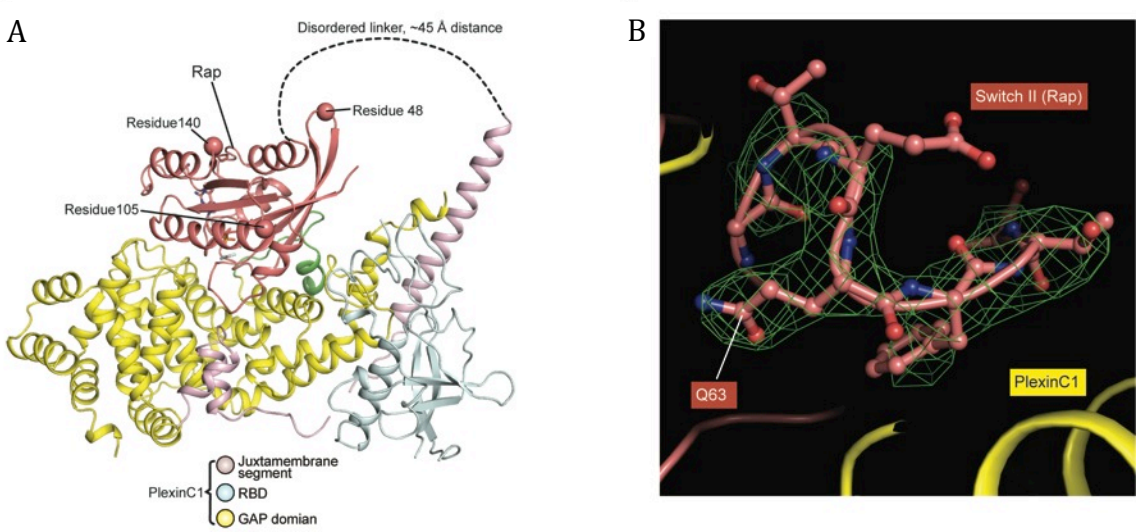

Figure 4-3. Additional validation of the structure.
(A) The overall structure of one PlexinC1$_{cyto}$/Rap1B complex in the asymmetric unit. The three residues that are not identical in human and zebrafish Rap1B are highlighted by spheres. They are located far away from the PlexinC1$_{cyto}$/Rap1B interface. The linker between the C-terminus of Rap1B and the N-terminus of PlexinC1$_{cyto}$ is not included in the structure due to lack of density. The distance between the two ends is ~45 Å, which can be spanned readily by the disordered linker of ~32 residues.

(B) Simulated annealing omit map of Switch II. A Sigma-A weighted simulated annealing omit map was calculated in Phenix by using the model with residues 60-66 in one of the Rap1B molecules removed. The map is contoured at 3σ in green, with the final model of the structure superimposed.

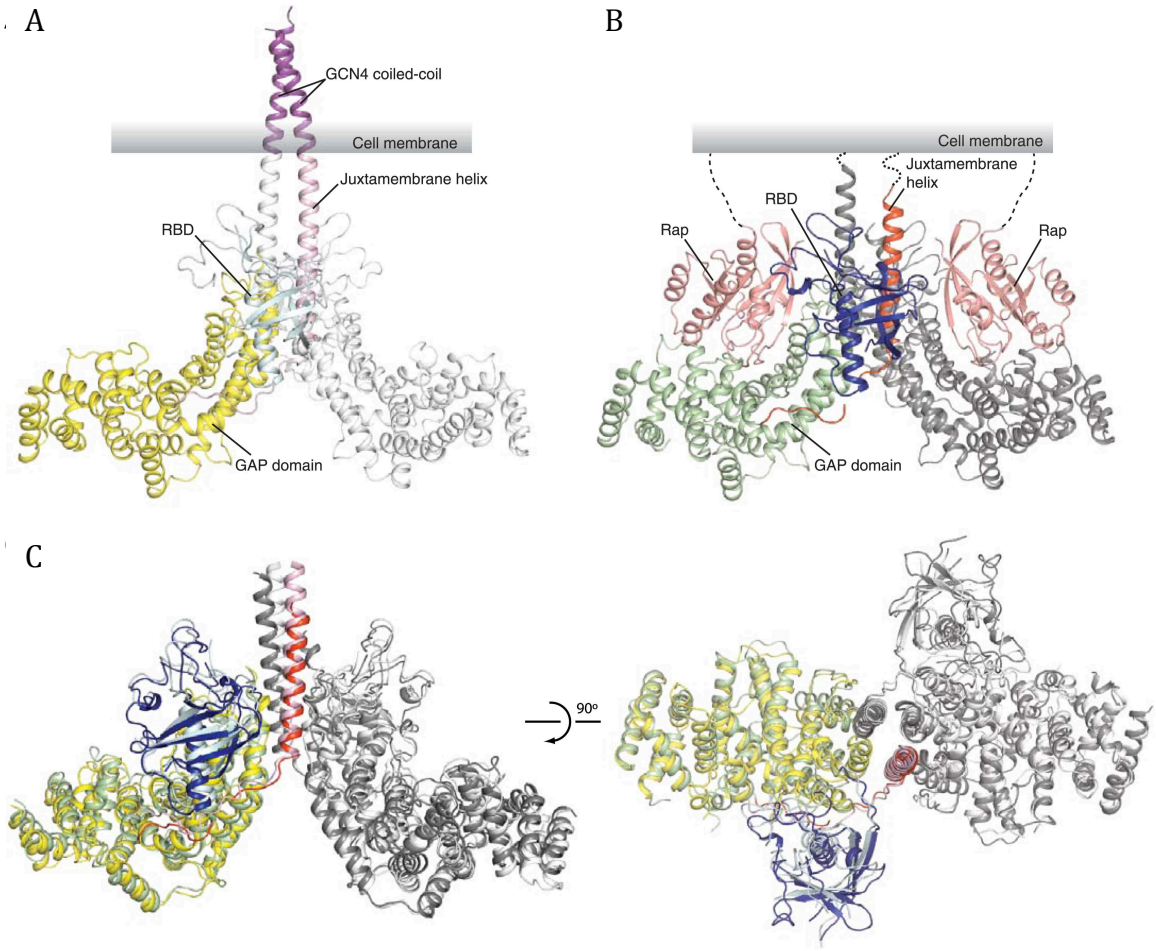

Figure 4-4. Overall structures of the zebrafish PlexinC1$_{cyto}$ active dimers.
(A) Structure of the coiled-coil induced active dimer of PlexinC1$_{cyto}$. PDB ID: 4M8M

(B) Structure of the Rap1B bound active dimer of PlexinC1$_{cyto}$. In both (A) and (B), domains from one plexin protomer are colored and labeled. The other plexin protomer is shown in white in (A) and in gray in (B). PDB ID: 4M8N

(C) Comparison of the active dimers seen in (A) and (B). The coiled-coil motif and Rap are omitted for clarity. Colors are the same as in (A) and (B).

Note: This figure and work was completed in collaboration with Yuxiao Wang who solved the coiled-coil PlexinC1$_{cyto}$ dimer crystal structure.

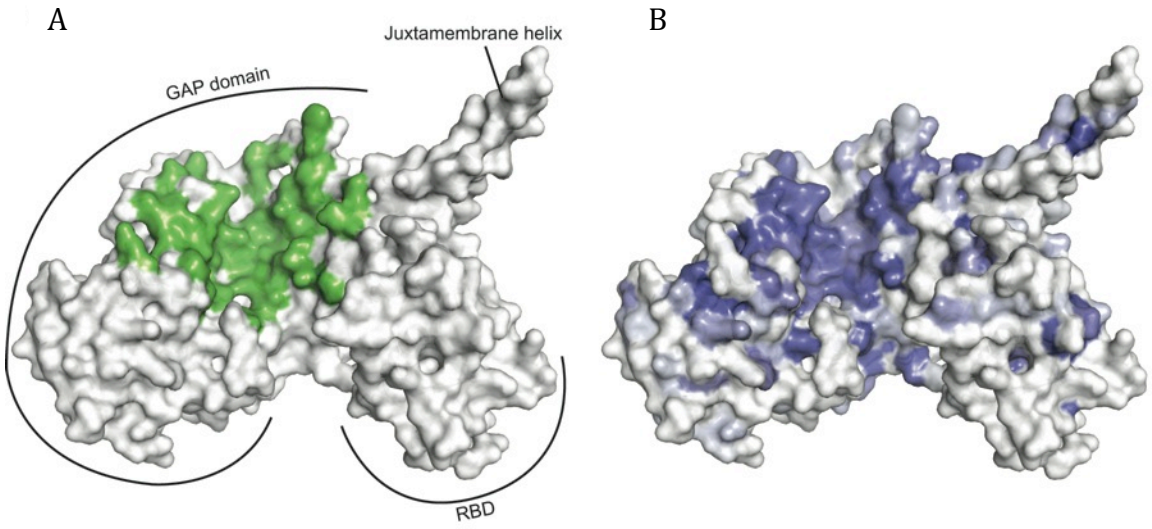

Figure 4-5. Sequence conservation at the Rap-binding surface of the plexin family. (A) Rap-binding surface in zebrafish PlexinC1$_{cyto}$. Residues in PlexinC1 within 4 Å distance of the bound Rap1B molecule are colored green.

(B) Sequence conservation projection on the molecular surface of PlexinC1$_{cyto}$. The conservation scores were calculated based on an alignment of zebrafish PlexinC1 and all the plexins from mouse (Plexin A1, A2, A3, A4, B1, B2, B3, C1 and D1). The color spectrum from white to dark blue indicates increasing levels of sequence conservation. The structures in (A) and (B) are shown in the same orientation. It is evident from the comparison between (A) and (B) that the Rap-binding surface is composed of highly conserved residues in plexins.

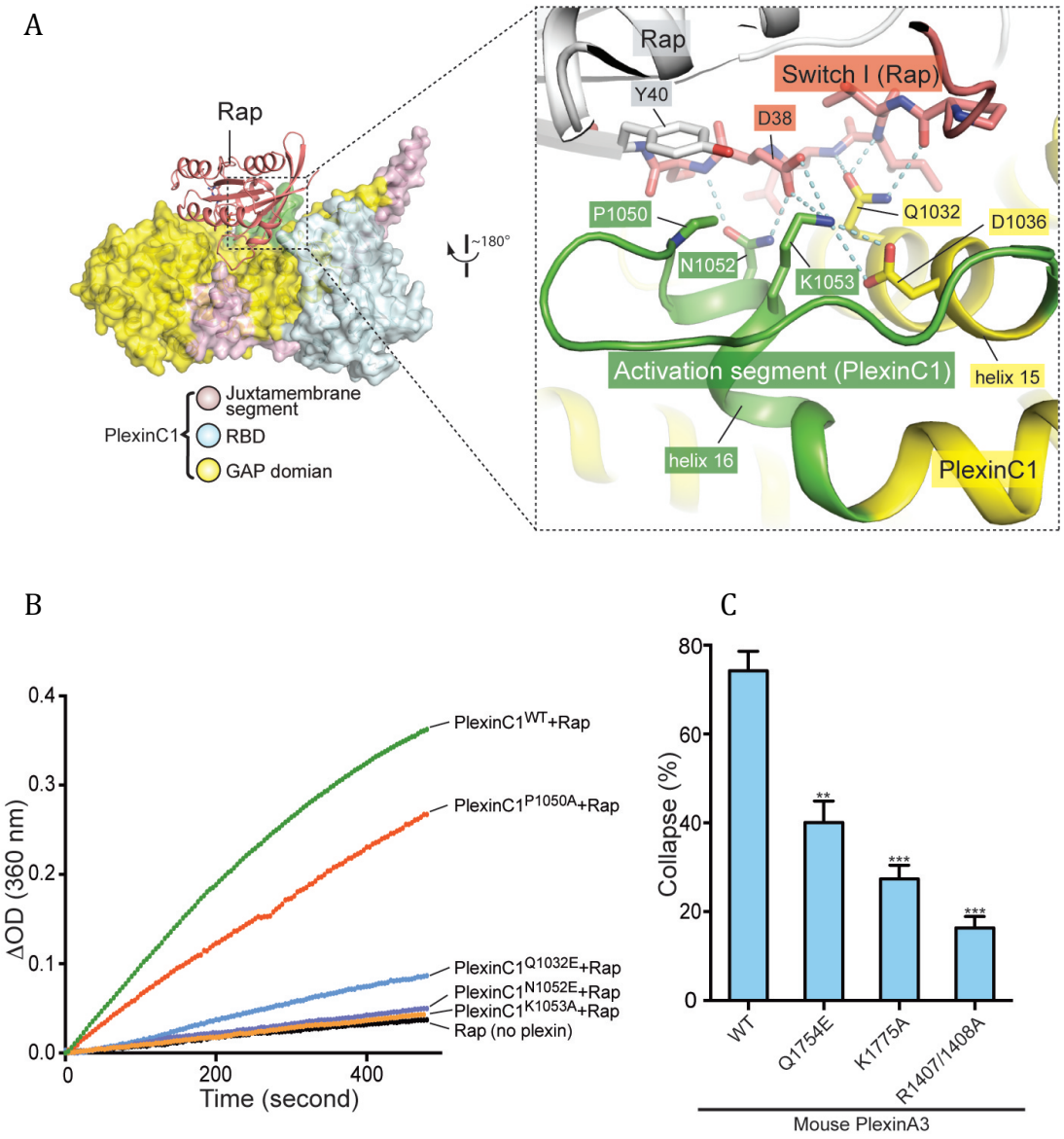

Figure 4-6. Interactions between the activation segment in PlexinC1 and Switch I in Rap.

(A) Detailed view of the interface between the activation segment and Switch I. Polar interactions and potential hydrogen bonds are indicated by dashed lines.

(B) GAP activity assays for $PlexinC1_{cyto}$ mutants at the activation segment/Switch I interface. The plots are representatives of 3 independent experiments.

(C) COS7 cell collapse assays for mutations at the activation segment/Switch I interface. Q1754E and K1775A of mouse PlexinA3 correspond to Q1032E and K1053A of zebrafish PlexinC1, respectively. The results for the wild type and the arginine-finger mutant (R1407/1408A) are shown as positive and negative controls, respectively. At least 150 cells were counted for each sample. Error bars: standard error of the mean from three independent experiments. Statistical significance is determined by two-tailed Student's t-test (** $p<0.01$; *** $p<0.001$).

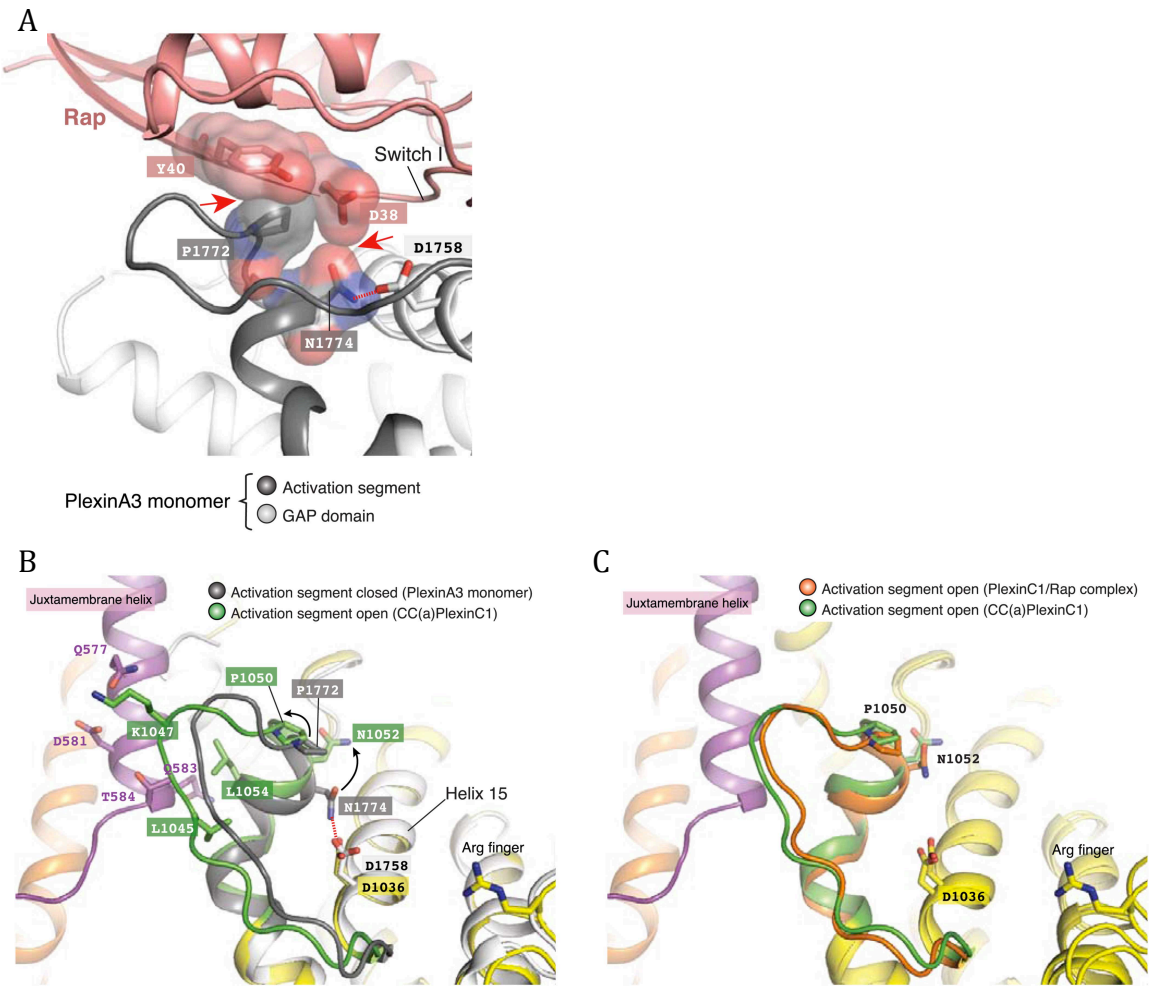

Figure 4-7. Dimerization-induced opening of the activation segment.
(A) Docking of Rap to the inactive PlexinA3$_{cyto}$ structure. The docking is based on a superimposition between PlexinA3 and PlexinC1 in the PlexinC1/Rap complex structure. Red dashed line indicates a hydrogen bond, red arrows indicate steric clashes and unfavorable interactions. PDB ID: 3IG3.

(B) Comparison of the activation segment in the structures of the coiled-coil PlexinC1$_{cyto}$ dimer and PlexinA3$_{cyto}$. Conformational differences important for GAP activation are highlighted by black arrows.

(C) Comparison of the activation segment in the structures of the coiled-coil PlexinC1$_{cyto}$ dimer and the PlexinC1$_{cyto}$/Rap complex dimer.

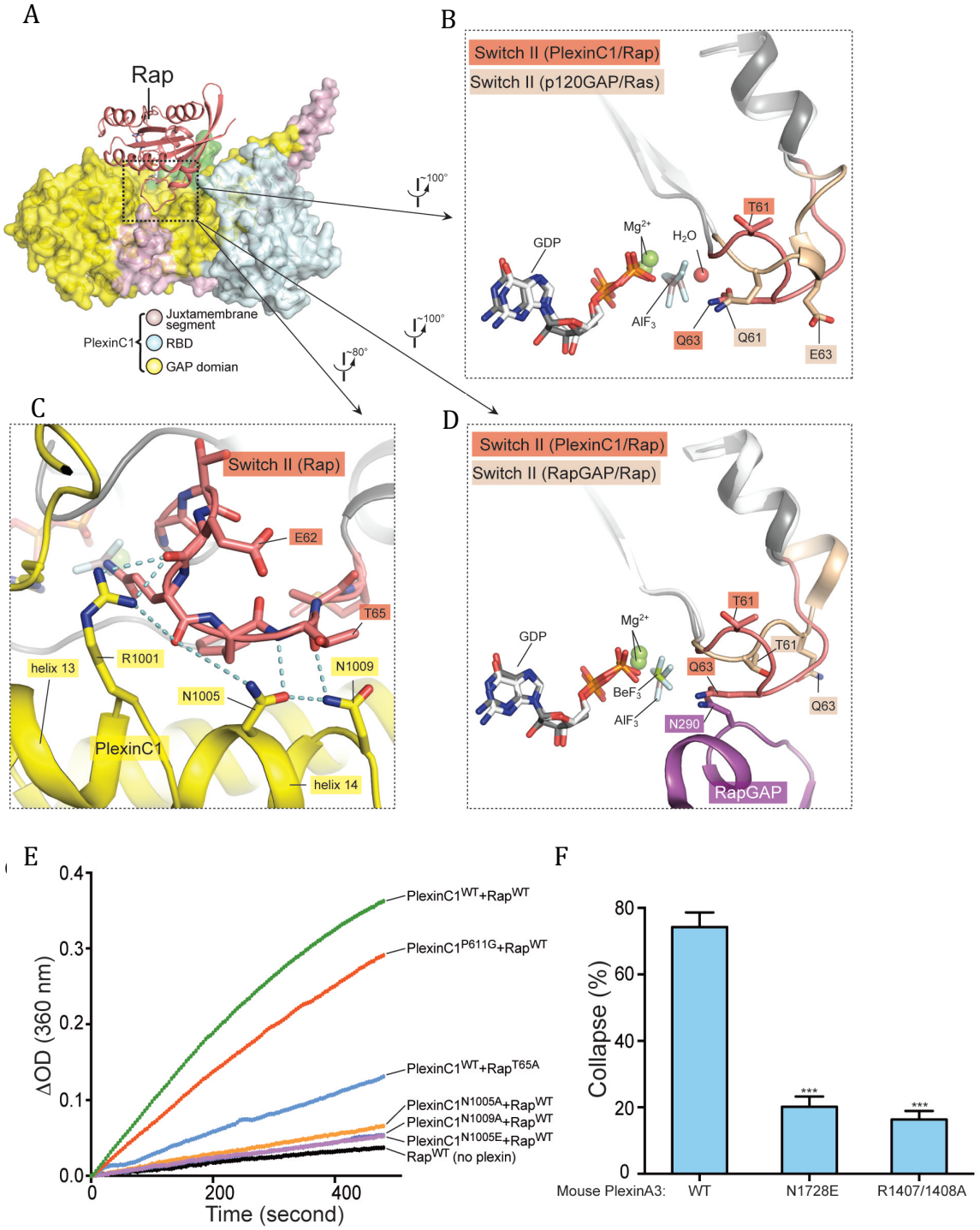

Figure 4-8. The Gln63-in conformation of Switch II in the PlexinC1$_{cyto}$/Rap1B complex.

(A) Overall structure of the complex. The box indicates the region that is shown in expanded views in (B), (C) and (D).

(B) Comparison of the Switch II conformation in the PlexinC1/Rap and the p120GAP/Ras (PDB ID: 1WQ1) complexes. The nucleophilic H_2O is not included in the $PlexinC1_{cyto}$/Rap1B structure due to low resolution of the density map.

(C) Comparison of the Switch II conformation in the PlexinC1/Rap and the RapGAP/Rap (PDB ID: 3BRW) complexes.

(D) Specific interactions between PlexinC1 and Switch II in Rap1B. Polar interactions and potential hydrogen bonds are indicated by dashed lines.

(E) GAP activity assays for mutations at the plexin/Switch II interface. The plots are representatives of 3 independent experiments.

(F) COS7 cell collapse assays for mutations at plexin/Switch II interface. N1728E of mouse PlexinA3 corresponds to N1005E of zebrafish PlexinC1. At least 150 cells were counted for each sample. Error bars: standard error of the mean from three independent experiments. Statistical significance is determined by two-tailed Student's t-test (*** $p<0.001$).

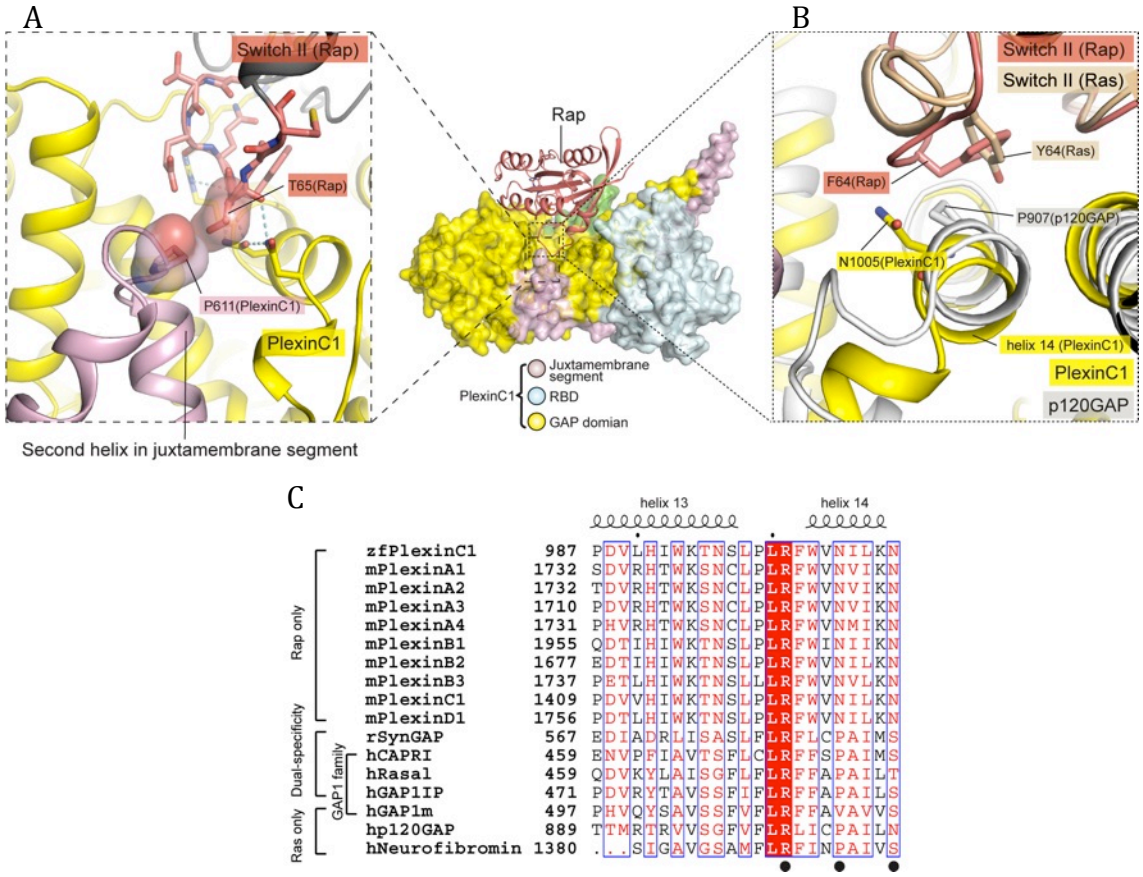

Figure 4-9. Comparison of Switch II-interacting region between plexin, RasGAPs and dual-specific GAPs.
(A) Interaction between Pro611 in PlexinC1 and Thr65 in Rap1B.

(B) Packing interactions made by Phe64 in Rap1B with PlexinC1 and Tyr64 in Ras with p120GAP. The PlexinC1$_{ctyo}$/Rap1B and the p120GAP/Ras structures are superimposed using Rap1B and Ras as references. Pro907 in p120GAP contributes to Ras binding by stacking against Tyr64 in Switch II of Ras. A valine residue at the position of Pro907 (Val515 in GAP1m in (C)) appears to be readily accommodated in this binding mode. While a proline residue at this position also seems compatible with the Gln63-in conformation of Rap, a valine residue with its bulkier sidechain likely clashes with Phe64 in Rap.

(C) Sequence alignment of the major Switch II-interacting segment in plexins, RasGAPs and dual-specificity GAPs. The black circles highlight the three residues (Arg1001, Asn1005 and Asn1009 in zebrafish PlexinC1) that make critical interactions with Switch II in Rap. zf: zebrafish; m: mouse; h: human; r: rat.

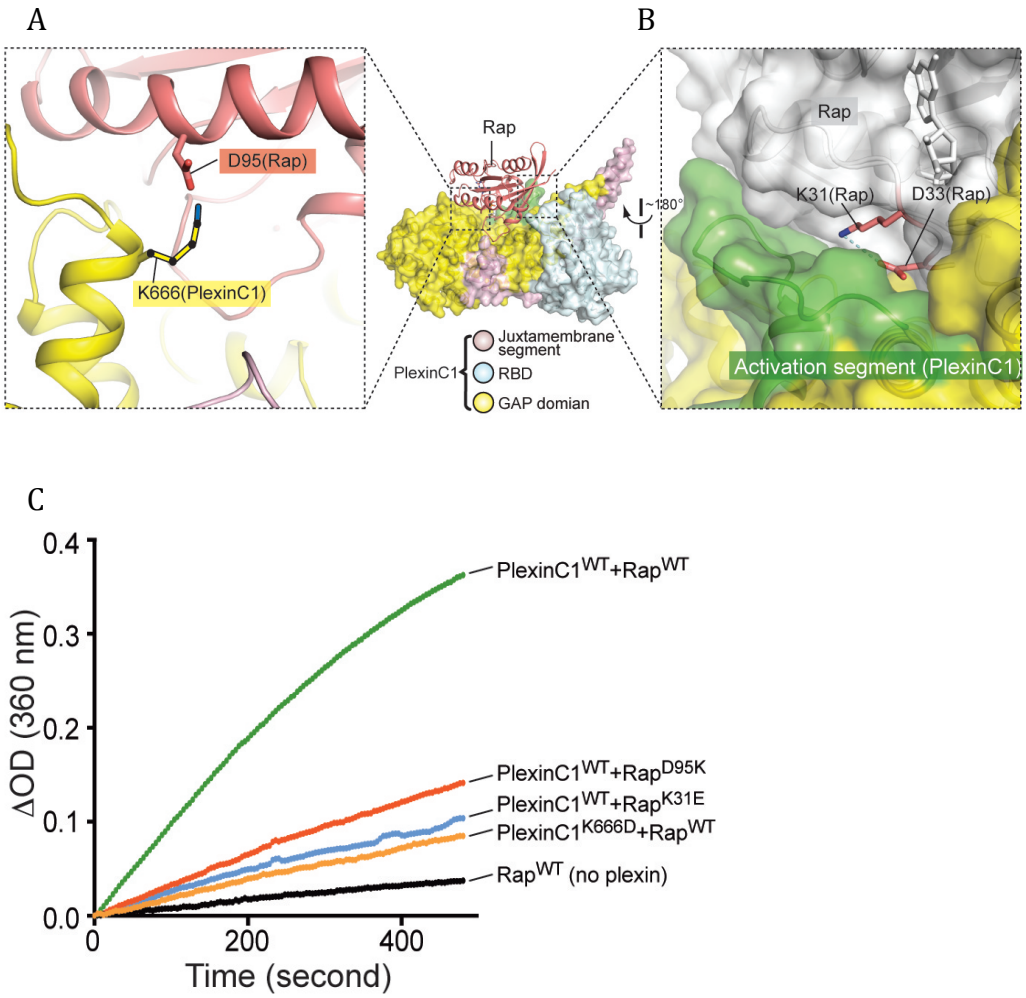

Figure 4-10. Additional specificity determinants in the PlexinC1/Rap1B complex.
(A) Potential interaction between Lys666 in PlexinC1 and Asp95 in Rap. The side chain of Lys666 in PlexinC1 is not built in the final model due to weak electron density. It is modeled to show its potential interaction with Asp95 in Rap.

(B) Burial of Lys31 in Rap1B at the PlexinC1/Rap1B interface.

(C) GAP activity assays for the specificity determinants. The plots are representatives of 3 independent experiments.

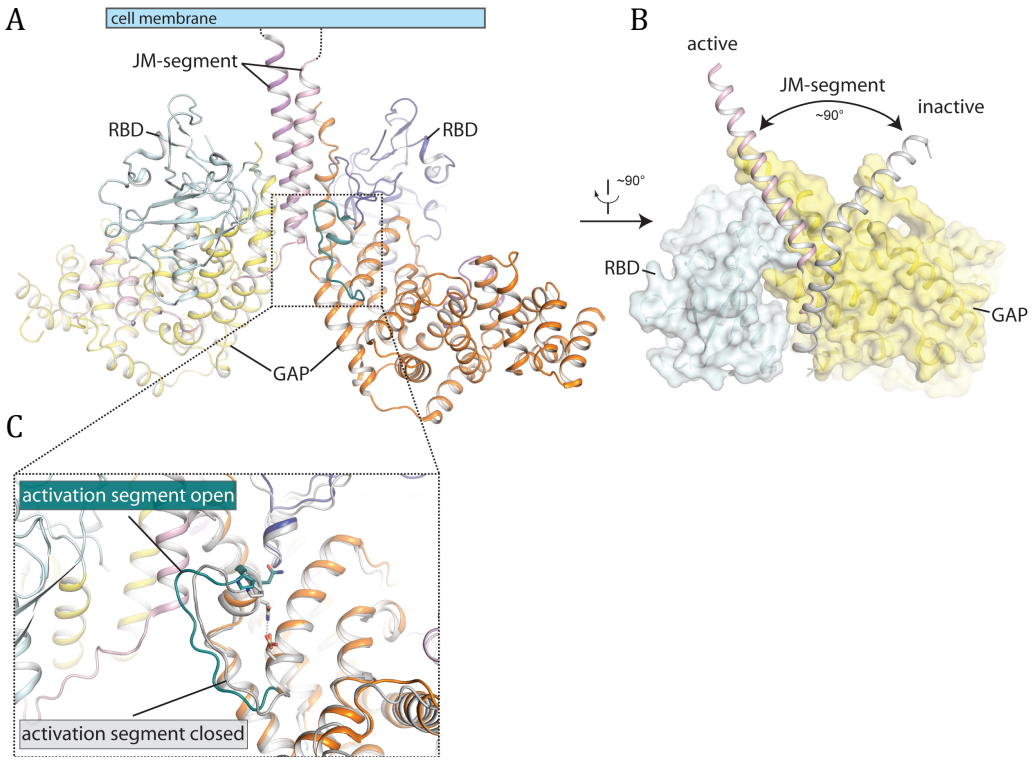

Figure 4-11. Dimerization-induced activation of the plexin cytoplasmic region.
(A) Structure of the active dimer of the cytoplasmic region of zebrafish PlexinC1. Domains are labeled and the bound Rap molecules have been omitted for clarity. PDB ID: 4M8N.

(B) Dimer-induced conformational change of the juxtamembrane region. The PlexinC1 subunit on the left from (A) is superimposed onto the structure of the inactive, monomeric PlexinA3 (PDB ID: 3IG3). The conformational difference between the two structures is highlighted.

(C) Dimer-induced conformational change of the activation segment. The conformations of the activation segment in the structure of PlexinA3 and the active dimer are compared.

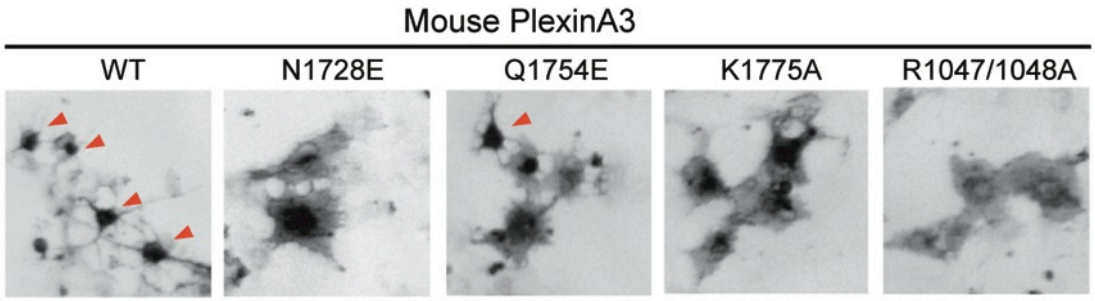

Figure 4-12. Representative images from the COS7 cell collapse assays.
Red arrowheads highlight collapsed cells.

Note: Yuxiao Wang performed collapse assays pictured above.

Table 4-1. Data collection and refinement statistics

Data collection	
Space group	P1
Cell dimensions	
a, *b*, *c* (Å)	76.47, 84.85, 138.91
a, *b*, *g* (°)	91.08, 95.08, 90.28
Resolution (Å)	50.0-3.30(3.36-3.30)*
R_{sym} (%)	5.2(48.7)
$I/\sigma I$	18.6(1.6)
Completeness (%)	91.0(89.2)
Redundancy	1.9(1.9)
Refinement	
Resolution (Å)	3.30
No. reflections	45104
R_{work}/ R_{free} (%)	23.8/30.1
No. atoms	22230
Protein	22088
Ligand/ion	132
Water	10
B-factors	
Protein	143.7
Ligand/ion	129.1
Water	91.4
R.m.s deviations	
Bond lengths (Å)	0.0039
Bond angles (°)	0.69
Ramanchandran plot	
Favored (%)	93.28
Allowed (%)	6.55
Disallowed (%)	0.17

*Highest resolution shell is shown in parenthesis.

CHAPTER FIVE

A Secondary PDZ Domain-Binding Site on Class B Plexins Enhances the Selectivity Towards PDZ-RhoGEF

Summary

PDZ domains are abundant protein interaction modules and typically recognize a short motif at the C-terminus of their ligands, with a few residues in the motif endowing binding specificity. The sequence-based rules however cannot fully account for the specificity between the vast number of PDZ domains and ligands in the cell. Plexins are transmembrane receptors that regulate processes such as axon guidance and angiogenesis. PDZ-RhoGEF and LARG use their PDZ domains to bind class B plexins and play critical roles in signaling. Here we present the crystal structure of the full-length cytoplasmic region of PlexinB2 in complex with the PDZ domain of PDZ-RhoGEF. The structure reveals that, in addition to the canonical C-terminal motif/PDZ interaction, the three-dimensional domain of PlexinB2 forms a secondary interface with the PDZ domain. Our biophysical and cell-based assays show that the secondary interface contributes to the specific interaction between plexin and PDZ-RhoGEF, and to signaling by plexin in the cell. Formation of secondary interfaces may be a general mechanism for increasing affinity and specificity of modular domain-mediated interactions.

Introduction

In addition to the common signaling pathways through the domains shared by all plexins, class B plexins (B1, B2 and B3) mediate a pathway through their unique C-terminal tail. The conserved "VTDL" motif at the C-terminus of these plexins binds specifically to the N-terminal PDZ (PSD-95/Discs-large/ZO-1) domains of the two related guanine nucleotide exchange factors (GEFs), PDZ-RhoGEF and LARG (leukemia-associated RhoGEF) (Aurandt, Vikis et al. 2002, Driessens, Olivo et al. 2002, Hirotani, Ohoka et al. 2002, Perrot, Vazquez-Prado et al. 2002, Swiercz, Kuner et al. 2002, Oinuma, Katoh et al. 2003). This interaction recruits PDZ-RhoGEF and LARG to the plasma membrane, where they promote the exchange of GDP for GTP for RhoA. GTP-bound active RhoA binds its downstream effectors and transduces signals that contribute to plexin-mediated regulation of axon guidance and angiogenesis (Driessens, Olivo et al. 2002, Perrot, Vazquez-Prado et al. 2002, Swiercz, Kuner et al. 2002, Basile, Barac et al. 2004). A recent study has shown that deletion of the C-terminal tail of PlexinB2 causes defects in the development of the liver vasculature in mice, highlighting the critical role of the PDZ-RhoGEF/LARG-RhoA pathway in plexin function in vivo (Worzfeld, Swiercz et al. 2014).

Over 250 PDZ domains exist in the human proteome, constituting one of the most abundant protein interaction modules (Luck, Charbonnier et al. 2012, Ye and Zhang 2013). Correspondingly, there are about 600 ligands for the PDZ domains (Kim, Kim et al. 2012). Due to these large numbers, a high degree of mutual specificity is expected between PDZ domains and their respective ligands to ensure faithful signaling in the cell. The fold of PDZ domains is composed of a six-stranded β-barrel and two α-helices. The canonical interaction mode between the PDZ domains and their ligands involves the

binding of the C-terminal tail of the ligand in an extended β-strand conformation to the groove between βB and αB in the PDZ domain. The C-terminal carboxyl group of the ligand forms two hydrogen bonds with the backbone of the conserved "GΦGF" motif (Φ: hydrophobic residue) in the βA-βB loop of the PDZ domain, which underlies the strong preference of PDZ domains for C-terminal tails. Previous studies have established the general rules of ligand specificity for PDZ domains (Songyang, Fanning et al. 1997). Class I PDZ domains recognize C-terminal motifs with the "T/S-X-Φ" (X: any residue; Φ: hydrophobic residue) sequence, whereas class II PDZ domains prefer the "Φ-X-Φ" sequence. The structural basis for this selectivity is relatively well understood (Ye and Zhang 2013). However, many PDZ domains are promiscuous towards short peptidic ligands and defy these simple rules of specificity. Particularly, the PDZ domains in PDZ-RhoGEF and LARG, assigned to class I PDZ domains based on their sequences, bind with similar affinities to many peptides of both classes I and II (Smietana, Kasztura et al. 2008).

Isolated C-terminal peptides from class B plexins showed modest affinities to the PDZ domains of PDZ-RhoGEF and LARG in earlier studies, with the dissociation constant (K_d) in the range of 10-40 μM (Paduch, Biernat et al. 2007, Liu, Zhang et al. 2008, Smietana, Kasztura et al. 2008). In contrast, the interaction between full-length class B plexins and PDZ-RhoGEF/LARG has been detected by various in vitro and cell-based experiments (Aurandt, Vikis et al. 2002, Driessens, Olivo et al. 2002, Perrot, Vazquez-Prado et al. 2002, Swiercz, Kuner et al. 2002, Oinuma, Katoh et al. 2003). Many other PDZ domains, however, failed to bind class B plexins under similar conditions (Aurandt, Vikis et al. 2002, Hirotani, Ohoka et al. 2002, Perrot, Vazquez-

Prado et al. 2002). It is not clear how class B plexins achieve this strong and specific interaction with PDZ-RhoGEF and LARG. More broadly, the sequence-based rules described above are likely an oversimplification of the mechanisms underlying specificity between the over 250 PDZ domains and 600 ligands. Most previous structural and binding analyses were conducted using isolated peptidic binding motifs derived from ligands of PDZ domains, leaving open the question of whether other regions in the ligands are involved in the interaction.

To address these questions, we determined the crystal structure of the complex between the full-length cytoplasmic region of PlexinB2 and the PDZ domain of PDZ-RhoGEF. The structure reveals a secondary interface between the PlexinB2 and the PDZ domain, in addition to the canonical interaction mediated by the C-terminal PDZ-binding motif of PlexinB2. Our structure-based mutational analyses show that the secondary interface plays an important role in the highly specific interaction between class B plexins and PDZ-RhoGEF.

Results

Crystal structure of the PlexinB2/PDZ complex reveals a secondary binding interface

To better understand the specificity between class B plexins and PDZ-RhoGEF/LARG, we determined the crystal structure of the full-length cytoplasmic region of mouse PlexinB2 ($PlexinB2_{cyto}$) in complex with the N-terminal PDZ domain from human PDZ-RhoGEF (Figure 5-1A). The PDZ domains from human and mouse PDZ-RhoGEF only have one non-identical residue, located outside of the plexin-binding interface (Figure 5-2). The same is true for the LARG PDZ domain. Therefore, the

species mismatch is not expected to affect the plexin/PDZ interaction. The asymmetric unit of the crystal contains one PlexinB2/PDZ complex (Figure 5-3). The N-terminal juxtamembrane helix in $PlexinB2_{cyto}$ is not present in the electron density map; it is probably disordered or degraded during crystallization. The rest of the $PlexinB2_{cyto}$ is similar to previously reported structures of other plexins (Figure 5-4) (He, Yang et al. 2009, Tong, Hota et al. 2009, Bell, Aricescu et al. 2011, Wang, He et al. 2012, Wang, Pascoe et al. 2013). The PDZ domain in the structure is similar to the NMR structure of the PDZ domain of LARG (Figure 5-5). $PlexinB2_{cyto}$ and the PDZ domain form a 1:1 complex, with the PlexinB2 C-terminal "VTDL" motif and the PDZ domain interacting in the typical PDZ/type I ligand binding mode. These interactions are similar to those seen in the NMR structure of the complex between the octameric tail peptide from PlexinB1 and the PDZ domain from LARG reported previously (Figure 5-1C and 5-4) (Liu, Zhang et al. 2008). In addition to these interactions, Lys1838 in PlexinB2, immediately upstream of the "VTDL" motif, makes an electrostatic contact with Asp64 in the PDZ domain. The equivalent interaction, between Lys2131 in the PlexinB1 peptide and Asp89 in the LARG PDZ domain, is also present in the NMR structure (Figure 5-5)(Liu, Zhang et al. 2008). Similar interactions have been extensively characterized for many type I PDZ domains and their ligands (Ye and Zhang 2013).

In addition to the canonical interface, our structure shows a secondary interface that is formed between the last two helices in the GAP domain of PlexinB2 and one face of the PDZ domain composed of β strands B through D (Figure 5-6A). The two interfaces together bury ~1500 $Å^2$ of solvent accessible surface area, with the canonical and the secondary interfaces contributing ~600 and ~900 $Å^2$ respectively. The center of the

secondary interface is mediated by hydrophobic interactions between Leu68 from the PDZ domain and two alanine residues (Ala1832 and Ala1833) from PlexinB2 (Figure 5-6A). Ile66 of the PDZ and Tyr1806 of PlexinB2 contribute additional hydrophobic contacts at the periphery of the interface. The interface is further stabilized by polar interactions. Arg88 and Asp64 from the PDZ domain interact with Asp1807 and Lys1838 from PlexinB2$_{cyto}$, respectively (Figure 5-6B). Tandem glutamine residues from PlexinB2 (Gln1829 and 1830) interact with the backbone carbonyls of Gly86 and Asp87 from the PDZ domain. Ser62 and Gln70 from the PDZ domain make polar interactions with the C-terminal end of the last helix in the PlexinB2 GAP domain (Figure 5-6B). Some of these interactions may be mediated by hydrogen bonds, but are not assigned due to the moderate resolution of the structure.

The PDZ domain of human LARG crystallized with PlexinB2$_{cyto}$ in a similar crystal form, yet these crystals diffracted relatively poorly. The comparable space groups and unit cell dimensions imply that the LARG and PDZ-RhoGEF PDZ domains bind PlexinB2 similarly. The residues in PlexinB2 mediating the secondary interface are highly conserved across class B plexins but not among plexins of classes A, C and D (Figure 5-6C). Ile66 and Leu68 in the PDZ domain of PDZ-RhoGEF are replaced by a proline and phenylalanine residue respectively in LARG, which maintain the hydrophobicity of the interface. Other residues involved in the secondary interface are identical between PDZ-RhoGEF and LARG from both human and mouse (Figure 5-2). These residues are however not conserved in PDZ domains from other proteins (Figure 5-2). These patterns of sequence conservation indicate that class B plexins and PDZ-

RhoGEF/LARG have co-evolved the secondary interface to enhance their mutual specificity, and the secondary interface is functionally important.

Tight binding between full-length PlexinB2$_{cyto}$ and the PDZ domain from PDZ-RhoGEF

Using fluorescence-based methods or isothermal titration calorimetry (ITC), several studies have determined the K_d value between isolated C-terminal peptides from PlexinB1 and the PDZ domain of PDZ-RhoGEF is in the range of 30-36 μM (Paduch, Biernat et al. 2007, Smietana, Kasztura et al. 2008). The PDZ domain of LARG shows similar affinity to the tail peptide from PlexinB1 (Paduch, Biernat et al. 2007, Liu, Zhang et al. 2008, Smietana, Kasztura et al. 2008). The peptides used in the studies of PDZ-RhoGEF included no more than the C-terminal 6 residues of human PlexinB1, which are identical to those in mouse PlexinB2. We analyzed the binding between PlexinB2$_{cyto}$ and the PDZ domain of PDZ-RhoGEF using ITC. PlexinB2$_{cyto}$ with the C-terminal 4 residues truncated (ΔVTDL) showed no detectable binding to the PDZ domain, consistent with the notion that the C-terminal motif is critical for the interaction (Figure 5-7A, B). Full-length PlexinB2$_{cyto}$ binds the PDZ domain with a K_d value of 2 μM (Figure 5-7A, B), which is over 10-fold tighter than that of the isolated C-terminal motif. These results suggest that the secondary interface as observed in our crystal structure significantly enhances the plexin/PDZ interaction.

Mutational analyses of the secondary interface

To buttress the contention that the secondary interface is important for the plexin/PDZ interaction, we assessed the effects of a series of mutations at this interface

by ITC (Figures 5-7B, C). Three mutations, Y1806A, A1832E and A1833E, were introduced individually into PlexinB2$_{cyto}$. The Y1806A mutant displayed moderately attenuated binding (K_d = 3.7 μM) compared to the wild type PlexinB2$_{cyto}$ (Figures 5-7A, B). In contrast, the A1832E and A1833E mutations significantly reduced the binding, yielding K_d values of 13 and 30 μM, respectively (Figure 3A-B). The A1833E mutation reduces the affinity to the level of the isolated C-terminal peptide of PlexinB1, effectively eliminating the contribution of the secondary interface. These results are consistent with the structural features of the secondary interface. Tyr1806 is located at the periphery of the interface, and the alanine mutation removes a portion of the hydrophobic interaction but does not sterically occlude binding. Introducing a charged, and significantly larger residue to the hydrophobic core of the interface as in the case of the A1832E and A1833E mutations, however, disrupts the secondary interface.

Similar to the mutations introduced to plexin, the mutations to PDZ also attenuated binding to various degrees consistent with the features of the secondary interface as seen in the structure. The PDZ R88A mutant increased K_d by ~3-fold to 6.4 μM (Figures 5-7A, B). Loss of the peripheral interaction between Arg88 in the PDZ domain and Asp1807 in PlexinB2$_{cyto}$ is not expected to actively disrupt the interface core or the ability of other contacts to form. The R88E mutation, which introduces charge/charge repulsion with Asp1807 in PlexinB2$_{cyto}$, reduced the affinity by 20-fold (K_d = 40 μM). Mutating Leu68 in the PDZ domain, which docks into the hydrophobic cavity created by Ala1832 and Ala1833 in PlexinB2$_{cyto}$, reduces the affinity by ~5-fold. Mutating a peripheral hydrophobic residue in the PDZ domain, I66A, moderately attenuated binding. Taken together these data demonstrate that the secondary interface is

responsible for the over 10-fold tighter binding to the PDZ domain by full-length PlexinB2$_{cyto}$ compared to the isolated PDZ-binding motif.

Both binding interfaces contribute to recruitment of PDZ-RhoGEF by Plexin

It has been shown previously that the GEF activity of PDZ-RhoGEF and its homologues can be facilitated by membrane recruitment to membrane-delimited substrates such as RhoA (Medina, Carter et al. 2013), and that this functional recruitment can mediate hormone signaling in cells (Carter, Gutowski et al. 2014). In the reconstituted system, GEFs were recruited to the surface of lipid vesicles that contained regulatory partners and substrates tethered to the membrane surface through interaction of poly-histidine tags with Ni-NTA-conjugated lipids. We used this system to examine the interaction of full-length PDZ-RhoGEF with PlexinB2$_{cyto}$ (Figures 5-8A, B, C). PDZ-RhoGEF in solution displayed modest nucleotide exchange activity towards RhoA tethered to lipid vesicles. Addition of His$_6$-PlexinB2$_{cyto}$ produced a concentration-dependent increase in the exchange activity (Figures 5-8A, B), suggesting effective and functional recruitment of PDZ-RhoGEF by His$_6$-PlexinB2$_{cyto}$ to membrane localized RhoA. Deletion of the C-terminal motif from PlexinB2 (ΔVTDL) eliminated the increase in the GEF activity (Figures 5-8B, C), consistent with an anticipated reduction in the recruitment. We further tested mutations in the secondary interface, two in the PDZ domain (R88E and R88A) and two in PlexinB2$_{cyto}$ (A1832E and A1833E). All four mutants attenuated the stimulatory effect of PlexinB2 on the GEF activity of PDZ-RhoGEF (Figure 5-8C). The partial reduction by the R88A mutation is consistent with its more moderate effect on binding affinity (Figure 5-7). These results implicate both the

primary and secondary interfaces in the recruitment of PDZ-RhoGEF by plexin. The sufficiency of this interaction is demonstrated by the recruitment of a chimeric protein containing the PDZ domain of PDZ-RhoGEF linked to an unrelated RacGEF, TRIO (triple functional domain protein) (Figure 5-8D). Here, His_6-$PlexinB2_{cyto}$ stimulates nucleotide exchange of membrane delimited Rac1 by the chimeric PDZ-TRIO, but not TRIO alone.

The secondary interface contributes to plexin-mediated activation of PDZ-RhoGEF in cells

Activation of class B plexins by semaphorin has been shown to activate PDZ-RhoGEF and LARG, leading to increased levels of GTP-bound RhoA in cells (Aurandt, Vikis et al. 2002, Driessens, Olivo et al. 2002, Hirotani, Ohoka et al. 2002, Perrot, Vazquez-Prado et al. 2002, Swiercz, Kuner et al. 2002, Oinuma, Katoh et al. 2003). To examine whether this plexin/PDZ-RhoGEF-mediated activation of RhoA is dependent on the secondary interface as seen in our crystal structure, we used a pull-down assay for quantifying RhoA(GTP) levels in the cell (Ren and Schwartz 2000). Full-length human PlexinB1, which is nearly identical in sequence to mouse PlexinB2 in both the C-terminal motif and the secondary interface, was used in these experiments. Consistent with previous studies, the results show that over-expression of PlexinB1 increased the levels of RhoA(GTP) in HEK293T cells, which express PDZ-RhoGEF endogenously (Figure 5-9) (Perrot, Vazquez-Prado et al. 2002, Basile, Barac et al. 2004). RhoA activation is further enhanced by semaphorin treatment. Deletion of the C-terminal "VTDL" motif in PlexinB1 (ΔVTDL) abolished RhoA activation in the presence or absence of semaphorin

treatment. These results are also consistent with previous studies(Perrot, Vazquez-Prado et al. 2002, Swiercz, Kuner et al. 2002). We then tested the effects on RhoA activation of the A2125E and A2126E mutations of PlexinB1, equivalent to the secondary interface mutations A1832E and A1833E of PlexinB2 respectively. The results show that these mutations both attenuated RhoA activation, although the reduction was not as server as that caused by the ΔVTDL mutation (Figure 5-9). Taken together, our data strongly support the hypothesis that the C-terminal motif and secondary interface in class B plexins together contribute to optimal recruitment of PDZ-RhoGEF and activation of RhoA for signal transduction in the cell.

Discussion

Protein interactions between modular domains such as PDZ, SH2 and SH3 domains and linear binding motifs are a common theme in biology (Pawson and Nash 2003). An established paradigm is that sequence variations of one or a few residues in the binding motifs determine the specificity. However, modules of the same types often show similar sequence preferences for the binding motifs, and similar or identical motifs often exist in different proteins. This paradigm is therefore inadequate for rationalizing the diverse yet specific interactions mediated by modular domains. In the case of PDZ domains, binding motifs of different classes do not always show large differences in affinity to cross-typed PDZ domains. Extensive investigations, including large-scale peptide library screening and bioinformatics analyses, have shown that residues beyond positions 0 and -2 in PDZ binding motifs are involved in fine-tuning the specificity (Luck, Charbonnier et al. 2012, Ye and Zhang 2013). Based on these studies, as many as 16 classes have been defined to account for the specificity profiles of PDZ domains

(Tonikian, Zhang et al. 2008). It has also been proposed that rather than distinguishing ligands based on classes, PDZ domains are evenly distributed throughout the selectivity space to avoid cross-reactivity, although the degree of selectivity conferred by this mechanism seems subtle (Stiffler, Chen et al. 2007). A recent study has shown that the PDZ domain in the protein PALS1 forms a structural supramodule with the SH3 and guanylate kinase domains, with all the three domains collectively contributing to tight and specific binding to the C-terminal tail of its ligand named crumbs (Li, Wei et al. 2014).

The above-mentioned analyses are largely limited to linear binding motifs in the PDZ ligands. Our finding here of the secondary interface mediated by the folded domains of class B plexins and PDZ-RhoGEF provides a new dimension to the mechanism by which PDZ domains achieve specificity. Interestingly, a recent study has shown that the C-terminal SH2 domain in phospholipase Cγ makes a functionally important secondary interface with the kinase domain of fibroblast growth factor receptor, in addition to the interaction between the SH2 domain and the phosphoryl-tyrosine motif (Bae, Lew et al. 2009). A secondary interface is also present in the complex between the SH3 domain of the Fyn kinase and Nef of the human immunodeficiency virus (Lee, Saksela et al. 1996). Secondary interactions mediated by three-dimensional domains may be broadly used by protein interaction modules for increasing affinity and specificity. Interfaces involving folded domains are less likely to be mimicked by non-specific interactions, as it requires both specific interactions between contacting residues and three-dimensional shape complementarity. This mode of interaction provides a solution for improving binding

affinity of modular domains to their cognate ligands while maintaining modest stickiness at the canonical motif-binding site.

It is currently unclear how the interaction between class B plexins and PDZ-RhoGEF/LARG is regulated by semaphorin binding to plexin. Prior to activation, plexin exists as an inactive monomer or inhibitory dimer (He, Yang et al. 2009, Wang, He et al. 2012). Semaphorin binding induces the formation of the active dimer of plexin(Janssen, Robinson et al. 2010, Liu, Juo et al. 2010, Nogi, Yasui et al. 2010, Janssen, Malinauskas et al. 2012, Wang, Pascoe et al. 2013). PDZ-RhoGEF and LARG also form dimers or oligomers, mediated primarily by their C-terminal coiled-coil region (Chikumi, Barac et al. 2004). The plexin active dimer and the PDZ-RhoGEF/LARG dimer may form a 2:2 complex (Figure 5-10A). Alternatively, dimeric PDZ-RhoGEF/LARG may bridge two copies of the active dimer of plexin, leading to their clustering on the cell surface (Figure 5-10B). The dimerization/oligomerization may increase the avidity between plexin and PDZ-RhoGEF/LARG. PDZ-RhoGEF and LARG both have other domains that help target them to the plasma membrane, such as the Pleckstrin-homology (PH) domain that interacts with GTP-bound RhoA (Chen, Medina et al. 2010). These factors together may facilitate the interaction between plexin and PDZ-RhoGEF/LARG, and thereby enhance their ability to discriminate against non-specific interactions.

Materials and Methods

Protein expression and purification

The construct for the cytoplasmic region of mouse PlexinB2 (residues 1226-1842) was obtained from OpenBiosystems and subcloned into a modified pET28 vector

(Novagen, Darmstadt) which encodes an N-terminal His_6 tag and a cleavage site for the human rhinovirus C3 protease (Wang, He et al. 2012). $PlexinB2_{cyto}$ proteins were expressed using the bacteria strain ArcticExpress (Stratagene) and purified as previously described (He, Yang et al. 2009, Wang, He et al. 2012, Wang, Pascoe et al. 2013). For the lipid vesicle assays, the N-terminal His_6 tag was left intact for tethering $PlexinB2_{cyto}$ to the Ni-NTA conjugated lipids. In all other cases, the His_6 tag was removed by addition of the human rhinovirus C3 proteases. Mutant constructs of PlexinB2 were generated using PCR-based mutagenesis.

The PDZ domains from human PDZ-RhoGEF and LARG (residues 42-125 and 67-150 respectively) were subcloned into the same modified pET28 vector as PlexinB2. The PDZ domain of PDZ-RhoGEF tends to form an inter-chain disulfide linkage by Cys47 (Paduch, Biernat et al. 2007). To avoid this issue, a C47S mutant was made for the ITC experiments. All interface mutations of the PDZ domain were introduced in the C47S background. PDZ domains were expressed using the bacteria strain BL21(DE3) and affinity purified using a 1 mL nickel conjugated column (HisTrap FF, GE Healthcare). The N-terminal His_6-tag was removed by the human rhinovirus C3 protease. Following protease digestion, proteins were further purified using a size exclusion column (Superdex 75 10/300 GL, GE Healthcare) and the monomeric species was collected.

The full length human cDNA of PDZ-RhoGEF (PRG) was cloned into pFastbac1 (Invitrogen) modified with an N-terminal EE-tag (EYMPME), expressed in *Spodoptera frugiperda* (SF9) cells with the Bac-to-Bac system (Invitrogen), and purified by affinity chromatography with anti-EE coupled Sepharose (BAbCO) as described (Wells, Liu et

al. 2002). Mutations in the PDZ domain were introduced by site directed mutagenesis. Preparation of full length RhoA with a C-terminal hexahistidine tag replacing the last four amino acids (RhoA-His_6) was described previously (Medina, Carter et al. 2013); Rac1 with a His_6-tag on its C-terminus (Rac1-His_6) was inserted into the same expression vector and purified similarly. The PDZ domain of PRG (residues 2 to 127) was cloned with a linker sequence (GSGTGSGIDGTGTGTG) onto the N-terminus of the first DH-PH domains of human Trio (residues 1226–1535) to create PDZ-TRIO, inserted into pGEX-KG-TEV, expressed in Escherichia coli strain BL21 (DE3), and purified as described (Chen, Medina et al. 2010, Chen, Guo et al. 2011).

The Rho-Binding Domain (RBD) construct of mouse Rhotekin (residues 7-89) was cloned into the pGEX-2T vector (GE Healthcare). The Rhotekin RBD was expressed using the bacteria strain BL21 (DE3) and affinity purified using a 1 mL GST column (GSTrap FF, GE Healthcare), followed by a size exclusion column (HiLoad 16/60 Superdex 200, GE Healthcare).

Crystallization and Structure determination

Various constructs of all three mouse class B plexins and the PDZ domains from both PDZ-RhoGEF and LARG were subjected to co-crystallization trials. Among these, the mouse $PlexinB2_{cyto}$ co-crystallized with the PDZ domains from either PDZ-RhoGEF or LARG. Initial screens were conducted with PlexinB2 and the PDZ domains mixed at 1:1 molar ratio using sitting drop 96-well plates. The $PlexinB2_{cyto}$/PDZ complexes crystallized at 20 °C against a well solution containing 0.2 M K/Na tartrate, 0.1 M Na citrate pH 5.6, and 2.0 M ammonium sulfate, with a mixture of PlexinB2 at 6 mg/mL and

the PDZ domains at 0.78 mg/mL. Larger crystals were grown using the PDZ domain from PDZ-RhoGEF by hanging drop vapor diffusion at 20 °C against a well solution containing 0.2 M K/Na tartrate, 0.1 M Na citrate pH 5.3, and 1.4 M ammonium sulfate. Larger crystals were also grown using the PDZ domain from LARG by hanging drop vapor diffusion at 4 °C in 0.2 M K/Na tartrate, 0.1 M Na Citrate pH 6, and 2.0 M ammonium sulfate. Crystals were cryo-protected using the crystallization solution supplemented with 25% (v/v) glycerol and flash cooled in liquid nitrogen. Diffraction data were collected at 100 K at the Advanced Photon Source (Argonne National Laboratory) on beamline 19ID. HKL2000 was used to index and scale the data (Otwinowski and Minor 1997). Diffraction of crystals grown using the PDZ domains from either PDZ-RhoGEF or LARG was consistent with the $P6_222$ space group. Only crystals grown using the PDZ domain of PDZ-RhoGEF, however, diffracted strongly with data extending to 3.2 Å. Data were highly anisotropic, with diffraction in the c* direction being much weaker than that in the a* and b* directions. Data was therefore processed with the 'auto-correction' option in HKL2000, which truncates and scales anisotropic data. The Phaser module of the Phenix software package was used for molecular replacement phasing (Adams, Grosse-Kunstleve et al. 2002, Mccoy, Grosse-Kunstleve et al. 2007). The structures of the cytoplasmic region of mouse PlexinA3 (PDB ID: 3IG3) and the PDZ domain of human LARG (PDB ID: 2OS6) were used as the search models.

Model building, refinement, and validation were performed using the Coot, Phenix, and MolProbity programs respectively (Adams, Grosse-Kunstleve et al. 2002, Emsley and Cowtan 2004, Chen, Arendall et al. 2010). Data collection and refinement

statistics are listed in Table 5-1. All structure figures were generated using the PyMOL program (the PyMOL Molecular Graphics System, Schrodinger). Protein sequence alignments were generated and rendered using the T-Coffee and ESPript programs respectively (Gouet, Courcelle et al. 1999, Notredame, Higgins et al. 2000). Buried surface area was calculated using the Get_Area function in PyMOL.

ITC experiments

All ITC experiments were conducted in triplicate using a MicroCal ITC200 instrument (GE Healthcare). All PDZ proteins used in these experiments contained the C47S mutation to avoid the inter-chain disulfide formation as mentioned above (Paduch, Biernat et al. 2007). The mutation site is distal to the binding interface and not expected to affect binding. Purified and concentrated proteins ($PlexinB2_{cyto}$ and PDZ) were dialyzed overnight at 4 °C against 1 L of buffer containing 10 mM Tris pH 8.0, 150 mM NaCl, 10% glycerol, and 1 mM Tris(2-carboxyethyl)phosphine. All proteins were thoroughly degassed before titration. PDZ proteins (300 or 500 μM) were placed in the syringe and $PlexinB2_{cyto}$ proteins (30 or 50 μM) were placed in the cell. Titrations of wild type PDZ into wild type $PlexinB2_{cyto}$ were carried out using 300 and 30 μM protein solutions respectively. Titration of wild type PDZ into $PlexinB2_{cyto}$ with the C-terminal 4 residue truncation was also performed at 300 and 30 μM respectively. All other mutant titrations were carried out using 50 μM $PlexinB2_{cyto}$ and 500 μM PDZ solutions. The PDZ was titrated into the cell over the course of 18 injections of 2 μL. All titrations were conducted at 20 °C with continuous stirring at 1000 RPM and 2 min intervals between injections. Data were integrated using NITPIC (Keller, Vargas et al. 2012) and passed to

SEDPHAT (Houtman, Brown et al. 2007) for fitting and global analysis. The 1:1 Hetero-Association model was used for all analysis with K_d, change in enthalpy (ΔH), and fraction of binding incompetent protein being fit. Global fit values for K_d and 1σ confidence intervals are reported. Confidence intervals were calculated in SEDPHAT using the "automatic confidence interval search with projection method" option. Representative isotherms and thermograms from each set of titrations are shown. All ITC data figures were generated with the GUSSI program (Brautigam 2015, in press).

Vesicle-based GEF activity assays

Assays with unilamellar phospholipid vesicles followed procedures described previously (Medina, Carter et al. 2013). Briefly, vesicles of approximately 100 nm diameter were prepared by extrusion through an Mini-Extruder using a 100-nm polycarbonate membrane (Avanti Polar Lipids). 1-Palmitoyl-2-oleoyl-*sn*-glycero-3-phosphoethanolamine, 1-palmitoyl-2-oleoyl-*sn*-glycero-3-phosphocholine, and 1,2-dioleoyl-*sn*-glycero-3-[(*N*-(5-amino-1-carboxypentyl)iminodiacetic acid)succinyl] (nickel salt) (18:1 DGS-NTA(Ni)) were incorporated in a mole ratio of 4.75:5:0.25, respectively. Vesicles (1.5 mM phospholipid) and N-methylanthraniloyl-GDP (mant-GDP) (5 μM) were mixed with 2 μM RhoA-His_6 or Rac1-His_6 as indicated. After incubation at 25 degrees C for 1 minute, exchange reactions were initiated by addition of the indicated GEF and monitored by a Fluorolog-3 spectrofluorometer. When included, His-tagged plexins were added to vesicles at the same time as His-tagged GTPases. In experiments using the PDZ-TRIO chimera, assay solutions were supplemented with 20 mM Imidazole to reduce non-specific binding of the protein to the Ni-NTA lipids; this low concentration

of imidazole did not effect functional association of polyhistidine tagged proteins. An increase in fluorescence was measured as Mant-GDP exchanged onto the GTPases in place of GDP. Total fluorescence change was measured with saturating concentrations of GEF and used to calculate molar binding of mant-GDP assuming a linear change for bound mant-GDP and saturation of the GTPase present in the assay. Initial rates of exchange were calculated with linear analysis or curve fitting depending on the shape of the response.

Cell-based RhoA activation assay

The full-length human PlexinB1 construct with an N-terminal VSV-G-tag in the pcDNA3.1 vector (Invitrogen) was obtained from K. Guan (UCSD). Empty pcDNA3.1 served as a vector control. The full-length human RhoA construct with an N-terminal HA-tag in the pCMV5 vector (ATCC) was obtained from M. Cobb (UTSW). The construct for the PlexinB1 ligand, Semaphorin4D, was obtained from R. Giger (U. Michigan) and used to express the ligand as previously described (He, Yang et al. 2009). PlexinB1 mutants were generated using PRC based mutagenesis.

Levels of RhoA activation in cells cotransfected with RhoA and wild type or mutant PlexinB1 were quantified by pulling down of RhoA(GTP) using a GST-Rhotekin RBD as previously described (Ren and Schwartz 2000). Briefly, HEK293T cells were seeded onto 60 mm dishes and grown to 70-80% confluence in Dubecco's Modified Eagle Medium (DMEM) medium supplemented with 10% FBS. Cells were transiently transfected with 0.5 μg of the RhoA plasmid and 4.5 μg of the PlexinB1 plasmid or the control vector using Lipofectamine2000 (Life Technologies). 36 hours after transfection,

cells were serum starved for 4 hours in DMEM supplemented with 0.2% FBS. Cells were treated with 10 nM Semaphorin4D or control medium for 15 minutes then washed in cold PBS and lysed in 300 μL lysis buffer (50 mM Tris pH 7.5, 30 mM $MgCl_2$, 5 mM EDTA, 150 mM NaCl, 1% NP-40, 2 mM DTT, Pierce Protease Inhibitor Mini Tablets #88666). Lysates were cleared by centrifugation for 10 minutes at 14,000 rmp at 4 °C. RhoA(GTP) was captured from lysates by incubation with 20 μg GST-Rhotekin and 25 uL Glutathione Sepharose 4B bead slurry (GE Healthcare) for 1 hour at 4 °C. Beads were washed 3 times with lysis buffer and the supernatant was removed. Bound proteins were eluted by addition of 30 μL SDS loading buffer (50 mM Tris pH 6.8, 5% β-mercaptoethanol, 1% SDS, 10% glycerol, and 0.02% Bromphenol Blue) prior to SDS-PAGE and Western blot analysis. GTP-loaded and total HA-tagged RhoA populations were detected by immunoblotting with a monoclonal anti-HA antibody (Cell Signaling #3724S). VSV-PlexinB1 expression was probed by immunoblotting cell lysates with a monoclonal anti-VSV-G antibody (Clone P5D4, Sigma).

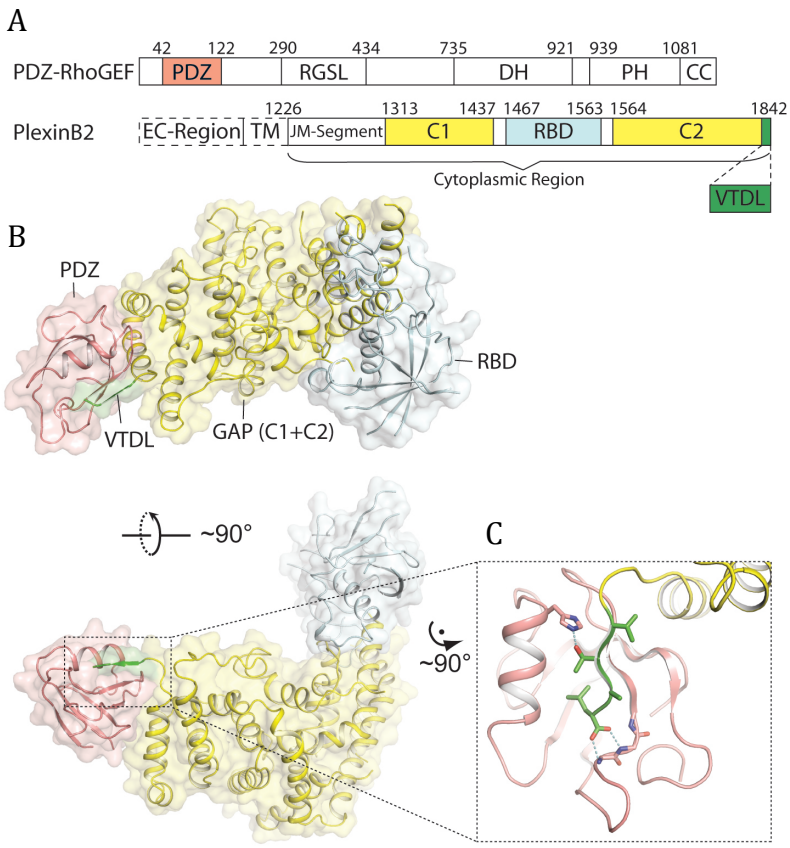

Figure 5-1. Crystal structure of the complex between PlexinB2$_{cyto}$ and the PDZ domain from PDZ-RhoGEF.

(A) Domain structure of PlexinB2 and PDZ-RhoGEF. Residues numbers are based on human PDZ-RhoGEF and mouse PlexinB2, respectively. RGSL: regulator of G-protein signaling-like domain; DH: Dbl-homology domain; PH: pleckstrin-homology domain; CC: coiled-coil domain; EC-region: extracellular region; TM: transmembrane region; JM-segment: juxtamembrane segment. The C1 and C2 segments in plexin together form the GAP domain.

(B) Overall structure of the PlexinB2$_{cyto}$/PDZ complex. The JM-segment in PlexinB2 is not visible in the structure. The color scheme is the same as in A.

(C) Detailed view of the interaction between the PDZ domain and the VTDL motif in PlexinB2. The sidechain of the aspartate residue is shown only to its β-carbon because of poor density.

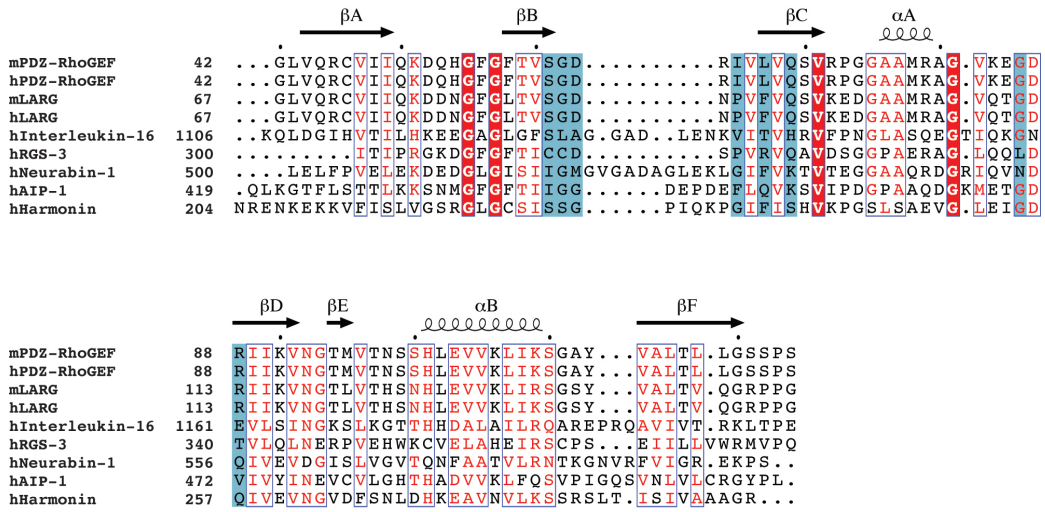

Figure 5-2. Sequence alignment of PDZ domains.
The sequences of the PDZ domains from PDZ-RhoGEF and LARG are aligned with a number of diverse PDZ domains. Residues involved in the secondary interface (blue) in PDZ-RhoGEF/LARG are not conserved across other PDZ domains. h: human; m: mouse.

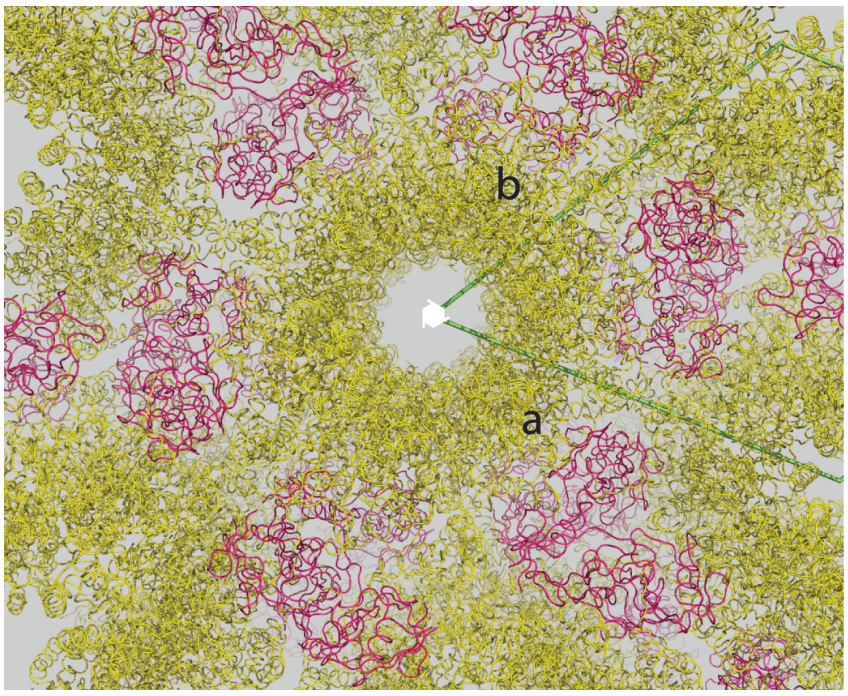

Figure 5-3. Crystal packing of the PlexinB2$_{cyto}$/PDZ complex.
PlexinB2 and the PDZ domain are colored yellow and red respectively. PlexinB2 molecules related by the crystallographic 6_2-fold screw axis form "helical columns". These columns do not contact one another, and PlexinB2 does not form any significant dimeric interactions in the crystal. One PDZ domain binds each PlexinB2, and also mediates crystal contacts between different PlexinB2 columns.

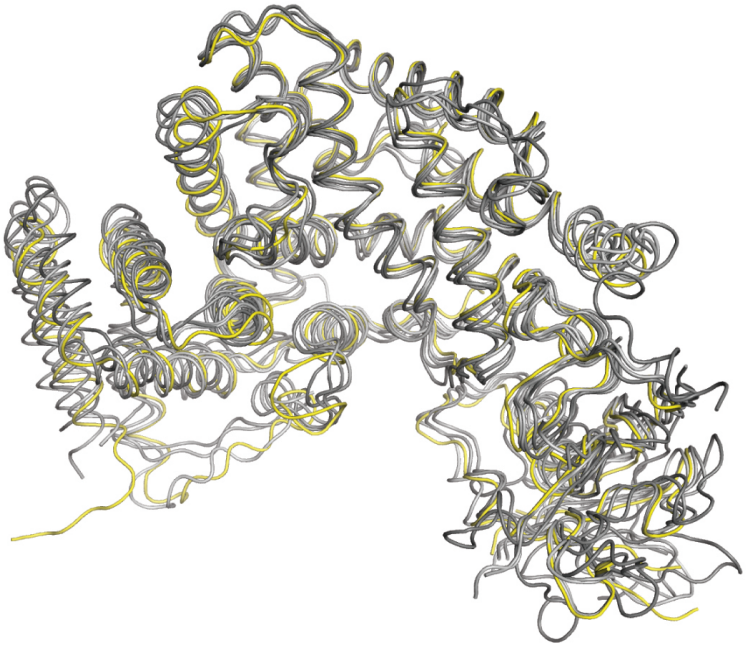

Figure 5-4. Structural similarity between PlexinB2$_{cyto}$ with several other plexin family members.
PlexinB2$_{cyto}$ from the PlexinB2$_{cyto}$/PDZ structure is shown in yellow. PlexinB1 (PDB ID: 3HM6), A3 (PDB ID: 3IG3), A1 (PDB ID: 3RYT), and C1 (PDB ID: 4M8N) are superimposed and colored from light to dark gray respectively. The juxtamembrane segment was not built in the PlexinB2$_{cyto}$ structure, and is also omitted from the other plexin structures.

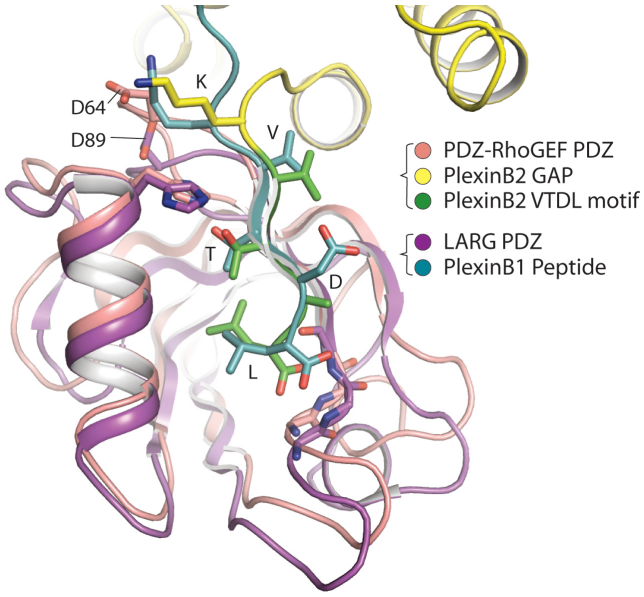

Figure 5-5. The PDZ domains from LARG and PDZ-RhoGEF bind the C-terminal motif in class B plexins in the same mode.
The NMR structure of the LARG PDZ domain in complex with the C-terminal motif from PlexinB1 (PDB ID: 2OS6) is superimposed on the PlexinB2/PDZ structure reported here.

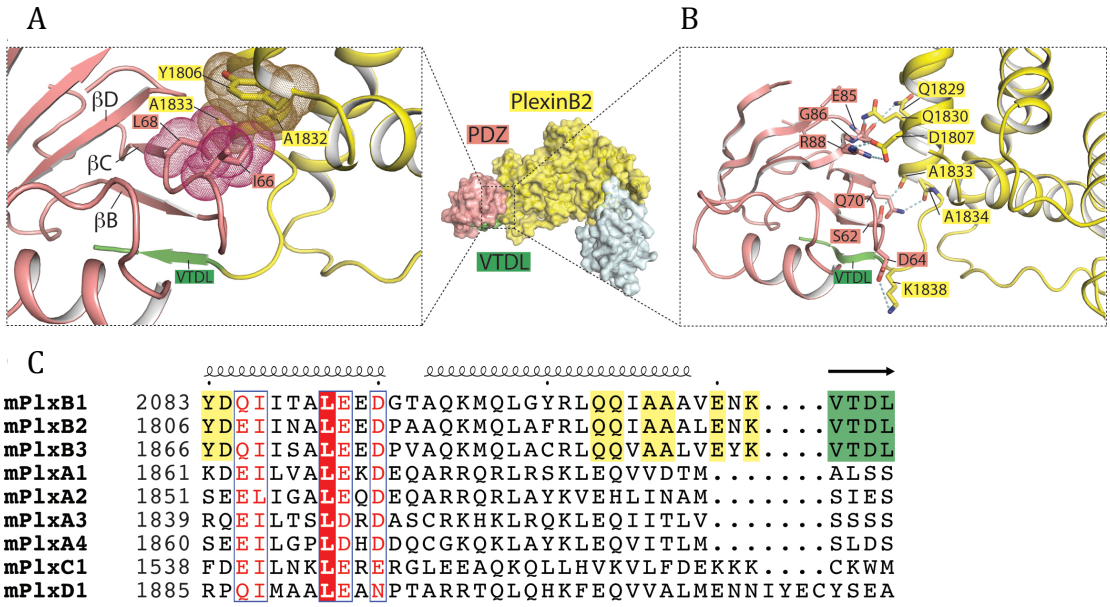

Figure 5-6. Secondary interface between PlexinB2 and the PDZ domain.
(A) Detailed view of the central hydrophobic interaction in the secondary interface. Van der Waals surfaces of residues are shown as dots.

(B) Detailed view of peripheral polar interactions in the secondary interface.

(C) Sequence alignment of the PDZ-binding region of mouse PlexinB2 with other plexin family members. Residues involved in the secondary interface are highlighted in yellow. The C-terminal VTDL motif is in green.

A

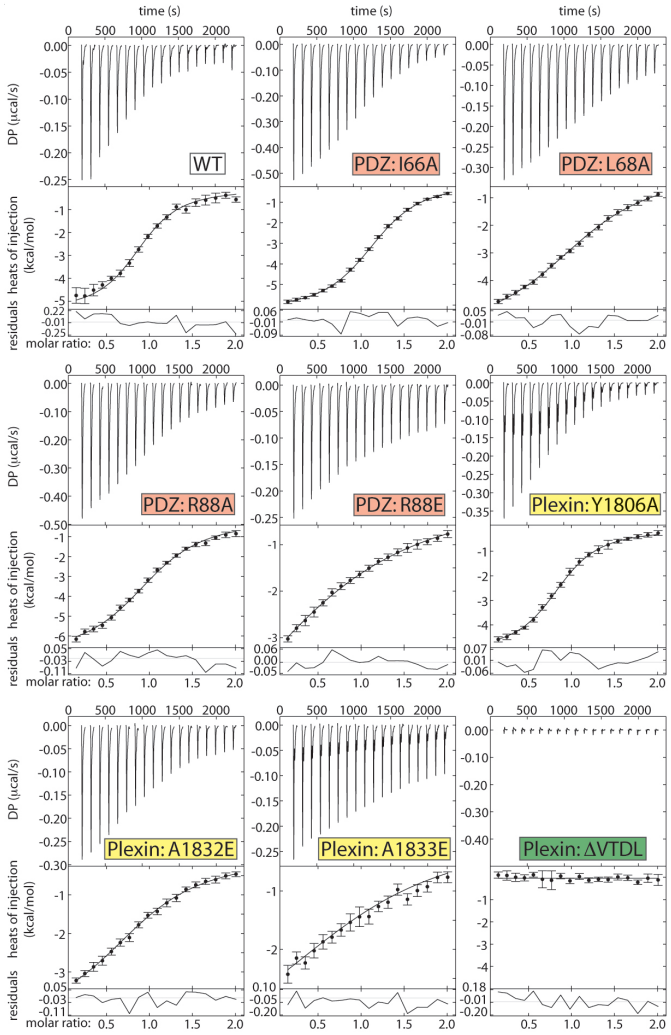

B

Plexin:	PDZ:	K_d (µM)	1σ (µM)
WT	WT	2.0	1.3-3.4
WT	I66A	3.2	2.8-3.5
WT	L68A	9.6	8.0-11.0
WT	R88A	6.4	5.3-7.8
WT	R88E	40.0	20.2-243.9
Y1806A	WT	3.7	3.4-4.0
A1832E	WT	13.2	9.0-20.8
A1833E	WT	30.0	12.0-72.0
ΔVTDL	WT	-	-
Peptide	WT	23-35	NA

C

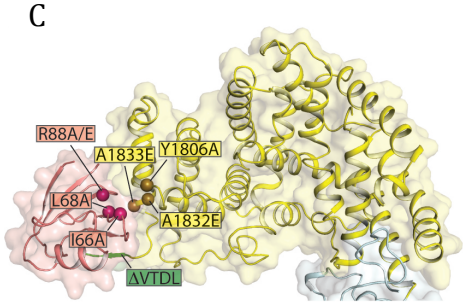

Figure 5-7. Mutational analysis of the secondary interface by ITC.
(A) Representative baseline-subtracted ITC thermograms (top panels), integrated titration heats (circles) with fits shown (lines, middle panels), and residuals plots (bottom panels).

(B) Values of K_d and 1σ confidence intervals from data in (A). The K_d values and confidence intervals are derived from a global analysis of triplicate datasets for each binding pair.

(C) Locations of the mutations in the crystal structure.

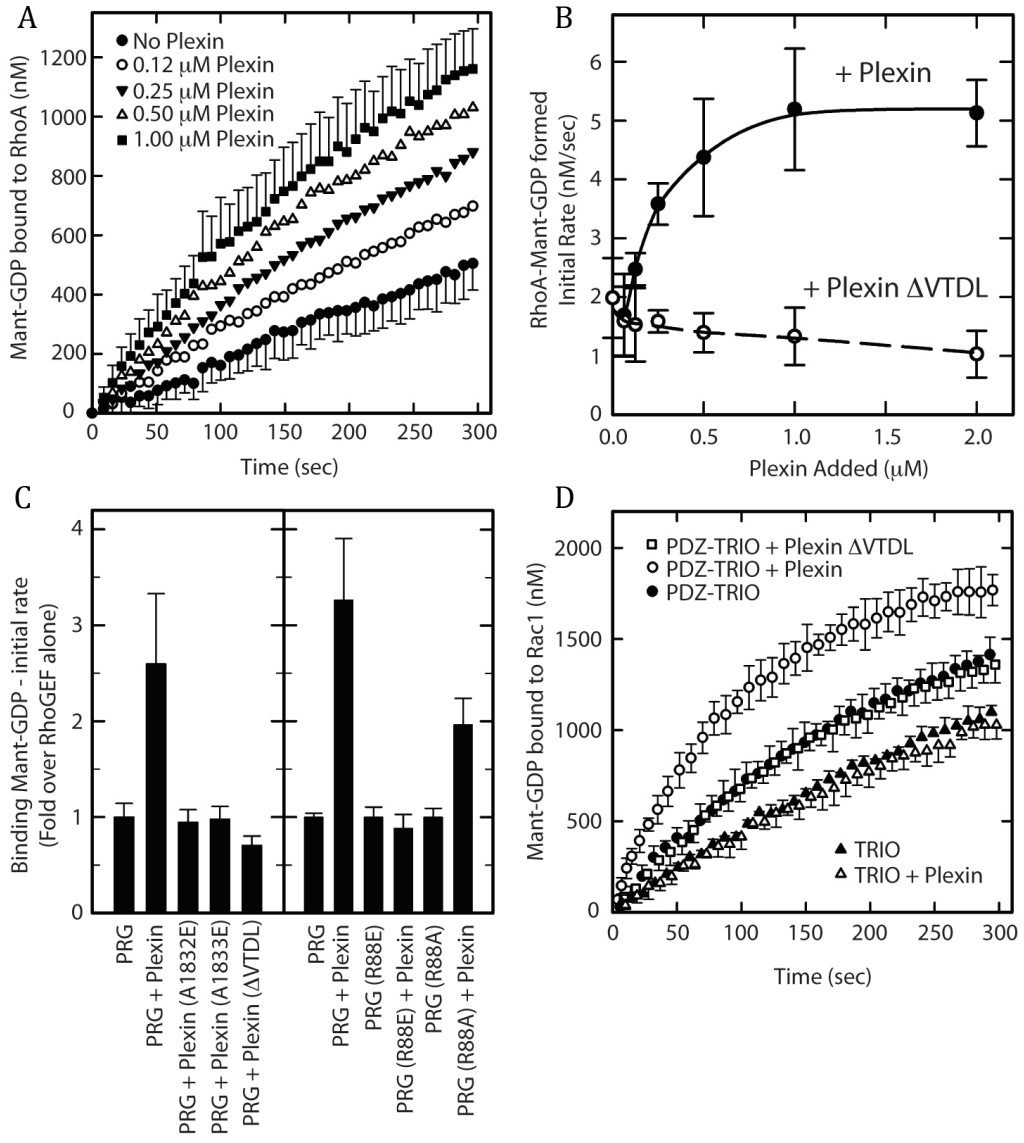

Figure 5-8. Recruitment of PDZ-RhoGEF by His_6-$PlexinB2_{cyto}$ to membrane-localized substrate.
Nucleotide exchange assays with lipid vesicles containing immobilized RhoA-His_6 or Rac1-His_6 is based on the change in fluorescence between bound and free mant-GDP.

(A) Time course of mant-GDP association to RhoA in the presence of 10 nM PDZ-RhoGEF (PRG) and increasing concentrations of His_6-$PlexinB2_{cyto}$. Example error bars indicate the general variance in signal among four measurements.

(B) Initial rates of exchange in the presence of increasing concentrations of the wild type or ΔVTDL mutant of His_6-PlexinB2. Results are the average of four titrations as in A; error bars are standard deviations.

(C) Initial rates of RhoA exchange stimulated by 10 nM wild type or mutants of PRG in the presence of 0.5 μM wild type or mutants of His_6-$PlexinB2_{cyto}$. Results are averages of 9 measurements; errors are standard deviations. All mutants showed no significant stimulation of PRG activity with one exception; the activity of PRG-R88A was stimulated by WT $PlexinB2_{cyto}$ but less so than PRG-WT ($p<0.0001$ for both comparisons, students T-test).

(D) Stimulation of chimeric PDZ-TRIO (150 nM) by 0.5 μM of the wild type or ΔVTDL mutant of His_6-$PlexinB2_{cyto}$. Results represent the average and standard deviation of triplicate measurements. Stimulation of PDZ-TRIO by 2-4 fold was significant ($p<0.05$) in two such experiments; no significant stimulation was observed with TRIO or with PlexinB2ΔVTDL.

Note: The above data was collected by Stephen Gutowski and the figure prepared by Paul Sternweis.

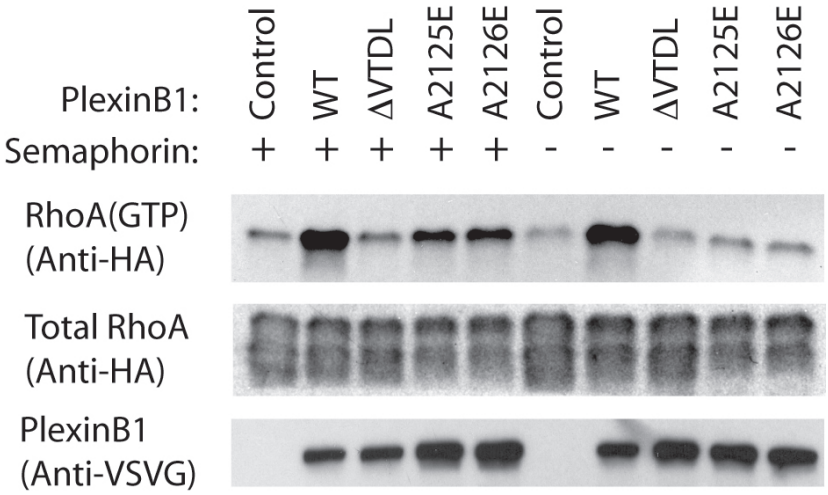

Figure 5-9. Contribution of the secondary interface between Plexin and the PDZ-RhoGEF to RhoA activation in cells.
Total expression levels of transfected PlexinB1 and RhoA were probed by anti-VSV-G and anti-HA antibodies, respectively. GTP-bound RhoA was pulled down by GST-Rotekin and probed by the same anti-HA antibody. The A2125E and A2126E mutations of human PlexinB1 correspond to the A1832E and A1833E mutations of mouse PlexinB2 in the secondary interface, respectively. Results shown are from one of the three independent repeats.

Note: The western blot pictured above was performed by Hua Chen.

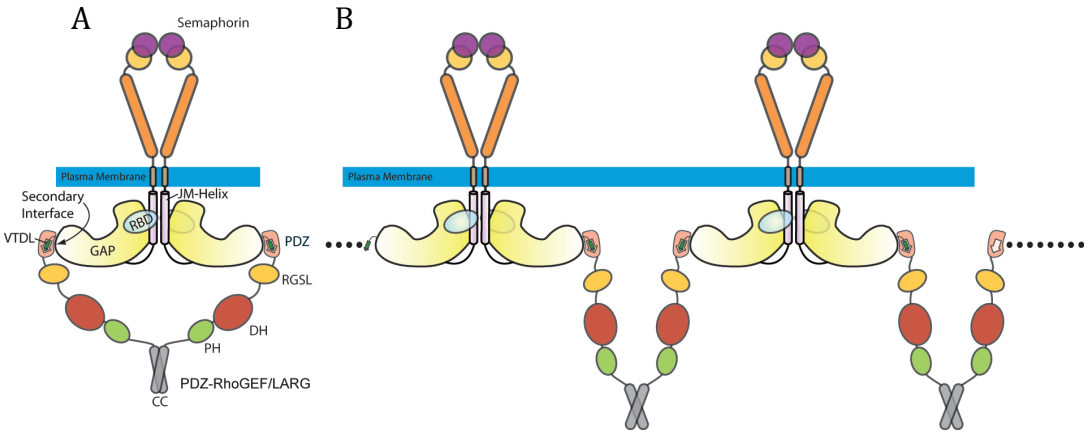

Figure 5-10. Model for the recruitment of PDZ-RhoGEF/LARG to the plasma membrane by class B plexins in the active state.
The PDZ/C-terminal motif interaction and the secondary interface contribute to the interaction together. The interaction may be further strengthened by bivalent engagement between dimeric PDZ-RhoGEF/LARG and the semaphorin-induced active dimer of plexin as shown in (A). An oligomeric complex may also form as shown in (B). The active dimer model of plexin is based on previous structural studies(Janssen, Robinson et al. 2010, Nogi, Yasui et al. 2010, Janssen, Malinauskas et al. 2012, Wang, Pascoe et al. 2013). Dimerization of PDZ-RhoGEF/LARG is likely mediated by the C-terminal coiled-coil domain(Chikumi, Barac et al. 2004), the structure of which is not known.

Table 5-1. Data collection and structure refinement statistics

Data collection	
Wavelength (Å)	0.98
Space group	$P6_222$
Cell Dimensions:	
a, b, c, (Å)	126.2, 126.2, 211.5
α, β, γ (°)	90, 90, 120
Resolution (Å)	50.0-3.20 (3.26-3.20)*
R_{sym} (%)	9.9 (>100)
I/σ	56.0 (1.3)
Completeness (%)	99.9 (100)
Redundancy	30.1 (27.4)
$CC_{1/2}$ of the highest resolution shell	0.74
Refinement	
Resolution (Å)	48.5-3.2
No. of reflections	14538
R_{work}/R_{free} (%)	25.4/29.7
No. of atoms	4478
Average B-factor	137.9
R.m.s. deviations:	
Bond lengths (Å)	0.004
Bond angles (°)	0.754
Ramachandran plot:	
Favored (%)	92.1
Allowed (%)	7.2
Disallowed (%)	0.7

*Numbers in parenthesis are for the highest resolution shell

CHAPTER SIX
Concluding Remarks and Future Directions

Investigations of the structural bases for plexin mediated signaling are ongoing. Major unanswered questions regarding plexin signaling, however, included: (1) what is the non-canonical RapGAP catalytic mechanism utilized by plexins, (2) how does dimerization induce plexin activity, and (3) how does the plexin GAP derive binding specificity for its Rap substrate. All of these questions were resolved by our work detailed in Chapter Four.

A framework for understanding the regulation and signaling mechanisms of plexin has emerged from our work and additional structural studies in the past few years (Figure 6-1). It is now clear how semaphorin binds plexin and induces its dimerization. This activation signal triggers the transition of the cytoplasmic region of plexin from the autoinhibited to the active dimer state. The activated cytoplasmic region transduces signal primarily by acting as a GAP for Rap using a non-canonical mechanism that takes advantage of Gln63 in Rap. Moreover, plexins have evolved to specifically recognize residues in Rap that have diverged from those in other Ras family small GTPases.

B family plexins also activate RhoA in response to semaphorin binding by activating the two RhoGEFs, PDZ-RhoGEF and LARG. How plexins specifically recognized these PDZ domains, however, remained unclear. We demonstrated that a secondary interface formed between the PDZ domains from these two GEFs and B family plexins provides a structural basis for ensuring PDZ selectivity and faithful signal transduction. Secondary interfaces may be a common theme utilized by modular protein-

protein interaction domains to achieve specificity. This work is described in Chapter Five.

These new insights set the stage for addressing remaining mechanistic questions, including the structural basis and functional role of the inhibitory dimer/oligomer of plexin, and how exactly the RhoGTPases regulate plexin activity. More broadly, it is also important to address how the many binding partners interact with plexin, and how the interactions are coordinated to trigger multiple signaling pathways that regulate a variety of the biological processes. Answering these questions may require the combination of structural studies and biophysical analyses in the context of the lipid membrane.

Finally, structural analyses of full-length plexin are ultimately required for elucidating the role of the transmembrane region, and the precise mechanism of the coupling between the extracellular and intracellular regions. This remains a major challenge, both for plexin specifically and for all single-pass transmembrane receptors in general. In Chapters Two and Three we described methods for generating fusion constructs of plexin and Rap suitable for X-ray crystallography studies, and a convenient method for measuring plexin GAP activity. By utilizing these methods along with the recent advances in membrane protein crystallography, cryo-electron microscopy and computational approaches, the goal may be within reach in the next few years.

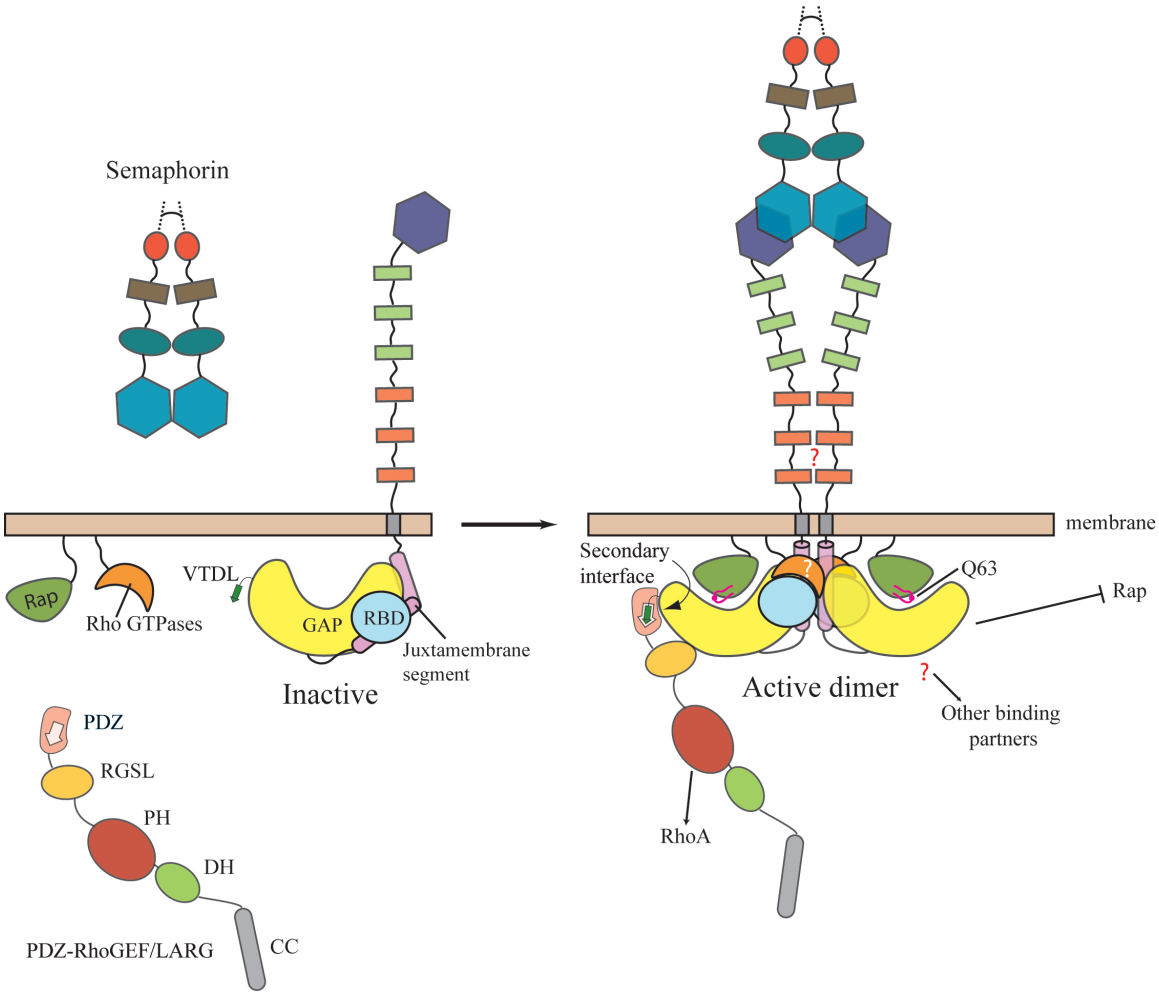

Figure 6-1. Overall model of plexin regulation and signaling.
The model describes semaphorin-induced transition of plexin from the inactive monomer to the active dimer state. Note that basal activity of plexin may be further suppressed by formation of an inhibitory dimer, which is not well characterized and therefore not shown. Questions marks indicate unanswered mechanistic questions. The interaction of PDZ-RhoGEF/LARG shown is specific to the B family plexins.

Bibliography

Adams, P. D., R. W. Grosse-Kunstleve, L. W. Hung, T. R. Ioerger, A. J. McCoy, N. W. Moriarty, R. J. Read, J. C. Sacchettini, N. K. Sauter and T. C. Terwilliger (2002). "PHENIX: building new software for automated crystallographic structure determination." Acta Crystallogr D Biol Crystallogr 58(Pt 11): 1948-1954.

Antipenko, A., J. P. Himanen, K. van Leyen, V. Nardi-Dei, J. Lesniak, W. A. Barton, K. R. Rajashankar, M. Lu, C. Hoemme, A. W. Puschel and D. B. Nikolov (2003). "Structure of the semaphorin-3A receptor binding module." Neuron 39(4): 589-598.

Aurandt, J., H. G. Vikis, J. S. Gutkind, N. Ahn and K. L. Guan (2002). "The semaphorin receptor plexin-B1 signals through a direct interaction with the Rho-specific nucleotide exchange factor, LARG." Proc Natl Acad Sci U S A 99(19): 12085-12090.

Bae, J. H., E. D. Lew, S. Yuzawa, F. Tome, I. Lax and J. Schlessinger (2009). "The selectivity of receptor tyrosine kinase signaling is controlled by a secondary SH2 domain binding site." Cell 138(3): 514-524.

Basile, J. R., A. Barac, T. Zhu, K. L. Guan and J. S. Gutkind (2004). "Class IV semaphorins promote angiogenesis by stimulating Rho-initiated pathways through plexin-B." Cancer Res 64(15): 5212-5224.

Bell, C. H., A. R. Aricescu, E. Y. Jones and C. Siebold (2011). "A dual binding mode for RhoGTPases in plexin signalling." PLoS Biol 9(8): e1001134.

Bos, J. L., H. Rehmann and A. Wittinghofer (2007). "GEFs and GAPs: critical elements in the control of small G proteins." Cell 129(5): 865-877.

Brautigam, C. A. (2015, in press). "Calculations and publication-quality illustrations for analytical ultracentrifugation data." Methods in Enzymology 562.

Cancer Genome Atlas Research, N. (2012). "Comprehensive genomic characterization of squamous cell lung cancers." Nature 489(7417): 519-525.

Carter, A. M., S. Gutowski and P. C. Sternweis (2014). "Regulated localization is sufficient for hormonal control of regulator of G protein signaling homology Rho guanine nucleotide exchange factors (RH-RhoGEFs)." J Biol Chem 289(28): 19737-19746.

Charpentier, T. H., G. L. Waldo, M. O. Barrett, W. Huang, Q. Zhang, T. K. Harden and J. Sondek (2014). "Membrane-induced allosteric control of phospholipase C-beta isozymes." J Biol Chem 289(43): 29545-29557.

Chen, V. B., W. B. Arendall, 3rd, J. J. Headd, D. A. Keedy, R. M. Immormino, G. J. Kapral, L. W. Murray, J. S. Richardson and D. C. Richardson (2010). "MolProbity: all-atom structure validation for macromolecular crystallography." Acta Crystallogr D Biol Crystallogr 66(Pt 1): 12-21.

Chen, Z., L. Guo, S. R. Sprang and P. C. Sternweis (2011). "Modulation of a GEF switch: autoinhibition of the intrinsic guanine nucleotide exchange activity of p115-RhoGEF." Protein Sci 20(1): 107-117.

Chen, Z., F. Medina, M. Y. Liu, C. Thomas, S. R. Sprang and P. C. Sternweis (2010). "Activated RhoA binds to the pleckstrin homology (PH) domain of PDZ-RhoGEF, a potential site for autoregulation." J Biol Chem 285(27): 21070-21081.

Chikumi, H., A. Barac, B. Behbahani, Y. Gao, H. Teramoto, Y. Zheng and J. S. Gutkind (2004). "Homo- and hetero-oligomerization of PDZ-RhoGEF, LARG and p115RhoGEF by their C-terminal region regulates their in vivo Rho GEF activity and transforming potential." Oncogene 23(1): 233-240.

Driessens, M. H., H. Hu, C. D. Nobes, A. Self, I. Jordens, C. S. Goodman and A. Hall (2001). "Plexin-B semaphorin receptors interact directly with active Rac and regulate the actin cytoskeleton by activating Rho." Curr Biol 11(5): 339-344.

Driessens, M. H., C. Olivo, K. Nagata, M. Inagaki and J. G. Collard (2002). "B plexins activate Rho through PDZ-RhoGEF." FEBS Lett 529(2-3): 168-172.

Emsley, P. and K. Cowtan (2004). "Coot: model-building tools for molecular graphics." Acta Crystallogr D Biol Crystallogr 60(Pt 12 Pt 1): 2126-2132.

Fansa, E. K., R. Dvorsky, S. C. Zhang, D. Fiegen and M. R. Ahmadian (2013). "Interaction characteristics of Plexin-B1 with Rho family proteins." Biochem Biophys Res Commun 434(4): 785-790.

Frech, M., J. John, V. Pizon, P. Chardin, A. Tavitian, R. Clark, F. McCormick and A. Wittinghofer (1990). "Inhibition of GTPase activating protein stimulation of Ras-p21 GTPase by the Krev-1 gene product." Science 249(4965): 169-171.

Gay, C. M., T. Zygmunt and J. Torres-Vazquez (2011). "Diverse functions for the semaphorin receptor PlexinD1 in development and disease." Developmental biology 349(1): 1-19.

Gitler, A. D., M. M. Lu and J. A. Epstein (2004). "PlexinD1 and semaphorin signaling are required in endothelial cells for cardiovascular development." Dev Cell 7(1): 107-116.

Gloerich, M. and J. L. Bos (2011). "Regulating Rap small G-proteins in time and space." Trends Cell Biol 21(10): 615-623.

Gouet, P., E. Courcelle, D. I. Stuart and F. Metoz (1999). "ESPript: analysis of multiple sequence alignments in PostScript." Bioinformatics 15(4): 305-308.

Gu, C. and E. Giraudo (2013). "The role of semaphorins and their receptors in vascular development and cancer." Exp Cell Res 319(9): 1306-1316.

Gu, C., Y. Yoshida, J. Livet, D. V. Reimert, F. Mann, J. Merte, C. E. Henderson, T. M. Jessell, A. L. Kolodkin and D. D. Ginty (2005). "Semaphorin 3E and plexin-D1 control vascular pattern independently of neuropilins." Science 307(5707): 265-268.

Hata, Y., A. Kikuchi, T. Sasaki, M. D. Schaber, J. B. Gibbs and Y. Takai (1990). "Inhibition of the ras p21 GTPase-activating protein-stimulated GTPase activity of c-Ha-ras p21 by smg p21 having the same putative effector domain as ras p21s." J Biol Chem 265(13): 7104-7107.

Hayashi, M., T. Nakashima, M. Taniguchi, T. Kodama, A. Kumanogoh and H. Takayanagi (2012). "Osteoprotection by semaphorin 3A." Nature 485(7396): 69-74.

He, H., T. Yang, J. R. Terman and X. Zhang (2009). "Crystal structure of the plexin A3 intracellular region reveals an autoinhibited conformation through active site sequestration." Proc Natl Acad Sci U S A 106(37): 15610-15615.

He, X., Y. C. Kuo, T. J. Rosche and X. Zhang (2013). "Structural Basis for Autoinhibition of the Guanine Nucleotide Exchange Factor FARP2." Structure 21(3): 355-364.

Hirotani, M., Y. Ohoka, T. Yamamoto, H. Nirasawa, T. Furuyama, M. Kogo, T. Matsuya and S. Inagaki (2002). "Interaction of plexin-B1 with PDZ domain-containing Rho guanine nucleotide exchange factors." Biochem Biophys Res Commun 297(1): 32-37.

Hota, P. K. and M. Buck (2009). "Thermodynamic characterization of two homologous protein complexes: associations of the semaphorin receptor plexin-B1 RhoGTPase binding domain with Rnd1 and active Rac1." Protein Sci 18(5): 1060-1071.

Hota, P. K. and M. Buck (2012). "Plexin structures are coming: opportunities for multilevel investigations of semaphorin guidance receptors, their cell signaling mechanisms, and functions." Cell Mol Life Sci 69(22): 3765-3805.

Houtman, J. C., P. H. Brown, B. Bowden, H. Yamaguchi, E. Appella, L. E. Samelson and P. Schuck (2007). "Studying multisite binary and ternary protein interactions by global analysis of isothermal titration calorimetry data in SEDPHAT: application to adaptor protein complexes in cell signaling." Protein Sci 16(1): 30-42.

Hu, H., T. F. Marton and C. S. Goodman (2001). "Plexin B mediates axon guidance in Drosophila by simultaneously inhibiting active Rac and enhancing RhoA signaling." Neuron 32(1): 39-51.

Ilangovan, U., H. Ton-That, J. Iwahara, O. Schneewind and R. T. Clubb (2001). "Structure of sortase, the transpeptidase that anchors proteins to the cell wall of Staphylococcus aureus." Proc Natl Acad Sci U S A 98(11): 6056-6061.

Janssen, B. J., T. Malinauskas, G. A. Weir, M. Z. Cader, C. Siebold and E. Y. Jones (2012). "Neuropilins lock secreted semaphorins onto plexins in a ternary signaling complex." Nat Struct Mol Biol 19(12): 1293-1299.

Janssen, B. J., R. A. Robinson, F. Perez-Branguli, C. H. Bell, K. J. Mitchell, C. Siebold and E. Y. Jones (2010). "Structural basis of semaphorin-plexin signalling." Nature 467(7319): 1118-1122.

Jeon, C. Y., H. J. Kim, J. Y. Lee, J. B. Kim, S. C. Kim and J. B. Park (2010). "p190RhoGAP and Rap-dependent RhoGAP (ARAP3) inactivate RhoA in response to nerve growth factor leading to neurite outgrowth from PC12 cells." Exp Mol Med 42(5): 335-344.

Jin, Z. and S. M. Strittmatter (1997). "Rac1 mediates collapsin-1-induced growth cone collapse." J Neurosci 17(16): 6256-6263.

Jones, E. Y. (2015). "Understanding cell signalling systems: paving the way for new therapies." Philos Trans A Math Phys Eng Sci 373(2036).

Kantor, D. B., O. Chivatakarn, K. L. Peer, S. F. Oster, M. Inatani, M. J. Hansen, J. G. Flanagan, Y. Yamaguchi, D. W. Sretavan, R. J. Giger and A. L. Kolodkin (2004). "Semaphorin 5A is a bifunctional axon guidance cue regulated by heparan and chondroitin sulfate proteoglycans." Neuron 44(6): 961-975.

Keller, S., C. Vargas, H. Zhao, G. Piszczek, C. A. Brautigam and P. Schuck (2012). "High-precision isothermal titration calorimetry with automated peak-shape analysis." Anal Chem 84(11): 5066-5073.

Kim, H., K. H. Siu, M. Raeeszadeh-Sarmazdeh, Q. Sun, Q. Chen and W. Chen (2015). "Bioengineering strategies to generate artificial protein complexes." Biotechnol Bioeng.

Kim, J., I. Kim, J. S. Yang, Y. E. Shin, J. Hwang, S. Park, Y. S. Choi and S. Kim (2012). "Rewiring of PDZ domain-ligand interaction network contributed to eukaryotic evolution." PLoS Genet 8(2): e1002510.

Klostermann, A., M. Lohrum, R. H. Adams and A. W. Puschel (1998). "The chemorepulsive activity of the axonal guidance signal semaphorin D requires dimerization." J Biol Chem 273(13): 7326-7331.

Kolodkin, A. L., D. J. Matthes and C. S. Goodman (1993). "The semaphorin genes encode a family of transmembrane and secreted growth cone guidance molecules." Cell 75(7): 1389-1399.

Koppel, A. M., L. Feiner, H. Kobayashi and J. A. Raper (1997). "A 70 amino acid region within the semaphorin domain activates specific cellular response of semaphorin family members." Neuron 19(3): 531-537.

Koppel, A. M. and J. A. Raper (1998). "Collapsin-1 covalently dimerizes, and dimerization is necessary for collapsing activity." J Biol Chem 273(25): 15708-15713.

Krapivinsky, G., I. Medina, L. Krapivinsky, S. Gapon and D. E. Clapham (2004). "SynGAP-MUPP1-CaMKII synaptic complexes regulate p38 MAP kinase activity and NMDA receptor-dependent synaptic AMPA receptor potentiation." Neuron 43(4): 563-574.

Kruger, R. P., J. Aurandt and K. L. Guan (2005). "Semaphorins command cells to move." Nat Rev Mol Cell Biol 6(10): 789-800.

Kuhn, T. B., M. D. Brown, C. L. Wilcox, J. A. Raper and J. R. Bamburg (1999). "Myelin and collapsin-1 induce motor neuron growth cone collapse through different pathways: inhibition of collapse by opposing mutants of rac1." J Neurosci 19(6): 1965-1975.

Kupzig, S., D. Bouyoucef-Cherchalli, S. Yarwood, R. Sessions and P. J. Cullen (2009). "The ability of GAP1IP4BP to function as a Rap1 GTPase-activating protein (GAP) requires its Ras GAP-related domain and an arginine finger rather than an asparagine thumb." Mol Cell Biol 29(14): 3929-3940.

Kupzig, S., D. Deaconescu, D. Bouyoucef, S. A. Walker, Q. Liu, C. L. Polte, O. Daumke, T. Ishizaki, P. J. Lockyer, A. Wittinghofer and P. J. Cullen (2006).

"GAP1 family members constitute bifunctional Ras and Rap GTPase-activating proteins." J Biol Chem 281(15): 9891-9900.

Laue, T. M., B. D. Shah, T. M. Ridgeway and S. L. Pelletier (1992). "Analytical ultracentrifugation in biochemistry and polymer science." Royal Society of Chemistry.

Lee, C. H., K. Saksela, U. A. Mirza, B. T. Chait and J. Kuriyan (1996). "Crystal structure of the conserved core of HIV-1 Nef complexed with a Src family SH3 domain." Cell 85(6): 931-942.

Li, S., S. Nakamura and S. Hattori (1997). "Activation of R-Ras GTPase by GTPase-activating proteins for Ras, Gap1(m), and p120GAP." J Biol Chem 272(31): 19328-19332.

Li, Y., Z. Wei, Y. Yan, Q. Wan, Q. Du and M. Zhang (2014). "Structure of Crumbs tail in complex with the PALS1 PDZ-SH3-GK tandem reveals a highly specific assembly mechanism for the apical Crumbs complex." Proc Natl Acad Sci U S A.

Liu, H., Z. S. Juo, A. H. Shim, P. J. Focia, X. Chen, K. C. Garcia and X. He (2010). "Structural basis of semaphorin-plexin recognition and viral mimicry from Sema7A and A39R complexes with PlexinC1." Cell 142(5): 749-761.

Liu, J., J. Zhang, Y. Yang, H. Huang, W. Shen, Q. Hu, X. Wang, J. Wu and Y. Shi (2008). "Conformational change upon ligand binding and dynamics of the PDZ domain from leukemia-associated Rho guanine nucleotide exchange factor." Protein Sci 17(6): 1003-1014.

Lorenz, T. C. (2012). "Polymerase chain reaction: basic protocol plus troubleshooting and optimization strategies." J Vis Exp(63): e3998.

Love, C. A., K. Harlos, N. Mavaddat, S. J. Davis, D. I. Stuart, E. Y. Jones and R. M. Esnouf (2003). "The ligand-binding face of the semaphorins revealed by the high-resolution crystal structure of SEMA4D." Nat Struct Biol 10(10): 843-848.

Luck, K., S. Charbonnier and G. Trave (2012). "The emerging contribution of sequence context to the specificity of protein interactions mediated by PDZ domains." FEBS Lett 586(17): 2648-2661.

Mccoy, A. J., R. W. Grosse-Kunstleve, P. D. Adams, M. D. Winn, L. C. Storoni and R. J. Read (2007). "Phaser crystallographic software." Journal of Applied Crystallography 40: 658-674.

Medina, F., A. M. Carter, O. Dada, S. Gutowski, J. Hadas, Z. Chen and P. C. Sternweis (2013). "Activated RhoA is a positive feedback regulator of the Lbc

family of Rho guanine nucleotide exchange factor proteins." J Biol Chem 288(16): 11325-11333.

Messersmith, E. K., E. D. Leonardo, C. J. Shatz, M. Tessier-Lavigne, C. S. Goodman and A. L. Kolodkin (1995). "Semaphorin III can function as a selective chemorepellent to pattern sensory projections in the spinal cord." Neuron 14(5): 949-959.

Nakamura, F., M. Tanaka, T. Takahashi, R. G. Kalb and S. M. Strittmatter (1998). "Neuropilin-1 extracellular domains mediate semaphorin D/III-induced growth cone collapse." Neuron 21(5): 1093-1100.

Nassar, N., G. Horn, C. Herrmann, C. Block, R. Janknecht and A. Wittinghofer (1996). "Ras/Rap effector specificity determined by charge reversal." Nat Struct Biol 3(8): 723-729.

Nogi, T., N. Yasui, E. Mihara, Y. Matsunaga, M. Noda, N. Yamashita, T. Toyofuku, S. Uchiyama, Y. Goshima, A. Kumanogoh and J. Takagi (2010). "Structural basis for semaphorin signalling through the plexin receptor." Nature 467(7319): 1123-1127.

Notredame, C., D. G. Higgins and J. Heringa (2000). "T-Coffee: A novel method for fast and accurate multiple sequence alignment." J Mol Biol 302(1): 205-217.

Ohba, Y., N. Mochizuki, S. Yamashita, A. M. Chan, J. W. Schrader, S. Hattori, K. Nagashima and M. Matsuda (2000). "Regulatory proteins of R-Ras, TC21/R-Ras2, and M-Ras/R-Ras3." J Biol Chem 275(26): 20020-20026.

Oinuma, I., Y. Ishikawa, H. Katoh and M. Negishi (2004). "The Semaphorin 4D receptor Plexin-B1 is a GTPase activating protein for R-Ras." Science 305(5685): 862-865.

Oinuma, I., H. Katoh, A. Harada and M. Negishi (2003). "Direct interaction of Rnd1 with Plexin-B1 regulates PDZ-RhoGEF-mediated Rho activation by Plexin-B1 and induces cell contraction in COS-7 cells." J Biol Chem 278(28): 25671-25677.

Oinuma, I., H. Katoh and M. Negishi (2004). "Molecular dissection of the semaphorin 4D receptor plexin-B1-stimulated R-Ras GTPase-activating protein activity and neurite remodeling in hippocampal neurons." J Neurosci 24(50): 11473-11480.

Okada, T., S. Sinha, I. Esposito, G. Schiavon, M. A. Lopez-Lago, W. Su, C. A. Pratilas, C. Abele, J. M. Hernandez, M. Ohara, M. Okada, A. Viale, A. Heguy, N. D.

Socci, A. Sapino, V. E. Seshan, S. Long, G. Inghirami, N. Rosen and F. G. Giancotti (2015). "The Rho GTPase Rnd1 suppresses mammary tumorigenesis and EMT by restraining Ras-MAPK signalling." Nat Cell Biol 17(1): 81-94.

Oster, S. F., M. O. Bodeker, F. He and D. W. Sretavan (2003). "Invariant Sema5A inhibition serves an ensheathing function during optic nerve development." Development 130(4): 775-784.

Otwinowski, Z. and W. Minor (1997). "Processing of X-ray Diffraction Data Collected in Oscillation Mode." Methods in Enzymology 276: 307-326.

Padilla, J. E. and T. O. Yeates (2003). "A statistic for local intensity differences: robustness to anisotropy and pseudo-centering and utility for detecting twinning." Acta Crystallogr D Biol Crystallogr 59(Pt 7): 1124-1130.

Paduch, M., M. Biernat, P. Stefanowicz, Z. S. Derewenda, Z. Szewczuk and J. Otlewski (2007). "Bivalent peptides as models for multimeric targets of PDZ domains." Chembiochem 8(4): 443-452.

Pawson, T. and P. Nash (2003). "Assembly of cell regulatory systems through protein interaction domains." Science 300(5618): 445-452.

Pena, V., M. Hothorn, A. Eberth, N. Kaschau, A. Parret, L. Gremer, F. Bonneau, M. R. Ahmadian and K. Scheffzek (2008). "The C2 domain of SynGAP is essential for stimulation of the Rap GTPase reaction." EMBO Rep 9(4): 350-355.

Perrot, V., J. Vazquez-Prado and J. S. Gutkind (2002). "Plexin B regulates Rho through the guanine nucleotide exchange factors leukemia-associated Rho GEF (LARG) and PDZ-RhoGEF." J Biol Chem 277(45): 43115-43120.

Popp, M. W., J. M. Antos and H. L. Ploegh (2009). "Site-specific protein labeling via sortase-mediated transpeptidation." Curr Protoc Protein Sci Chapter 15: Unit 15 13.

Proft, T. (2010). "Sortase-mediated protein ligation: an emerging biotechnology tool for protein modification and immobilisation." Biotechnol Lett 32(1): 1-10.

Quilliam, L. A., A. F. Castro, K. S. Rogers-Graham, C. B. Martin, C. J. Der and C. Bi (1999). "M-Ras/R-Ras3, a transforming ras protein regulated by Sos1, GRF1, and p120 Ras GTPase-activating protein, interacts with the putative Ras effector AF6." J Biol Chem 274(34): 23850-23857.

Ren, X. D. and M. A. Schwartz (2000). "Determination of GTP loading on Rho." Methods Enzymol 325: 264-272.

Rohm, B., B. Rahim, B. Kleiber, I. Hovatta and A. W. Puschel (2000). "The semaphorin 3A receptor may directly regulate the activity of small GTPases." FEBS Lett 486(1): 68-72.

Saito, Y., I. Oinuma, S. Fujimoto and M. Negishi (2009). "Plexin-B1 is a GTPase activating protein for M-Ras, remodelling dendrite morphology." EMBO Rep 10(6): 614-621.

Sakurai, A., C. Doci and J. S. Gutkind (2012). "Semaphorin signaling in angiogenesis, lymphangiogenesis and cancer." Cell Res 22(1): 23-32.

Sakurai, A., J. Gavard, Y. Annas-Linhares, J. R. Basile, P. Amornphimoltham, T. R. Palmby, H. Yagi, F. Zhang, P. A. Randazzo, X. Li, R. Weigert and J. S. Gutkind (2010). "Semaphorin 3E initiates antiangiogenic signaling through plexin D1 by regulating Arf6 and R-Ras." Mol Cell Biol 30(12): 3086-3098.

Scheffzek, K., M. R. Ahmadian, W. Kabsch, L. Wiesmuller, A. Lautwein, F. Schmitz and A. Wittinghofer (1997). "The Ras-RasGAP complex: structural basis for GTPase activation and its loss in oncogenic Ras mutants." Science 277(5324): 333-338.

Scheffzek, K., M. R. Ahmadian, L. Wiesmuller, W. Kabsch, P. Stege, F. Schmitz and A. Wittinghofer (1998). "Structural analysis of the GAP-related domain from neurofibromin and its implications." Embo J 17(15): 4313-4327.

Schuck, P. (2000). "Size-distribution analysis of macromolecules by sedimentation velocity ultracentrifugation and lamm equation modeling." Biophys J 78(3): 1606-1619.

Schuck, P. and B. Demeler (1999). "Direct sedimentation analysis of interference optical data in analytical ultracentrifugation." Biophys J 76(4): 2288-2296.

Scrima, A., C. Thomas, D. Deaconescu and A. Wittinghofer (2008). "The Rap-RapGAP complex: GTP hydrolysis without catalytic glutamine and arginine residues." Embo J 27(7): 1145-1153.

Semaphorin_Nomenclature_Committee (1999). "Unified nomenclature for the semaphorins/collapsins. Semaphorin Nomenclature Committee." Cell 97(5): 551-552.

Serini, G., D. Valdembri, S. Zanivan, G. Morterra, C. Burkhardt, F. Caccavari, L. Zammataro, L. Primo, L. Tamagnone, M. Logan, M. Tessier-Lavigne, M. Taniguchi, A. W. Puschel and F. Bussolino (2003). "Class 3 semaphorins

control vascular morphogenesis by inhibiting integrin function." Nature 424(6947): 391-397.

Seshagiri, S., E. W. Stawiski, S. Durinck, Z. Modrusan, E. E. Storm, C. B. Conboy, S. Chaudhuri, Y. Guan, V. Janakiraman, B. S. Jaiswal, J. Guillory, C. Ha, G. J. Dijkgraaf, J. Stinson, F. Gnad, M. A. Huntley, J. D. Degenhardt, P. M. Haverty, R. Bourgon, W. Wang, H. Koeppen, R. Gentleman, T. K. Starr, Z. Zhang, D. A. Largaespada, T. D. Wu and F. J. de Sauvage (2012). "Recurrent R-spondin fusions in colon cancer." Nature 488(7413): 660-664.

Siebold, C. and E. Y. Jones (2013). "Structural insights into semaphorins and their receptors." Semin Cell Dev Biol 24(3): 139-145.

Smietana, K., M. Kasztura, M. Paduch, U. Derewenda, Z. S. Derewenda and J. Otlewski (2008). "Degenerate specificity of PDZ domains from RhoA-specific nucleotide exchange factors PDZRhoGEF and LARG." Acta Biochim Pol 55(2): 269-280.

Song, H., G. Ming, Z. He, M. Lehmann, L. McKerracher, M. Tessier-Lavigne and M. Poo (1998). "Conversion of neuronal growth cone responses from repulsion to attraction by cyclic nucleotides." Science 281(5382): 1515-1518.

Songyang, Z., A. S. Fanning, C. Fu, J. Xu, S. M. Marfatia, A. H. Chishti, A. Crompton, A. C. Chan, J. M. Anderson and L. C. Cantley (1997). "Recognition of unique carboxyl-terminal motifs by distinct PDZ domains." Science 275(5296): 73-77.

Sot, B., C. Kotting, D. Deaconescu, Y. Suveyzdis, K. Gerwert and A. Wittinghofer (2010). "Unravelling the mechanism of dual-specificity GAPs." EMBO J 29(7): 1205-1214.

Stiffler, M. A., J. R. Chen, V. P. Grantcharova, Y. Lei, D. Fuchs, J. E. Allen, L. A. Zaslavskaia and G. MacBeath (2007). "PDZ domain binding selectivity is optimized across the mouse proteome." Science 317(5836): 364-369.

Swiercz, J. M., R. Kuner, J. Behrens and S. Offermanns (2002). "Plexin-B1 directly interacts with PDZ-RhoGEF/LARG to regulate RhoA and growth cone morphology." Neuron 35(1): 51-63.

Takahashi, T., A. Fournier, F. Nakamura, L. H. Wang, Y. Murakami, R. G. Kalb, H. Fujisawa and S. M. Strittmatter (1999). "Plexin-neuropilin-1 complexes form functional semaphorin-3A receptors." Cell 99(1): 59-69.

Takahashi, T. and S. M. Strittmatter (2001). "Plexina1 autoinhibition by the plexin sema domain." Neuron 29(2): 429-439.

Takamatsu, H. and A. Kumanogoh (2012). "Diverse roles for semaphorin-plexin signaling in the immune system." Trends Immunol 33(3): 127-135.

Tamagnone, L. (2012). "Emerging role of semaphorins as major regulatory signals and potential therapeutic targets in cancer." Cancer Cell 22(2): 145-152.

Tamagnone, L., S. Artigiani, H. Chen, Z. He, G. I. Ming, H. Song, A. Chedotal, M. L. Winberg, C. S. Goodman, M. Poo, M. Tessier-Lavigne and P. M. Comoglio (1999). "Plexins are a large family of receptors for transmembrane, secreted, and GPI-anchored semaphorins in vertebrates." Cell 99(1): 71-80.

Tian, B. X. and L. A. Eriksson (2011). "Catalytic mechanism and roles of Arg197 and Thr183 in the Staphylococcus aureus sortase A enzyme." J Phys Chem B 115(44): 13003-13011.

Ton-That, H., G. Liu, S. K. Mazmanian, K. F. Faull and O. Schneewind (1999). "Purification and characterization of sortase, the transpeptidase that cleaves surface proteins of Staphylococcus aureus at the LPXTG motif." Proc Natl Acad Sci U S A 96(22): 12424-12429.

Tong, Y., P. Chugha, P. K. Hota, R. S. Alviani, M. Li, W. Tempel, L. Shen, H. W. Park and M. Buck (2007). "Binding of Rac1, Rnd1, and RhoD to a Novel Rho GTPase Interaction Motif Destabilizes Dimerization of the Plexin-B1 Effector Domain." J Biol Chem 282(51): 37215-37224.

Tong, Y., P. K. Hota, J. Y. Penachioni, M. B. Hamaneh, S. Kim, R. S. Alviani, L. Shen, H. He, W. Tempel, L. Tamagnone, H. W. Park and M. Buck (2009). "Structure and function of the intracellular region of the plexin-b1 transmembrane receptor." J Biol Chem 284(51): 35962-35972.

Tonikian, R., Y. Zhang, S. L. Sazinsky, B. Currell, J. H. Yeh, B. Reva, H. A. Held, B. A. Appleton, M. Evangelista, Y. Wu, X. Xin, A. C. Chan, S. Seshagiri, L. A. Lasky, C. Sander, C. Boone, G. D. Bader and S. S. Sidhu (2008). "A specificity map for the PDZ domain family." PLoS Biol 6(9): e239.

Toyofuku, T., J. Yoshida, T. Sugimoto, H. Zhang, A. Kumanogoh, M. Hori and H. Kikutani (2005). "FARP2 triggers signals for Sema3A-mediated axonal repulsion." Nat Neurosci 8(12): 1712-1719.

Tran, T. S., A. L. Kolodkin and R. Bharadwaj (2007). "Semaphorin regulation of cellular morphology." Annu Rev Cell Dev Biol 23: 263-292.

Turner, L. J., S. Nicholls and A. Hall (2004). "The activity of the plexin-A1 receptor is regulated by Rac." J Biol Chem 279(32): 33199-33205.

Vikis, H. G., W. Li and K. L. Guan (2002). "The plexin-B1/Rac interaction inhibits PAK activation and enhances Sema4D ligand binding." Genes Dev 16(7): 836-845.

Vikis, H. G., W. Li, Z. He and K. L. Guan (2000). "The semaphorin receptor plexin-B1 specifically interacts with active Rac in a ligand-dependent manner." Proc Natl Acad Sci U S A 97(23): 12457-12462.

Walzer, T., L. Galibert, M. R. Comeau and T. De Smedt (2005). "Plexin C1 engagement on mouse dendritic cells by viral semaphorin A39R induces actin cytoskeleton rearrangement and inhibits integrin-mediated adhesion and chemokine-induced migration." J Immunol 174(1): 51-59.

Walzer, T., L. Galibert and T. De Smedt (2005). "Poxvirus semaphorin A39R inhibits phagocytosis by dendritic cells and neutrophils." Eur J Immunol 35(2): 391-398.

Wang, H., P. K. Hota, Y. Tong, B. Li, L. Shen, L. Nedyalkova, S. Borthakur, S. Kim, W. Tempel, M. Buck and H. W. Park (2011). "Structural basis of Rnd1 binding to plexin Rho GTPase binding domains (RBDs)." J Biol Chem 286(29): 26093-26106.

Wang, Y., H. He, N. Srivastava, S. Vikarunnessa, Y. B. Chen, J. Jiang, C. W. Cowan and X. Zhang (2012). "Plexins Are GTPase-Activating Proteins for Rap and Are Activated by Induced Dimerization." Sci Signal 5(207): ra6.

Wang, Y., H. G. Pascoe, C. A. Brautigam, H. He and X. Zhang (2013). "Structural basis for activation and non-canonical catalysis of the Rap GTPase activating protein domain of plexin." Elife 2: e01279.

Webb, M. R. (1992). "A continuous spectrophotometric assay for inorganic phosphate and for measuring phosphate release kinetics in biological systems." Proc Natl Acad Sci U S A 89(June): 4884-4887.

Webb, M. R. and J. L. Hunter (1992). "Interaction of GTPase-activating protein with p21ras, measured using a continuous assay for inorganic phosphate release." Biochem J 287 (Pt 2): 555-559.

Wells, C. D., M. Y. Liu, M. Jackson, S. Gutowski, P. M. Sternweis, J. D. Rothstein, T. Kozasa and P. C. Sternweis (2002). "Mechanisms for reversible regulation between G13 and Rho exchange factors." J Biol Chem 277(2): 1174-1181.

Wiesmuller, L. and A. Wittinghofer (1992). "Expression of the GTPase Activating Domain of the Neurofibromatosis Type 1 (NF1) Gene in Escherichia

coli and Role of the Conserved Lysine Residue." The Journal of Biolgical Chemistry 267(May): 10207-10210.

Winberg, M. L., J. N. Noordermeer, L. Tamagnone, P. M. Comoglio, M. K. Spriggs, M. Tessier-Lavigne and C. S. Goodman (1998). "Plexin A is a neuronal semaphorin receptor that controls axon guidance." Cell 95(7): 903-916.

Winn, M. D., C. C. Ballard, K. D. Cowtan, E. J. Dodson, P. Emsley, P. R. Evans, R. M. Keegan, E. B. Krissinel, A. G. Leslie, A. McCoy, S. J. McNicholas, G. N. Murshudov, N. S. Pannu, E. A. Potterton, H. R. Powell, R. J. Read, A. Vagin and K. S. Wilson (2011). "Overview of the CCP4 suite and current developments." Acta Crystallogr D Biol Crystallogr 67(Pt 4): 235-242.

Worzfeld, T., J. M. Swiercz, A. Senturk, B. Genz, A. Korostylev, S. Deng, J. Xia, M. Hoshino, J. A. Epstein, A. M. Chan, B. Vollmar, A. Acker-Palmer, R. Kuner and S. Offermanns (2014). "Genetic dissection of plexin signaling in vivo." Proc Natl Acad Sci U S A 111(6): 2194-2199.

Yamada, A., K. Kubo, T. Takeshita, N. Harashima, K. Kawano, T. Mine, K. Sagawa, K. Sugamura and K. Itoh (1999). "Molecular cloning of a glycosylphosphatidylinositol-anchored molecule CDw108." J Immunol 162(7): 4094-4100.

Yamada, T., T. Sakisaka, S. Hisata, T. Baba and Y. Takai (2005). "RA-RhoGAP, Rap-activated Rho GTPase-activating protein implicated in neurite outgrowth through Rho." J Biol Chem 280(38): 33026-33034.

Yaron, A. and B. Zheng (2007). "Navigating their way to the clinic: emerging roles for axon guidance molecules in neurological disorders and injury." Dev Neurobiol 67(9): 1216-1231.

Yatani, A., L. A. Quilliam, A. M. Brown and G. M. Bokoch (1991). "Rap1A antagonizes the ability of Ras and Ras-Gap to inhibit muscarinic K+ channels." J Biol Chem 266(33): 22222-22226.

Yazdani, U. and J. R. Terman (2006). "The semaphorins." Genome Biol 7(3): 211.

Ye, F. and M. Zhang (2013). "Structures and target recognition modes of PDZ domains: recurring themes and emerging pictures." Biochem J 455(1): 1-14.

Zanata, S. M., I. Hovatta, B. Rohm and A. W. Puschel (2002). "Antagonistic effects of Rnd1 and RhoD GTPases regulate receptor activity in Semaphorin 3A-induced cytoskeletal collapse." J Neurosci 22(2): 471-477.

Zhao, H., R. Ghirlando, G. Piszczek, U. Curth, C. A. Brautigam and P. Schuck (2013). "Recorded scan times can limit the accuracy of sedimentation coefficients in analytical ultracentrifugation." Anal Biochem 437(1): 104-108.

Zhuang, B., Y. S. Su and S. Sockanathan (2009). "FARP1 promotes the dendritic growth of spinal motor neuron subtypes through transmembrane Semaphorin6A and PlexinA4 signaling." Neuron 61(3): 359-372.